

Lawrence Berkeley National Laboratory

Lawrence Berkeley National Laboratory

Title

DENSITY AND MAGNETIC FIELD MEASUREMENTS IN THE TORMAC IV-c
PLASMA

Permalink

<https://escholarship.org/uc/item/70s6r86x>

Author

Coonrod Jr., John Walter

Publication Date

1978-09-01

DENSITY AND MAGNETIC FIELD MEASUREMENTS

IN THE TORMAC IV-c PLASMA

John Walter Coonrod, Jr.

**Lawrence Berkeley Laboratory
Berkeley, California 94720**

NOTICE
This report was prepared as an account of work sponsored by the United States Government. Neither the United States nor the United States Department of Energy, nor any of their employees, nor any of their contractors, subcontractors, or their employees, makes any warranty, express or implied, or assumes any legal liability or responsibility for the accuracy, completeness or usefulness of any information, apparatus, product or process disclosed, or represents that its use would not infringe privately owned rights.

TABLE OF CONTENTS

ABSTRACT	vii
PREFACE	ix
1. INTRODUCTION	1
1.1 Tormac Concept	1
1.2 Tormac IV	5
1.3 Experimental Sequence	5
1.4 Motivation for Tormac IV-c	7
1.5 Diagnostics	9
1.5.1 Table of Typical Tormac IV-c Values	10
1.6 Questions and Conclusions	11
1.7 References	13
2. EXPERIMENTAL DATA AND ANALYSIS	15
2.1 Data Summary	15
2.2 Overall Picture	16
2.3 Spectral Measurements	17
2.3.1 Reconstruction Technique	18
2.3.4 Problems with Reconstruction	24
2.3.3 D _g Profiles and Density	25
2.3.4 He 4686 Profiles and Fluctuations	37
2.4 Thomson Scattering	44
2.5 Magnetic Measurements	48
2.5.1 Flux Exclusion	50
2.5.2 Description of Small Probes	55
2.5.3 Small Probe Data	59
2.6 Interferometer Measurements	73
2.6.1 Description and Access	73
2.6.2 Alignment and Calibration Procedure	77
2.6.3 Analysis Technique	78
2.6.4 Radial Density Profiles	79
2.7 Overall Particle Accounting	79
2.8 References	105
3. EXPERIMENT LAYOUT AND CONSTRUCTION	107
3.1 Glass Vessel	107
3.2 Cusp Winding	110
3.3 Cusp Bank and Switches	113
3.4 Bias Circuit	116
3.5 Pre-ionize Circuit	116
3.6 Heater Circuit	117
3.7 Floor Plan	118
3.8 Vacuum System	118
3.9 Safety Interlocks	122
3.10 References	123

4.	NUMERICAL CALCULATIONS	124
4.1	Vacuum Code PSIVAC	124
4.2	CGL Plasma Equilibrium Code	126
4.3	Tormac IV-c Results	129
4.4	References	129
5.	DATA ACQUISITION	133
5.1	Reticon System	133
5.1.1	Organization	134
5.1.2	Data Transmission Scheme	137
5.1.3	Channel Control and Selection	138
5.1.4	Operation Cycles	138
5.1.5	Circuit Description	141
5.1.5.1	Reticon system circuitry	141
5.1.5.2	Multiplexer circuitry	148
5.2	Computer System	152
5.2.1	Present Configuration	153
5.2.1.1	Hardware	154
5.2.1.2	Software	155
5.2.2	System Evolution	156
5.2.3	Descriptions of Special Programs	158
5.3	References	171
	ACKNOWLEDGMENTS	172

FIGURES

CHAPTER I

- 1.1 Comparison of Tokamak and Tormac Geometry
- 1.2 Tormac Confinement
- 1.3 Tormac IV Geometry
- 1.4 Typical Current Waveforms
- 1.5 Fluctuations in a Simulated Compression

CHAPTER II

- 2.1 Polychromator and Light Probe
- 2.2 Raw Data from Computer Data Acquisition Program "TAKE"
- 2.3 Calibration Parameter Display from "TAKE"
- 2.4 Output from Spectral Line Fitting Routine "FIT"
- 2.5 Doppler and Holtzmark Broadening
- 2.6 Typical D_{β} Profile
- 2.7 Typical output from the TIMEFIT Program
- 2.8 Radial profiles of D_{β} at characteristic times
- 2.9 Time dependence of D_{β} intensity and implied density
- 2.10 Estimated time dependent compression along z
- 2.11 Line of sight z profiles of D_{β} derived density
- 2.12 Typical 4686 line profile
- 2.13 Voight fit to the 4686 line
- 2.14 Raw 4686 data taken at a fast time scale
- 2.15 Fast time dependence of 4686 intensity and width
- 2.16 4686 light during preionization
- 2.18 Thomson scattering apparatus
- 2.19 Amplitude vs T_e for scattered light in polychromator channels
- 2.20 Typical scattering waveforms
- 2.21 T_e vs Time
- 2.22 Location of magnetic probes
- 2.23 Current waveforms
- 2.24 Plasma current waveforms
- 2.25 Typical flux loop and current waveforms
- 2.26 Output of subtraction circuit (flux exclusion)
- 2.27 Small probes
- 2.29 Vacuum magnetic field profiles
- 2.30 a-c Probe waveforms in the plasma
- 2.31 Field Oscillations vs Fill Pressure
- 2.32 a-e Field profiles
- 2.33 Probe waveforms during pre-ionization
- 2.34 Diagram of laser interferometer
- 2.35 Photo of interferometer in position
- 2.36 a,b Raw and unfolded data for one case
- 2.37 a-f Total Ionization vs. Time
- 2.38 a-o Radial Profiles of Line Density
- 2.39 Evolution of density gradient

CHAPTER III

- 3.1 Pyrex vessel for Tormac IV-c
- 3.2 Cusp winding
- 3.3 Winding endplate during construction
- 3.4 Martin Greenwald applying epoxy to outer cylinder
- 3.5 High voltage system schematic
- 3.6 Experiment floor plan
- 3.7 Vacuum and gas fill system

CHAPTER IV

- 4.1 Vacuum and plasma solutions in Tormac V
- 4.2 Vacuum (B) contours in Tormac IV-c
- 4.3 Vacuum poloidal field lines in Tormac IV-c

CHAPTER V

- 5.1 SAM chip organization
- 5.2 Data path
- 5.3 Computer system
- 5.4 Command word format
- 5.5 Photo of Reticon box
- 5.6 Photo of boards
- 5.7 Photo of Multiplexer box
- 5.8 SAM board
- 5.9 Control board
- 5.10 ADC board
- 5.11 Multiplexer address board
- 5.12 Multiplexer interface board

DENSITY AND MAGNETIC FIELD MEASUREMENTS
IN THE TORMAC IV-c PLASMA

John Walter Coonrod, Jr.

Accelerator and Fusion Research Division
Lawrence Berkeley Laboratory
Berkeley, California 94720

ABSTRACT

Tormac is a concept for magnetically confining a high- β fusion plasma in a toroidal, stuffed line cusp. A Tormac plasma has two regions: an interior confined on the closed toroidal field lines of the stuffing field, and an exterior sheath on open, cusped field lines. The interior plasma gives the device a longer confinement time than a standard mirror, while the favorable curvature of the cusp fields allow the plasma to be stable at higher values of β (the ratio of plasma pressure to magnetic pressure) than a totally closed configuration like Tokamak.

Tormac IV-c is an attempt to create and study a Tormac plasma with two cusp lines, a bi-cusp. It is a pulsed experiment. 10-50 mTorr of gas is preionized in a .5 meter diameter glass vessel in the presence of a 300 Gauss bias field. A 3-4 kG compression field then rises in 8.3 μ sec, sweeping up the plasma, and decays with $\tau = 80 \mu$ sec. During that time, data are taken by Thomson scattering, laser interferometry, magnetic probes, and spectroscopy, and stored by an online computer.

The results indicate that the plasma is incompletely ionized, cold ($T_e < 5$ eV) and in contact with the wall at small major radius. The bicusp configuration depends on a combination of toroidal and poloidal fields forming the magnetic piston which compresses the plasma. This occurs at the outer radius where the field is primarily poloidal, but fails at the inner wall as the toroidal field penetrates rapidly throughout the plasma.

This thesis describes the design, construction and operation of Tormac IV-c, and reports on the results, with emphasis on describing the behavior of the density compression and field penetration.

PREFACE

This thesis describes the construction, operation, and results of Tormac IV-c, a plasma confinement device built by Martin J. Greenwald and myself at the Lawrence Berkeley Laboratory. His thesis, "Temperature Measurements in the Tormac IV-c plasma" (LBL-8166), and this form complementary volumes in emphasis, although each is an independently complete description of the apparatus and data.

I have organized this paper in five chapters, each of which could be read separately. The introduction and the summary section of the data chapter describe the results, and the rest contains details. The work on data acquisition in Chapter 5 is useful to any experiment using computers, and is not restricted to plasma experiments per se.

This experiment is an integral part of the Tormac Project led by Morton A. Levine, which resides in the Magnetic Fusion Energy Program at LBL led by Wulf Kunkel. It was done with the collaboration and support of a large number of physicists and technicians. Participants over the last four years include (in approximate seniority):

EXPERIMENTAL PHYSICISTS

Morton A. Levine

Ian G. Brown

W.I.B. Smith

Booth R. Myers

Benedict Feinberg

Rory Niland

Philip Pincosy

Bruno Vaucher

John Coonrod

Martin Greenwald

Robert Shaw

TECHNICAL SUPPORT

Robert A. Peterson

Gus Saucedo

Gary Tabler

Joe Holdener

Eloy Salinas

Phil Smith

Jim Galvin

PROGRAMMING SUPPORT

Ludmilla Soroka

1. INTRODUCTION

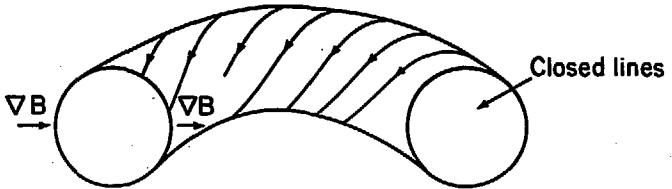
1.1 Tormac Concept

Tormac (toroidal magnetic cusp) is a magnetic configuration for confining a fusion plasma. This report is about Tormac IV-c, a fast-pulsed experiment at the Lawrence Berkeley Laboratory. It is the most recent of six devices built in the Tormac project.

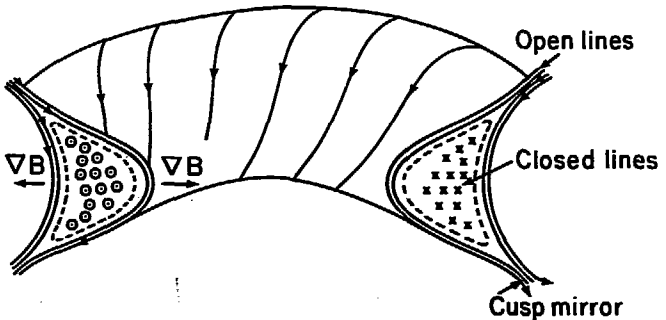
Tormac is an alternate concept in the U.S. effort to develop commercial fusion power. The leading contender, tokamak, has limitations which may make tokamak reactors uneconomical or impossible to build; primarily, it might have to be too large. If Tormac works, a reactor could be built at a comparatively smaller size and with conventional magnet technology.

Tormac is a high β device. The quality of magnetic confinement is usually described by β , the ratio of plasma pressure to magnetic field pressure. Tokamaks are grossly unstable for β larger than a few percent, which implies the need for large fields and lower densities. At low density, a much larger volume is required to produce power.

A plasma is subject to interchange instabilities whenever the confining magnetic field decreases in the direction away from the plasma surface (Figure 1.1), i.e. any plasma perturbation experiences less and less restoring force as it moves outward. It is equivalent to say that field lines must be convex toward the plasma for MHD stability.¹ Tokamaks



Tokamak average minimum-B geometry



Tormac absolute minimum-B geometry

FIGURE 1.1

XBL 789-2222

SCHEMATIC OF THE TORMAC ABSOLUTE MINIMUM B CONFIGURATION CONTRASTED WITH THE TOKAMAK AVERAGE MINIMUM B. IN BOTH CASES, TOROIDAL FIELDS WITH A $1/R$ DEPENDENCE PROVIDE FAVORABLE CURVATURE AT SMALL MAJOR RADIUS.

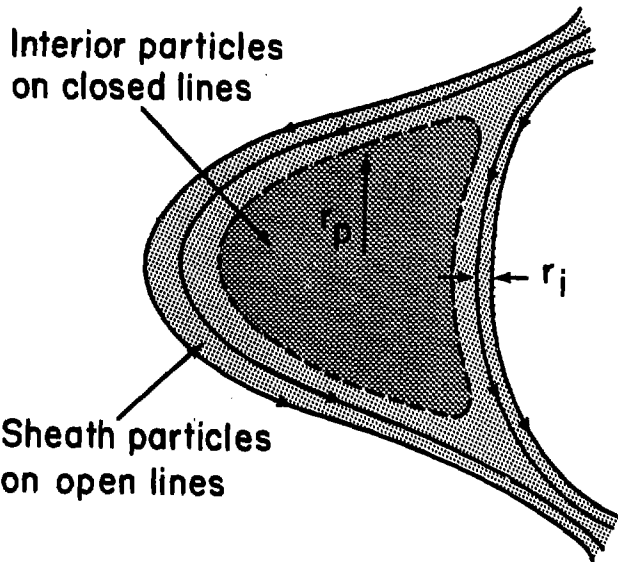
are average minimum-B stable. For low values of β , the plasma communicates with both convex and concave field regions faster than it could go unstable, and on average experiences a net stabilizing effect.

It is topologically impossible to have an absolute minimum-B torus without opening some of the field lines. Plasma losses are enhanced on open lines, so the region of open lines ought to be limited to as small a fraction of the plasma as possible.

Tormac² is an absolute minimum-B configuration in which there are two field regions: An inside set of closed lines, and a boundary set of open lines in the plasma sheath (figure 1.2).

The internal closed field lines have the minimum field strength required to conserve the adiabatic invariant. A second canonical invariant is conserved due to the device's axial symmetry.³

The simplest model for Tormac confinement assumes that the internal plasma is confined for a time long compared to the loss time in the sheath. Sheath particles are mirrored at the cusps, and enter the loss cone in an ion-ion collision time. The sheath thickness is the order of an ion gyro-radius, and remains this due to the rapid losses.⁴ Picture the confined plasma, then, as an onion losing one layer every collision time until it is eaten away. A steady state reactor would require a scheme to inject both particles and flux to re-inflate the plasma.⁵



Tormac confinement

FIGURE 1.2

XBL 789-2224

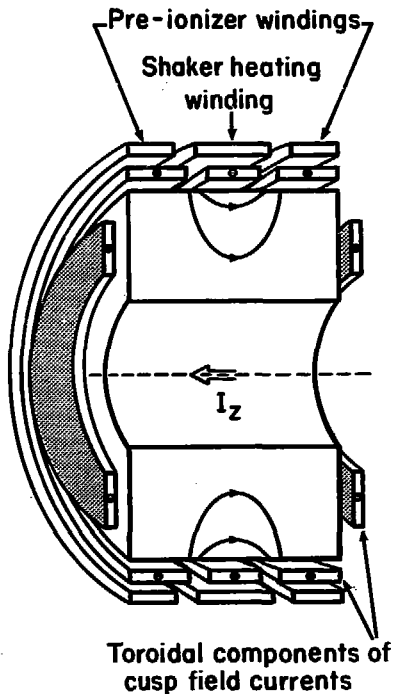
1.2 Tormac IV

The purpose of Tormac IV is to investigate and develop the concept in a small scale experiment. The objectives were (1) to create a Tormac plasma configuration during a 100 μ sec field pulse, and (2) to evaluate the "Shaker" heating scheme.⁶ Shaker heating is the absorption of magnetoacoustic waves launched into the plasma from an external winding as the field shakes the plasma surface.

The Tormac IV vessel is a rectangular pyrex torus with an 18" major diameter. The vessel is evacuated, then filled with a mixture of deuterium and helium. The gas is ionized, and then compressed by the cusp field (Figure 1.3).

1.3 Experimental Sequence

- 1) The glass vessel is evacuated to 5×10^{-7} torr.
- 2) The vacuum pump is gated off and the vessel is filled with 10 to 70 microns of gas (85% Deuterium, plus 15% Helium used for spectral diagnostics).
- 3) A 300 gauss toroidal bias field rises in 160 μ sec.
- 4) High and low frequency pre-ionize coils ring for 20 μ sec, breaking down the gas. The plasma is held by the bias field in an oscillating Z-pinch equilibrium, as the pre-ionize coils drive large (40 kA) currents in the plasma.
- 5) The pre-ionize current is crowbarred, and the main cusp compression field rises in 8.3 μ sec. The



Tormac IV geometry

FIGURE 1.3

XBL 789-2223

SCHEMATIC OF TORMAC IV SHOWING THE PLACEMENT OF THE WINDINGS AND THE GLASS VESSEL. THE TOROIDAL AND POLOIDAL CURRENTS ARE SHOWN SEPARATED FOR CLARITY. IN THE ACTUAL EXPERIMENT, BOTH COMPONENTS OF THE CUSP FIELD ARE CREATED BY A SINGLE WINDING.

initial bias current is frozen into the plasma, and is compressed into the interior closed field lines.

- 6) During the compression or at the peak the heater coil may be fired.
- 7) At the peak compression the cusp current is crowbarred, falling in 80 μ sec.

Fig. 1.4 shows the relationship of these currents.

The primary problems in performing such an experiment are:

- 1) Achieving full preionization of the gas
- 2) Excluding the open field lines from the central region. Can a relatively slowly-pulsed magnetic field be excluded from the plasma, or will it penetrate too quickly?
- 3) Diagnosing a hot, high- β plasma. The complex Tormac coil structure allows very little access.

1.4 Motivation for Tormac IV-c

Three similar Tormac IV experiments have been built. Tormac IV-a was built in 1973 by Gallagher and Levine at the Air Force Cambridge Research Labs, and moved to LBL in 1974. The primary diagnostics on Tormac IV-a were intensities and widths of spectral emission lines from the hot gas. Of particular interest was a measurement of T_i from the Doppler broadened 4686 angstrom ionized helium line. Measurements by Myers and Levine have been reported⁸ and indicated spectacular success: a strongly compressed, high- β plasma with $n_e = 3 \times 10^{15}$, $T_i > 150$ eV, being contained for $\tau > 30$ μ sec.

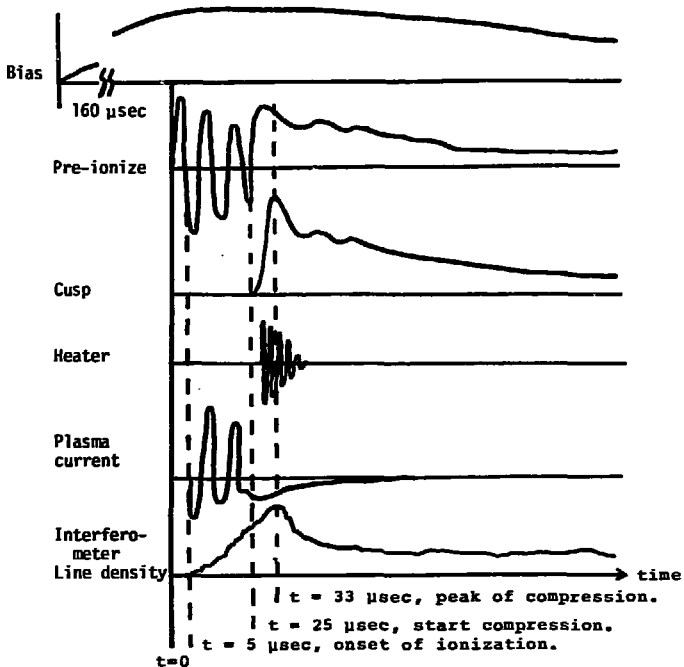


FIGURE 1.4 TYPICAL CURRENT WAVEFORMS IN TORMAC IV-C.

XBL 789-11362

In 1975 a second device, Tormac IV-b was built at LBL and used only briefly as it appeared to have a leak that could not be repaired.

Late in 1977 Martin Greenwald and I began constructing Tormac IV-c. Our goal was to duplicate the conditions of Tormac IV-a, and to permit a more thorough diagnosis, particularly by Thomson scattering and interferometry. Results of these experiments led to different conclusions, although the spectral data was nearly identical. Scattering gave $T_e \sim 5$ eV, while interferometry showed incomplete ionization and the plasma in contact with the wall.

1.5 Diagnostics

Tormac IV-c was designed to be able to duplicate any measurements from Tormac IV-a, and to allow more thorough and varied diagnostics to be added. These include:

Magnetic measurements:

- Rogowski coils on all banks, windings and switches
- Rogowski coil around the plasma vessel
- Flux loop around the plasma vessel
- Magnetic probes, moving through the plasma in r and z

Spectral measurements:

- Adjustable external light probe, connected to a 16 channel polychromator

Interferometer

- HeNe Laser Michelson Interferometer, radial scan

Thomson scattering.

1.5.1 Table of a Typical Tormac IV-c Values⁹

Bias Field	300 Gauss
Preionize field	800 Gauss $\omega = 7.9 \times 10^5 \text{ sec}^{-1}$ loop voltage = 30 kV
Cusp circuit	$I_{\text{peak}} = 268 \text{ kAmps}$ $B_T(r = 15 \text{ cm}) = 3.6 \text{ kG}$ $B_P(r = 20 \text{ cm}) = 3.0 \text{ kG}$
Gas Fill	10-50 mTorr 85% D ₂ 15%He
Peak T _e	5 eV
Peak n _e	$6 \times 10^{15} \text{ cm}^{-3}$ (36 mTorr gas fill)

Field Penetration:

Calculated for 5 cm, classical	70 μsec
Observed for B _T	-1 μsec
Observed for B _P	-8 μsec

Density Compression

$$n_{\text{peak}}/n_{\text{avg}} = 6 \times 10^{15}/2 \times 10^{15} = 3$$

$$V_{\text{peak}}/V_{\text{total}} = 3.2 \times 10^4/6.6 \times 10^3 = 4.8$$

Collision Frequencies (sec⁻¹) Larmor Frequencies (sec⁻¹)
($n=5 \times 10^{15} \text{ cm}^{-3}$) (3.5 kG)

$\nu_{ei} = 9.8 \times 10^9$	$\omega_{ce} = 6.2 \times 10^{10}$
$\nu_{ii} = 2.2 \times 10^8$	$\omega_{ci} = 3.3 \times 10^7$
$\omega_p = 4.0 \times 10^{12}$	$r_i = .1 \text{ cm}$

Alfven Speed (10 cm) = 1.3 μsec

$$ZnA = 7.3$$

$$\lambda_D = 2.35 \times 10^{-5} \text{ cm}$$

T_e/T_i equilibration: $\nu_c = 5.2 \times 10^6 \text{ sec}^{-1}$
 $\tau_c = 1.9 \times 10^{-7} \text{ sec}$

1.6 Questions and Conclusions

The primary conclusion of density studies in Tormac IV-c is that under these conditions the experiment does not form a plasma in the bicusp configuration. The plasma that is formed is slightly compressed and swept in from the outer wall, but is in direct contact with, and is never lifted away from, the inner wall.

The sweep-up problem in pulsed Tormac experiments is complex, particularly for a bicusp. The magnetic well of the cusp field must become a magnetic piston, which drives the plasma in from all directions at once. If we imagine the initial plasma to contain only a toroidal bias field, then the compression field is parallel to the bias at small major radius, and perpendicular at large major radius. Earlier experiments on pinches¹⁰ have shown that parallel fields fail to form a magnetic piston, even for risetimes relatively faster than in Tormac IV-c. This will be discussed in detail below.

The question which arose in Tormac IV-a was "is it really as hot as the line broadening indicates, and if not, what mechanism is broadening the lines?" This is a paradox which has arisen in pinch experiments as well.¹¹ The Thomson scattering on IV-c conclusively demonstrates an electron temperature < 5 eV at all times. At these temperatures and densities $T_e = T_i$, leaving us to discover an alternate broadening mechanism.

One part of that answer is fluctuations. During the

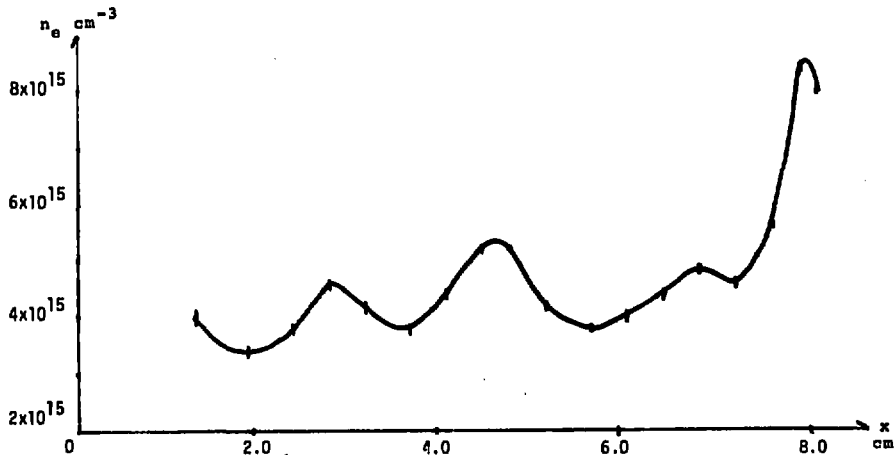


FIGURE 1.5 DENSITY FLUCTUATIONS IN A SIMULATED COMPRESSION.

A 1-D simulation of a Tormac IV-c compression is performed using a hybrid code. This shows density fluctuations at 4 sec into a 8.3 μsec cusp rise. The x coordinate is given in cm. From work by M. Vella, S. Hamasaki, H. Berk, to be published.

XBL 789-11364

cusplike rise, there are large amplitude (60%) local magnetic fluctuations which appear to propagate into the plasma from the outside major radius. They appear also in the helium line emission, in the intensity and in the wings. The line could be broadened by consequent E fields, or by mass motion. If we assume the oscillations are an Alfvén disturbance the mass velocity would be the Alfvén velocity multiplied by the fractional amplitude of the perturbation. Taking $n = 5 \times 10^{15}$, $B = 3\text{kG}$ gives $V_{\text{mass}} = 4.3 \times 10^6$ cm/sec, corresponding to a thermal velocity at 80 eV. This is approximate in that I have assumed the deuterium provides all the mass density and the helium moves with it.

The existence of fluctuations is not surprising, considering that the rise time of the field is not very different from an Alfvén transit time of the plasma, although we did not expect them to be so large. They have been observed, though, in 1-D simulations performed recently by M.C. Vella¹² using a hybrid code developed at Science Applications, Inc. by S. Hamasaki, and shown in Figure 1.5.

The question to arise from this study is, could a modified Tormac IV-c succeed in producing a Tormac configuration? Possible first steps would be, (1) a definite poloidal field to sweep the plasma away from small major radii, such as a 4-pole cusp described in reference 2, and (2) a greatly increased pre-ionizer field. A 4-pole cusp avoids the problem of compression by fields parallel to the bias, which is not central to the Tormac concept.

1.7 References

1. N.A. Krall and A.W. Trivelpiece, Principles of Plasma Physics, Section 5.8. McGraw-Hill, N.Y. (1973).
2. U. Berkowitz et al., 2nd Int. Conf. Peaceful Uses of Atomic Energy (Proc. Conf. Genevo, 1958) 31, 171 UN, N.Y. (1958).
L.S. Combes, C.C. Gallagher, and M.A. Levine, Phys. Fluids 5, 1070 (1962).
3. M.A. Levine, A.H. Boozer, G. Kalman, and P. Bakshi, Phys. Rev. Lett. 28, 1323 (1972).
4. A.H. Boozer and M.A. Levine, Phys. Rev. Lett. 31, 1287 (1973).
5. M.A. Levine, I.G. Brown, and W.B. Kunkel, LBL-4491 (1976).
6. M.A. Levine, I.G. Brown, and C.C. Gallagher. Pulsed High Beta Plasmas (Proc. 3rd Topical Conf. Culham U.K. 1975) ed. D.E. Evans. p. 382. Pergamon, Oxford (1976).
7. C.C. Gallagher and M.A. Levine, "Design and Construction of Tormac IV, a Toroidal, Bi-Cusp Plasma Containment Device," Tech. Rpt. AFCRL-T4-74-0122.
8. B.R. Myers and M.A. Levine, Bull. Am. Phys. Soc. 22, 1068 (1977).
9. Numerical calculations from D.L. Book, Revised NRL Plasma Formulary GPO 909-039.
10. A.W. DeSilva, W.F. Dove, I.J. Spaulding, and G.C. Goldenbaum, Phys. Fluids 14, 42 (1971).
11. P.R. Forman, private communication.
12. Michael C. Vella, LBL, private communication.

2. EXPERIMENTAL DATA AND ANALYSIS

2.1 Data Summary

Data were taken by Martin Greenwald and myself during March, June and August 1978. About 800 shots were recorded and stored by the computer data acquisition system described in the final chapter; several hundred others were recorded as photographs of oscilloscope traces.

With the exception of magnetic probes, the Tormac diagnostics were designed to diagnose a plasma with $T > 100$ eV. They have worked for the present plasma, although in some cases the interpretation changes in the low temperature regime.

The strategy for data taking was to reproduce the experiments performed on Tormac IV-a using spectral data, and then to thoroughly investigate the plasma using "non-ambiguous" diagnostics.

There has been an emphasis in Tormac experiments to gather information from a great many shots. The emission spectra, for instance, has in the past been computer reconstructed from a great many views to determine the emission from each point in the plasma cross section. Interferometer and probe traces from many shots have been collected to form profiles in r and z . This work depends on the shot to shot repeatability of the experiment. For most diagnostics this is very good, i.e. variations are smaller between shots than they are between positions.

The data were taken with the device in two different

configurations: with and without a pair of conducting rings circling the device outside the cusp lines, at a 23" diameter. These rings were added to simulate rings on Tormac IV-a, used at one time to distribute current.

In each of these configurations data was taken with and without the cusp field, and with three different gas filling pressures corresponding to cycling the gas fill plenum 1, 2 or 3 times (see Chapter 3.8).

2.2 Overall Picture

All the data for Tormac IV-c fit together in a straightforward way, with the exception of the broadening of the 4686 Å line. This latter is more complex and can be reasonably explained by a combination of effects other than high ion temperature.

During the second half phase of the ringing pre-ionizer, ionization begins and a large toroidal current (40 kA) is driven in the plasma in phase with the ringing. A very short burst (< 1 μ sec) of 4686 light appears during the first plasma current oscillation indicating runaway electrons. (In Toramc IV-a, a burst of x-rays was detected at this same time.) Electron density and total ionization rise smoothly, to about 35%, during 15 μ sec of pre-ionization. The ionization is strongest near the inner cylinder, and falls off smoothly with radius. If no cusp field is applied, the ionization falls off with $\tau \sim 30$ μ sec.

When the cusp field is turned on, plasma is pushed away from the outer wall, while the total ionization is increased to about 70%.

The bicus configuration requires that plasma pressure be confined by poloidal fields at large radii and toroidal fields at small radii. The plasma excludes the poloidal field briefly, creating a sharp boundary at the outside for about 10 μ sec.

Appearance of the toroidal field, however, is delayed for about 1 μ sec at small radii, and then jumps into large oscillations about the vacuum value, until the cusp peak. No boundary appears at small radii, and the plasma is presumably supported by the wall.

These oscillations appear at the plasma boundary, and damp out shortly after the peak of the cusp. They appear in some form on all the diagnostics.

After the peak of the cusp, the plasma boundary relaxes in about 10 μ sec, and the total ionization decays at $\tau = 80 \mu$ sec.

2.3 Spectral Measurements

Tormac IV is ideal for studying visible emission spectra as the bottle is clear glass. Helium is used in the gas mixture specifically as a diagnostic of ion temperature by Doppler broadening of the 4686 angstrom line. One should also expect to measure the plasma density by the Holtzmark

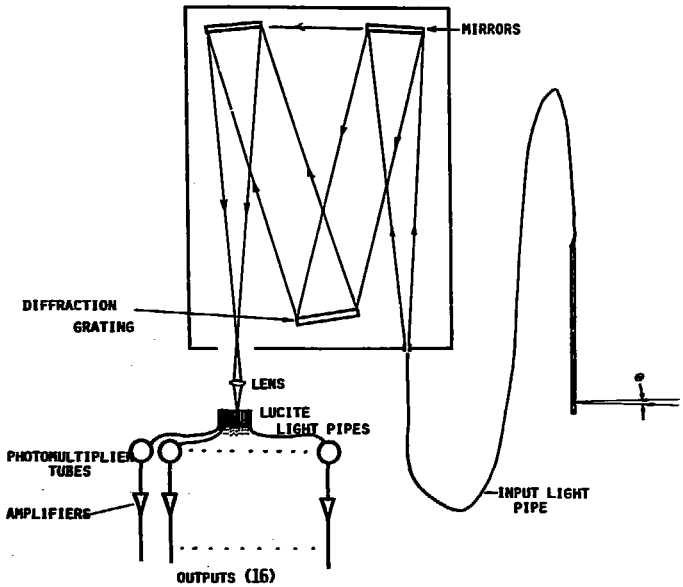
(E-field) broadening of the neutral deuterium D_0 line.

Both lines are affected to some extent by both broadening mechanisms, and to this extent the diagnostic is ambiguous. A cold, dense plasma broadens the line as much as a hot tenuous plasma. In addition, light is collected along a line of sight which passes through both confined and colder, unconfined plasma. At temperatures above a few eV, the intensity of the line should fall due to burn out, and the collected light would primarily represent the cold background plasma.

2.3.1 Reconstruction Technique

Information on the light emitted by the plasma center can be extracted by computerized tomographic reconstruction,¹ the method used in medicine to take sectional x-rays of the brain. To do this, line of sight measurements are taken at many positions and angles. The cross section is treated as a matrix of emitting elements, and finding the emission at each element is equivalent to solving a large system of linear equations. Many algorithms have been developed to do this.²

The procedure developed on Tormac IV-a uses 88 total views, taken at 4 different angles: 0° , 90° , 45° and 135° . A thin probe containing interchangeable mirrors and a lens is slipped under the magnet winding, and along the vessel (Figure 2.1). Views are made along r and z at 1/2 inch intervals.³



SIXTEEN CHANNEL POLYCHROMATOR AND LIGHT PROBE. SEPARATION BETWEEN CHANNELS IS .39 A.

FIGURE 2.1

XBL 789-10876

Light collected by the probe is focused onto a light fiber bundle and carried to the input slit of a Spex 3/4 meter Czerny-Turner spectrometer. At the output slit is a stack of 16 flat light guides which distribute the different wavelengths to 16 type 4840 photomultiplier tubes. Mounted on the polychromator are adjustable gain amplifiers and emitter follower line drivers. Each signal is recorded on a separate data acquisition channel. At each shot, a full line profile is recorded at 128 time steps. Between shots, subroutines in the data acquisition program automatically fit the data to Gaussian or Lorentzian line shapes and display the results.

Figure 2.2 is an example of the display of a raw data shot. The first 8 traces represent different current waveforms, and the last 16 are the polychromator channels. The channels in the wings are often operated at higher gains. The full system, from light pipe to computer, is calibrated together using a white light "solar simulator", and a special computer program.

The calibration coefficients and amplifier gain settings are stored in a parameter array in the computer program and stored with each shot, this is displayed in Figure 2.3. Output from the 4 parameter fit routine (height, center, width, and continuum level) developed by Rory Niland is shown in Figure 2.4.

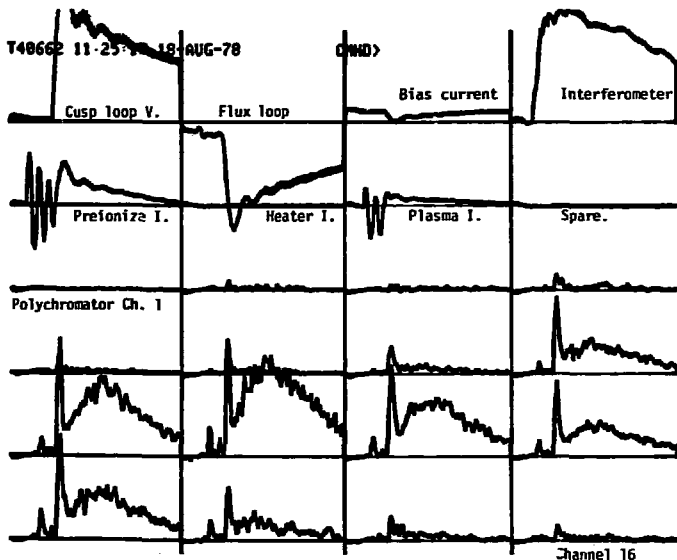


FIGURE 2.2 RAW DATA FROM COMPUTER DATA ACQUISITION PROGRAM TAKE.

Immediately after a shot, the data from 24 Reticon channels is displayed on a graphics terminal and a hard copy can be made. The shot number, time and date are displayed and are stored with the data on disk.

XBL 789-11366

HEADER PARAMETERS--T40789 17:02:51 23-AUG-78

POLYCHROMETER SETTING & CALIBRATION--I>GS PC

1>20	1.0000	2>20	0.9900	3>20	1.0200	4>20	0.9700
5>20	0.9700	6>20	0.9900	7>20	0.9800	8>20	1.0200
9>20	0.9900	10>20	1.0300	11>20	1.0000	12>20	1.0400
13>20	1.0900	14>20	1.0700	15>20	1.1300	16>20	1.0000

VOLTAGES & TIMINGS

BIAS	2000VOLTS	1USEC
PREI	30000VOLTS	330USEC
CUSP	15000VOLTS	345USEC
LAUS	0VOLTS	0USEC
LASR	0VOLTS	0USEC
INTF	3VOLTS	0USEC
PHOT	750VOLTS	0USEC
COMP	0VOLTS	325USEC

RETICON CHANNELS

1> 0 2> 1 3> 2 4> 3 5> 4 6> 5 7> 6 8> 7 9> 8 10> 9
11>10 12>11 13>12 14>13 15>14 16>15 17>16 18>17 19>18 20>19
21>20 22>21 23>22 24>23 25>-1
CHANGE??

FIGURE 2.3 CALIBRATION PARAMETER DISPLAY FROM TAKE.

A header record is stored with each shot which contains calibration information for the polychromator, as well as Reticon channel assignments, bank settings, and a 64 character comment (not shown).

XBL 789-11365

A= 0.99
B= 6.90
C= 3.51 with .005 noise
D= 0.81
T= 57.45 E11

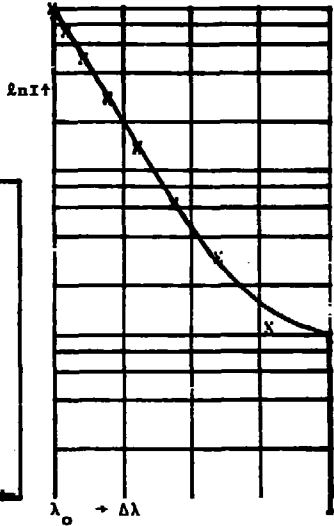


FIGURE 2.4 OUTPUT FROM THE FIT ROUTINE.

A subroutine in the TAKE program calibrates the raw polychromator data and fits it to a Gaussian, for a given time step. Here a test run fits a computed Gaussian with added noise.

2.3.2 Problems with Reconstructions

While we initially took spectra data and performed a reconstruction of the 4686 line, for comparison with Tormac IV-a, we later abandoned this method. The spatial resolution of a reconstruction depends on the number of angular views. Work done by Rory Niland⁴ discovered that 4 angles limited the resolution to one quarter to one half the chamber size.

In general a rule of thumb in tomography is to have 4 times as many rays as grid squares, to insure the system of equations is overdetermined⁵ (not all rays are independent). The reconstructions on Tormac IV had 88 rays and 200 grid squares and hence were greatly underdetermined.

2.3.3 D_β Profiles and Density

The problem of burnout in the center is not an issue in the low temperature case. Hence useful information can be gained from looking at profiles composed of the line-of-sight data taken at different positions.

Broadening of the neutral deuterium D_β line (4861 angstroms) is primarily due to density. The Stark effect caused by microscopic electric fields broadens the radiation from individual atoms, and the collection of contributions from a random distribution is called Holtzmark broadening. The density is related to the line width by⁶

$$[2.1] \quad n = C(n,T) \Delta\lambda^{3/2}$$

where $\Delta\lambda$ is the full width and C is a tabulated coefficient, only weakly dependent on n. Figure 2.5 plots this and the Doppler broadening for a range of plasma parameters.

A scan along the vessel radius of D_β was made, and each point in time was fit using the computer program TIMEFIT, which displays the four fit parameters, the error and the total line intensity (Figure 2.7). This intermediate analysis routine lets the final routines know the error so they can eliminate the poor data from the final results.

Figures 2.8 a-c were reduced from TIMEFIT by TPROF to produce radial profiles at different times. These are in good qualitative agreement with similar plots taken from the interferometer data. Quantitatively, by comparing these with the interferometer, one can estimate the plasma size along z

$$[2.2] \quad L \sim \frac{(\int n_e dx)_{intf}}{\langle n_e \rangle_{D_\beta}}$$

This ignores the actual shape, and the weighting is due to intensity variation of the light, but it gives a relative width.

Figures 2.9 a-d give the time dependent D_β intensity and implied density: again these can be compared with the interferometer Figure 2.36a. The comparison in formula [2.2] leads to a compression estimate shown in Figure 2.10. This can be compared to the line of sight profile taken along z, in Figure 2.11.

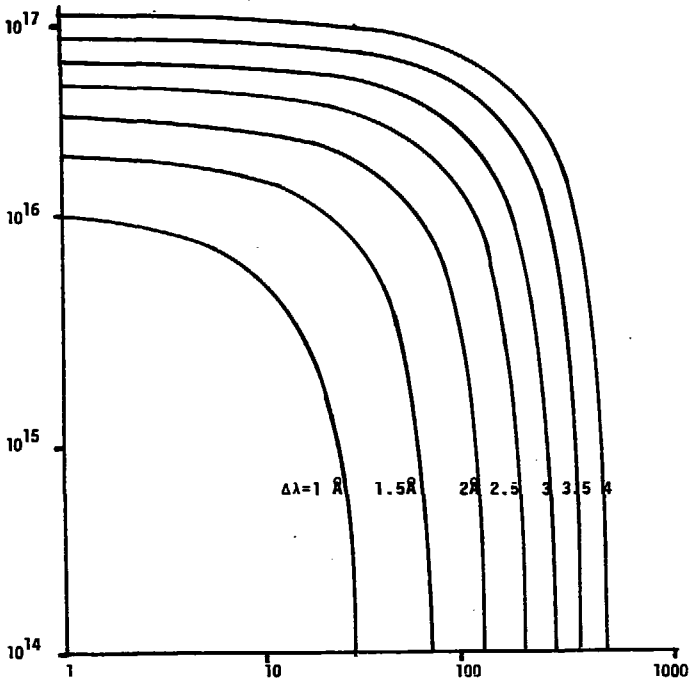


FIGURE 2.5 DOPPLER AND HOLTZMARK BROADENING OF THE He_{II} 4686 ANGSTROM LINE.

XBL 789-11341

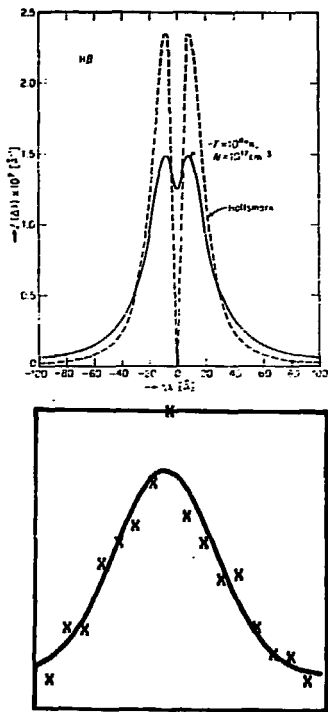


FIGURE 2.6 TYPICAL D_β PROFILE.

Top: Theoretical curves by Griem for the Holtzmark and detailed Stark broadening of the hydrogen 4861 line. Note that while the shapes vary, the half-width is nearly constant. Bottom: An experimental deuterium line curve showing the component shift wiped out by other effects. The width is determined by a Gaussian fit routine.

30-AUG-78 15:41 44 NUMBER OF SHOTS=10
FILE #= 845 846 847 848 849 850 851 852 853 854

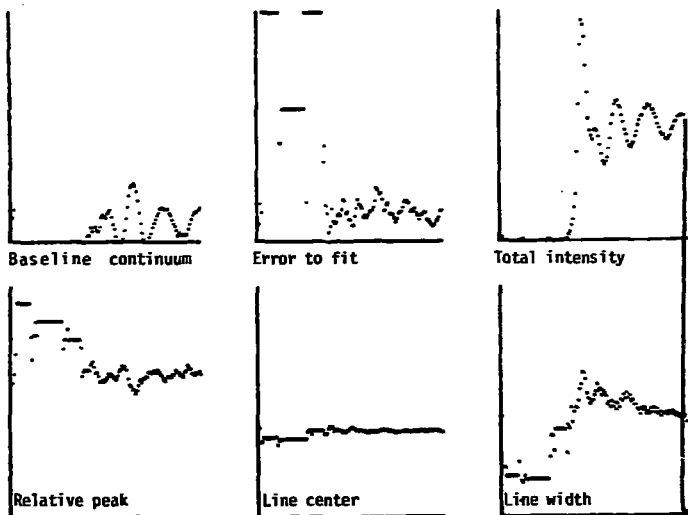


FIGURE 2.7 TYPICAL OUTPUT FROM THE TIMEFIT PROGRAM.

TIMEFIT has averaged the data from 10 shots, and fit the line shapes to 4 parameters. Data points falling on horizontal dashes have been given artificial values when the FIT routine has failed to fit a given time step. 4686 angstrom line on a fast time scale (200 nsec between samples).

XBL 789-11333

DENSITY PROFILE FROM 4861 WIDTH 15-SEP-78 13:10:16

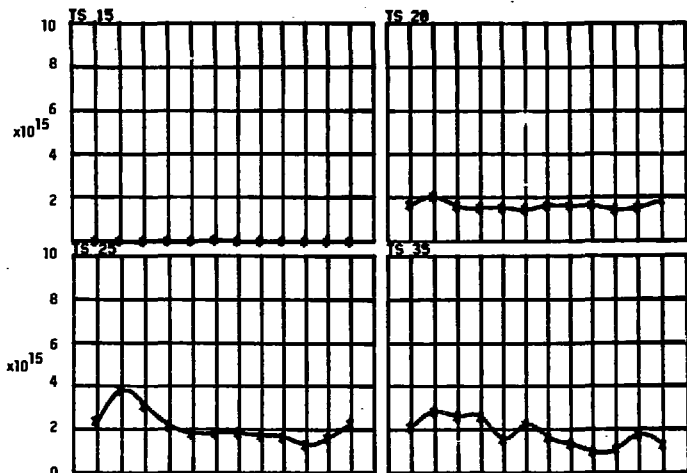


FIGURE 2.8A RADIAL PROFILES OF D_β DERIVED DENSITY.

Electron density is inferred from the line broadening of the deuterium 4861 angstrom line. Times are given above each graph. Each horizontal division represents one cm.

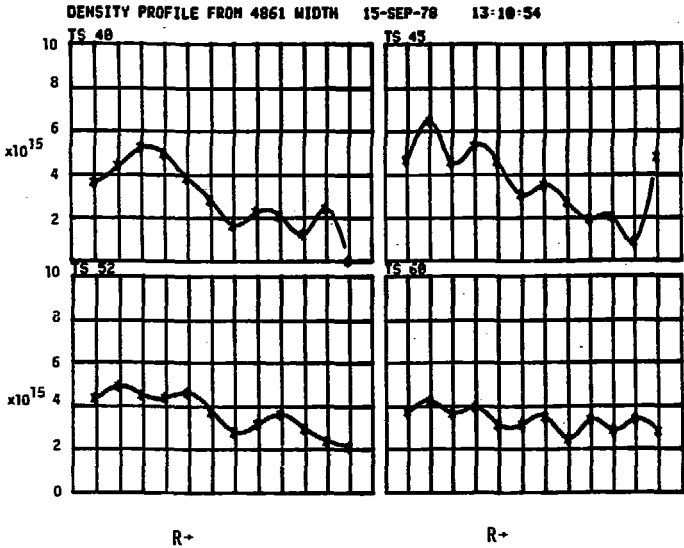


FIGURE 2.88 RADIAL PROFILES OF D_β DERIVED DENSITY.

Electron density is inferred from the line broadening of the Deuterium 4861 angstrom line. Times are given above each graph. Each horizontal division represents one cm.

XBL 789-11354

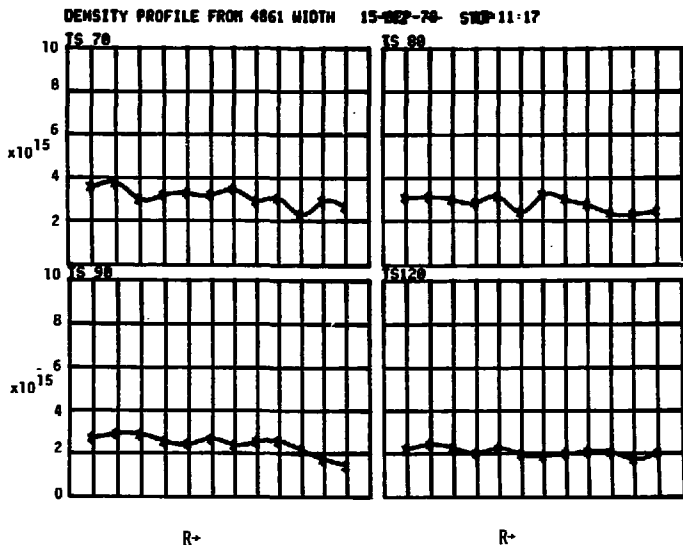
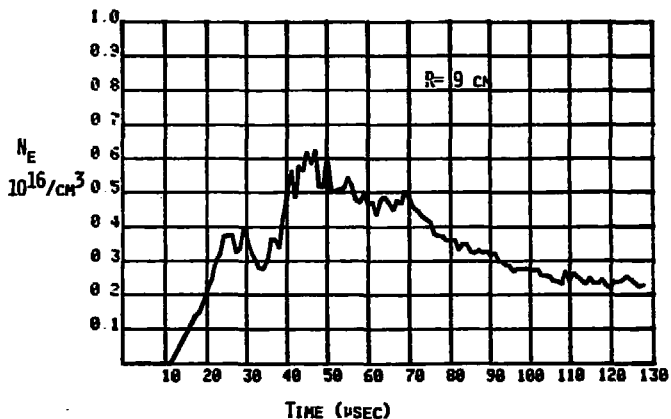


FIGURE 2.8c RADIAL PROFILES OF D_β DERIVED DENSITY.

Electron density is inferred from the line broadening of the Deuterium 4861 angstrom line. Times are given above each graph. Each horizontal division represents one cm.

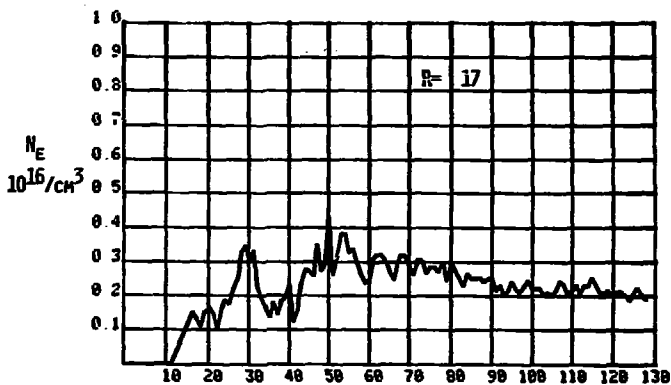
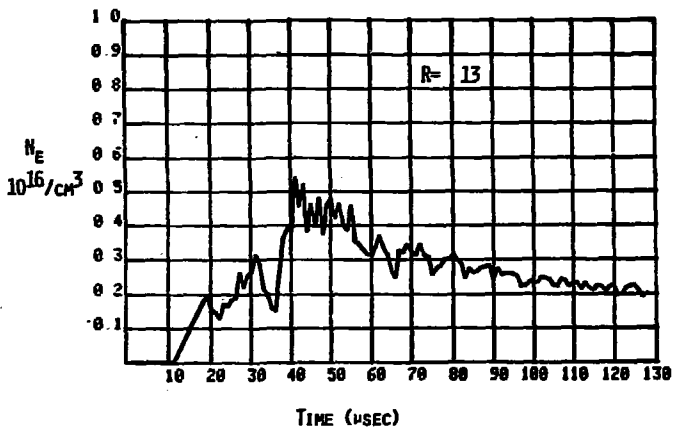
XBL 789-11355



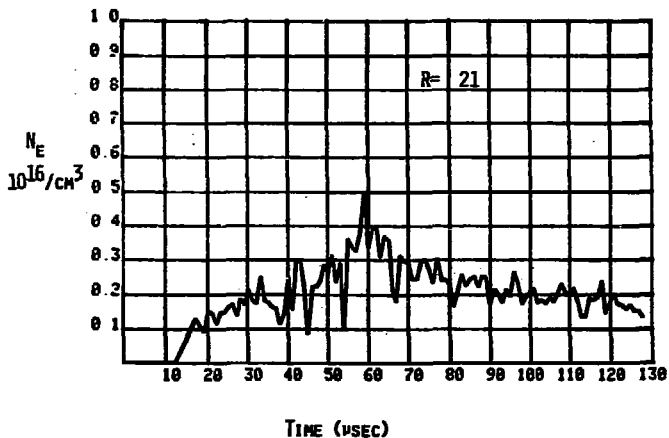
ELECTRON DENSITIES AT $R = 9\text{CM}$ INFERRED FROM D_{β} LINE BROADENING VS TIME. THE CUSP RISE BEGINS AT 25 μSEC AND PEAKS AT 33 μSEC .

FIGURE 2.9A

XBL 789-10854



ELECTRON DENSITIES AT $R=17$ CM INFERRED FROM D_β



ELECTRON DENSITIES AT R=21 CM INFERRED FROM D_B

FIGURE 2.9D

XBL 789-10852

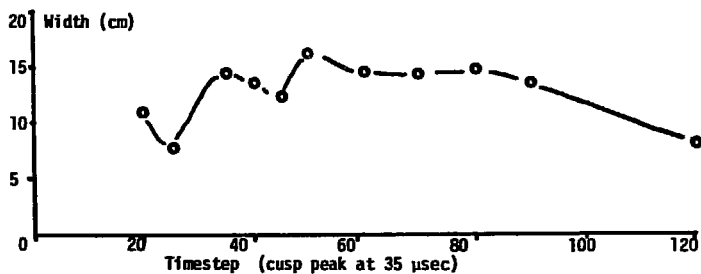


FIGURE 2.10 ESTIMATE OF WIDTH ALONG Z FROM D_B WIDTH.

XBL 789-11349

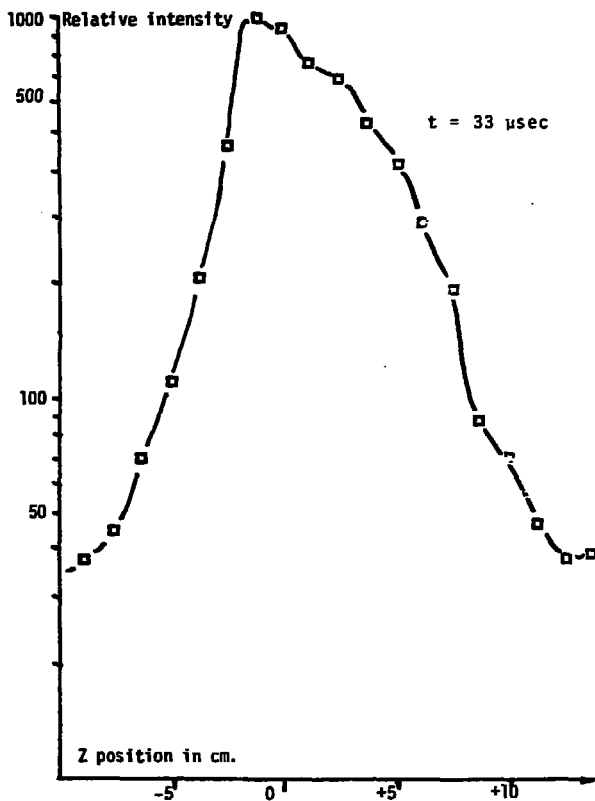


FIGURE 2.11 LINE OF SIGHT INTENSITY PROFILE ALONG Z, FROM TORMAC IV-A.

XBL 789-11352

2.3.4 He 4686 Profiles and Fluctuations

Figure 2.12 shows the principle enigma in the experiment, the broadening of the singly ionized helium line at 4686 angstroms. The shape is quite Gaussian, as a line Doppler broadened by a hot Maxwellian plasma ought to be.⁷ When one interprets the line width as pure Doppler broadening, the resulting ion temperature is > 100 eV. This is inconsistent with the electron temperature obtained from Thomson scattering, and with energy considerations: 1) not enough energy has been transferred from the magnetic field to heat the plasma; 2) at this density and ion temperature the plasma pressure is greater than the available magnetic pressure, i.e. $\beta > 1$.

A less naive procedure is to de-convolve the density and pressure broadening. The Stark coefficient C for this state is 2.74×10^{16} , indicating much less broadening than for deuterium ($C = 3.3 \times 10^{14}$). Figure 2.13 shows the results of Voigt fits performed by Robert Shaw.⁸ The density is reasonable, but the temperature is still too high. Other effects, such as fine structure, Zeeman splitting or instrumental broadening could account for no more than 20eV of the apparent temperature.

Figure 2.16 shows the time dependence of the 4686 light, during the preionization and compression phases. Note especially that the line is broad at the very onset of ionization, and during the rise of the cusp. These are times

@VND0 86
B= 9.01
C= 3.30
D= 0.05

T40212 13 33 32 14-MAR-78 STEP= 31

TI=148 79 E¹¹

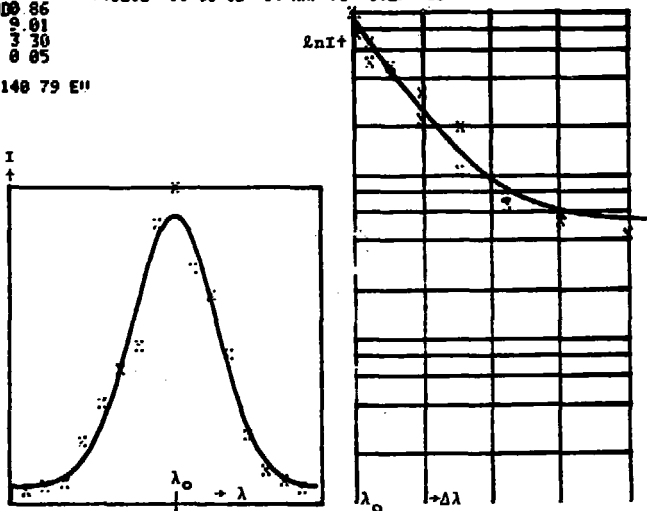


FIGURE 2.12 TYPICAL 4686 LINE PROFILE.

The HeII 4686 line broadening is interpreted as due to an ion temperature of 141ev.

XBL 789-11347

INPUT RMIN,RMAX,ZMIN,ZMAX(I2)
3.6,8,12

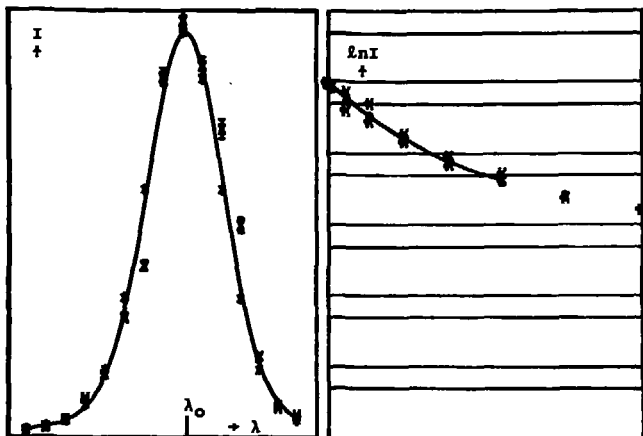
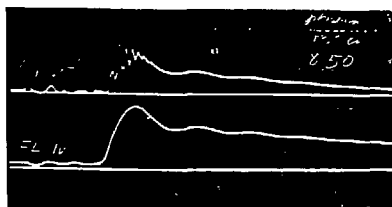


FIGURE 2.13 VOIGT FIT TO A 4686 LINE.

The central 20 grid squares from a computer reconstruction of HeI 4686 light emission have been averaged and fit to a Voigt profile. Doppler and Holtzmark broadening are taken into account, and the background continuum is assumed to be 0. Resulting fit has $n_e = 4 \times 10^{15}$, $T_i = 80$ ev. Gas fill = 50 mTorr. Data from Torvac IV-c, reconstruction and fit by Robert Shaw.

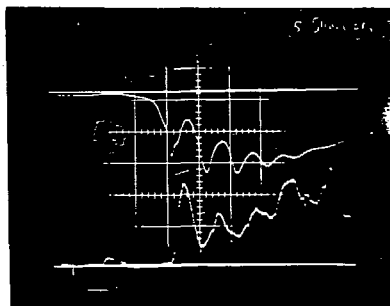
when the plasma can be nowhere near equilibrium. Hence the broadening could be due to the effects of an instability. As mentioned above, a strong magnetic fluctuation is seen during the cusp rise on the magnetic probes. Figure 2.14 shows the raw data of a shot. Channel 7, the toroidal field probe, shows the fluctuations, and the 4880 light is obviously correlated with it. The problem would be greatly simplified if we saw the width fluctuate. Figure 2.15 shows the intensity and width at this fast time scale, and while the intensity fluctuation is strong the width varies quite slowly. Figure 2.7 shows the output of TIMEFIT. The large fluctuations in the "continuum" parameter are an interesting feature. Since the polychromator does not read far into the wings, this probably reflects activity in the wings rather than in the continuum. Another interesting possibility also fails: oscillations in the line center would indicate the Doppler shift of mass motion, and this does not appear.

Possible, and likely, interpretations include some combination of action due to fluctuating electric fields and due to very symmetrical mass motions, so that line of sight views all see an averaged effect. This unsolved problem is a subject for further studies.



SMALL PROBE MEASUREMENT
OF TOROIDAL FIELD IN
PLASMA, AT $R=13.9$ CM
2000 GAUSS/DIV

FLUX LOOP
VERTICAL 1V/DIV
HORIZONTAL 10 USEC/DIV



SMALL PROBE, B_T
774 GAUSS/DIV

4686 Å INTENSITY
HORIZONTAL 2 USEC/DIV

FIGURE 2.14
FLUCTUATIONS IN TOROIDAL FIELD AND 4686 Å EMISSION
DURING CUSP CURRENT RISE.

FIT846.FIT

30-AUG-70

16:43:42

RELATIVE INTENSITY

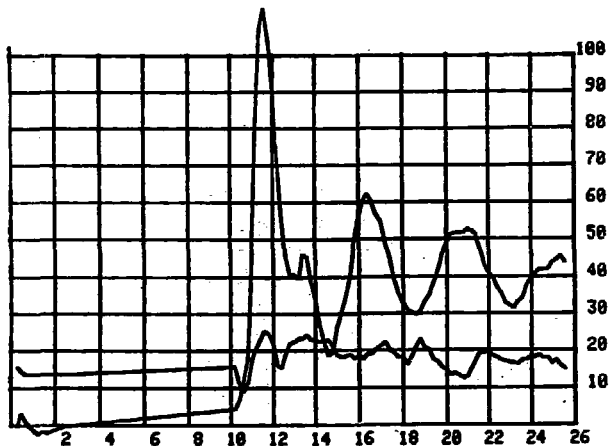


FIGURE 2.15 FAST TIME DEPENDENCE OF 4686 INTENSITY AND WIDTH.

The flat portions of the trace are artificial and represent the timesteps when the FIT routine failed due to insufficient data (too little light).

XBL 789-11345

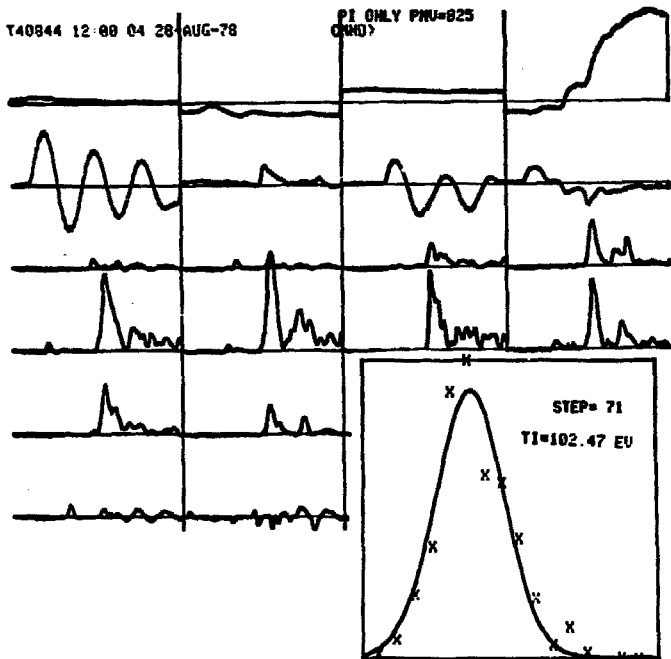


FIGURE 2.16 4686 LIGHT DURING PREIONIZATION.

During preionization, a burst of 4686 light appears, with a substantial width.

2.4 Thomson Scattering

Particle density and velocity distribution functions may be measured from the spectrum of light scattered from an intense pulse of ruby laser light.⁹ On Tormac IV-c, relative density and electron temperature measurements are made from light scattered at 90°. The formula for the scattering intensity spectrum is¹⁰

$$I(\lambda) = e^{-\left(\frac{\lambda - \lambda_0}{19.46}\right)^2} \frac{1}{T_e}$$

if one assumes cooperative effects are unimportant. Here λ is the observed wavelength in angstroms, λ_0 is the incident wavelength, and θ is the scattering angle.

The scattering apparatus is shown in Figure 2.18 and in the floor plan, Figure 3.6. The incident beam can be moved to any of 3 input ports, spaced radially at 11.4, 15.2 and 18.4 cm. A special triple grating 7 channel polychromator was designed by W.I.S. Smith and Martin Greenwald for use on this experiment and on Tormac V.¹¹ Figure 2.19 shows the relative amplitude of different channels as a function of T_e . The central temperature the polychromator was designed for is 300 eV: at the low temperatures in Tormac IV-c no scattering at all is detected in channels 3-7. Typical scope traces for channels 1 and 2 are shown in Figure 2.20. The second channel is more sensitive; the relative calibration is 1.5:1. The calibrated ratio of these two channels gives

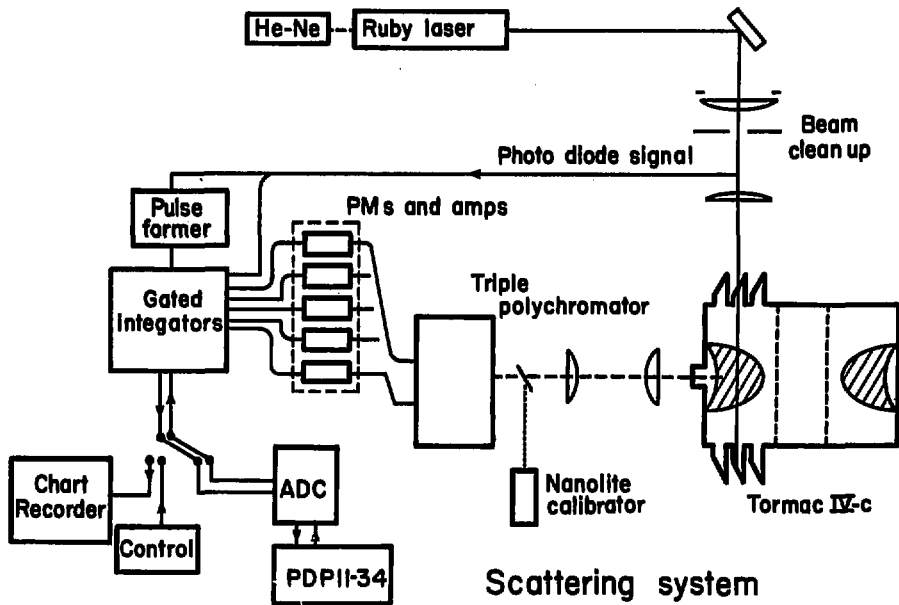


FIGURE 2.18

XBL 789-2208

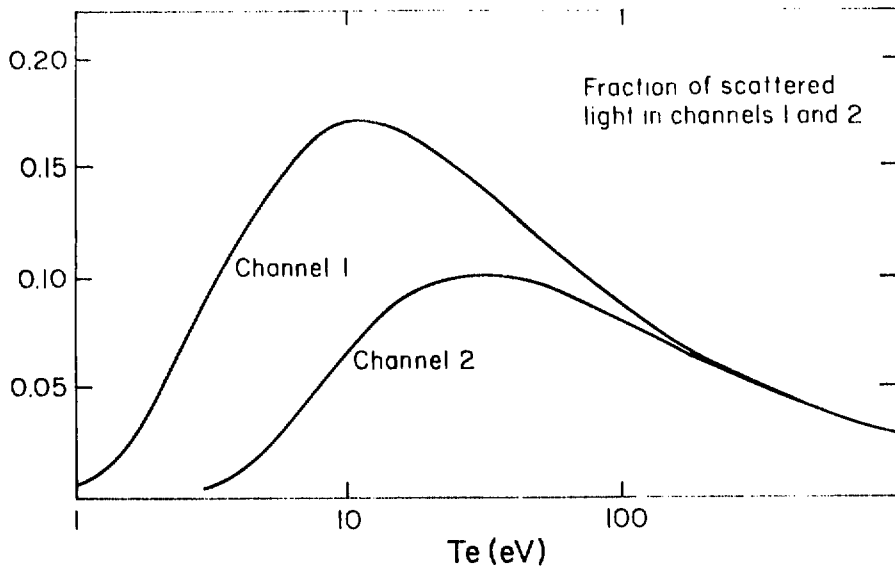
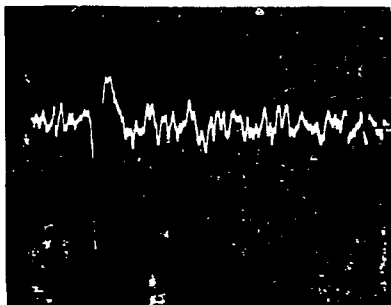


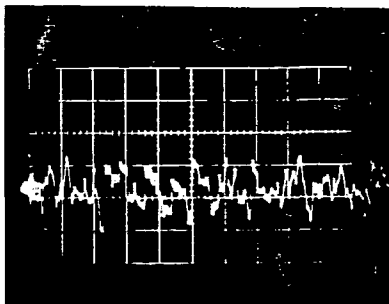
FIGURE 2.19

FRACTION OF SCATTERED LIGHT WITHIN THE SPECTRAL RANGE OF POLYCHROMATOR CHANNELS 1 AND 2 PLOTTED VS ELECTRON TEMPERATURE. FOR TEMPERATURES LESS THAN 10 eV, SCATTERING INTO CHANNELS 3 AND ABOVE IS INSIGNIFICANT.

XBL 789-2214



CHANNEL 1
VERTICAL 10 mV/cm
HORIZONTAL 200 nsec/cm
SENSITIVITY 44



CHANNEL 2
VERTICAL 50 mV/cm
HORIZONTAL 200 nsec/cm
SENSITIVITY 340

Typical Thomson Scattering Data, taken at the peak of the cusp field. The scattering signal is seen a little more than 2 cm from the start of the trace. When corrected for photomultiplier sensitivity, the ratio of channel 1 to 2 is 5.6 implying an electron temperature of 5.5 eV.

FIGURE 2.20 TYPICAL SCATTERING WAVEFORMS.

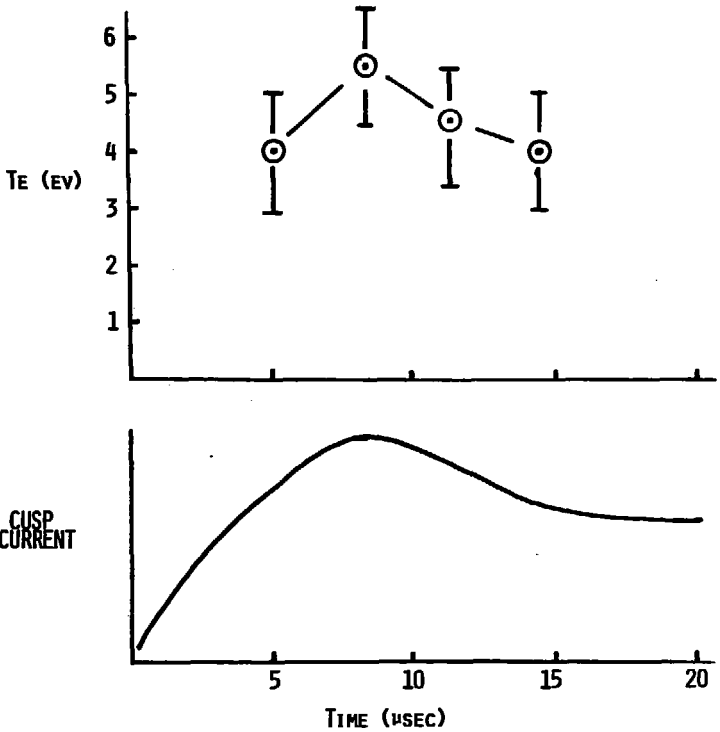
T_e . Scattering in channel 2 is limited to $T_e > 4$ eV, and only appears at times near the cusp peak. A short curve for T_e versus time is given in Figure 2.21.

This value of T_e was found to be independent of fill pressure. The intensity increased with fill pressure from 17 to 51 microns and then remained flat through 100 microns. This corresponds to the ionization limit with fill pressure observed in interferometry. T_e also was independent of the fraction of helium, and did not go up as the cusp bank voltage was increased from 15 to 17 kV.

2.5 Magnetic Measurements

Figure 2.22 is a map of the magnetic probes. An important consideration in a pulsed experiment is the fraction of capacitor bank energy which makes it into field energy, as there are substantial losses. All the probes used are simple coils inductively coupled to the field. A Rogowski coil is a simple solenoid wrapped into a torus around a conductor. By Ampere's law, it gives a measure of current in the conductor independent of its position.

The table below summarizes the measurements of the device currents.



ELECTRON TEMPERATURE vs TIME

FIGURE 2.21

XBL 789-10851

	BIAS	PREIONIZER	CUSP	HEATER
Bank voltage	2kV	30kV	15kV	40kV
Bank capacitance	375 μ F	2 μ F	112 μ F	.9 μ F
Bank energy	750J	900J	12.6J	720J
Ringing f	-	125khz	30khz	500khz
1/4 period rise	160 μ sec	2 μ sec	8.3 μ sec	.5 μ sec
decay τ	>1msec	30 μ sec	80 μ sec	10 μ sec
B, plasma center	300G	800G	3.5kG	700G

Figure 2.23 shows typical waveforms for each signal.

Figure 2.24 shows measurements of the plasma toroidal current. The oscillating waveform is the current induced by the pre-ionizer. Notice that the oscillation is not symmetric. This may be due to turbulence in the pre-ionized plasma, which appears in plasma probe signals, or to the fact that each succeeding half-cycle is more fully excluded than the last.

When the cusp goes on, it appears to drive a net current. However, the vacuum trace shows a similar offset. When this is subtracted it leaves a 5 μ sec pulse at 10 kA, and a long term net current <2 kA, compared to the peak current of 40 kA.

2.5.1 Flux exclusion

If a high- β plasma exists over a region of the vessel, it is reasonable to expect one could measure that by a measurement of the diamagnetically excluded toroidal flux.¹² This is done by a single turn loop about the plasma vessel

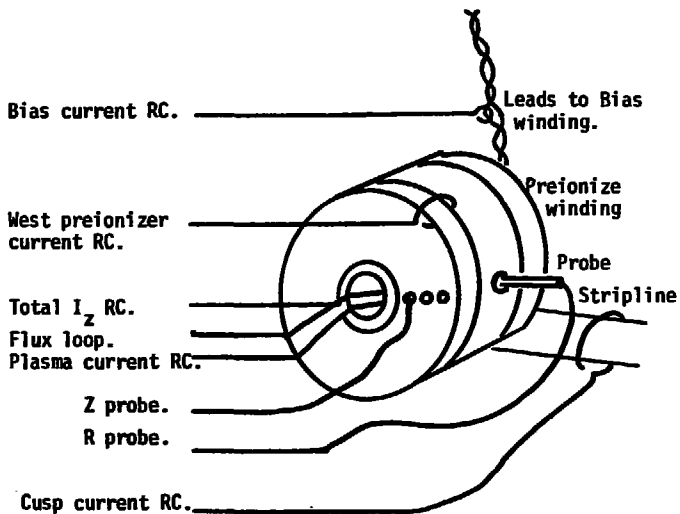
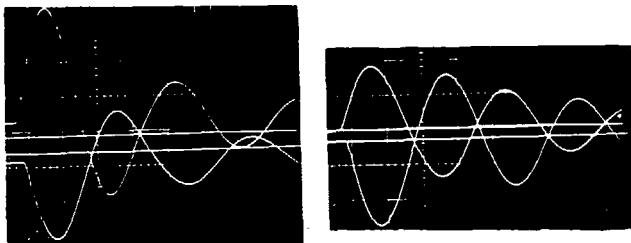
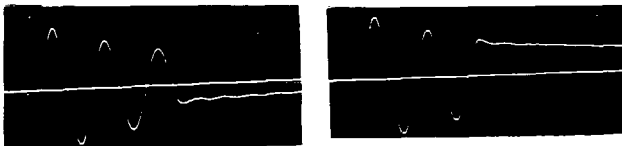


FIGURE 2.22 LOCATION OF MAGNETIC PROBES.

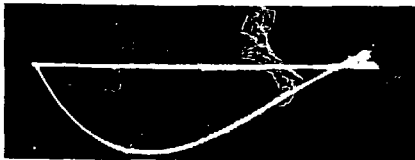
XBL 789-11350



Cusp waveform allowed to ring (no crowbar) to measure damping. Photo on left is with the bias, and shows much more damping than the photo on the right with the bias disconnected. Each photo show the Rogowski coil and flux loop. Upper left trace has gain turned up.



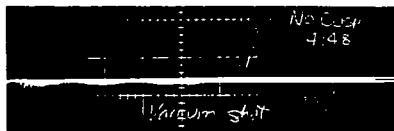
Pre-ionize waveform, with crowbar triggered at delay to demonstrate both polarities.



Bias current, shown from the flux loop signal.

XBB 789-12550

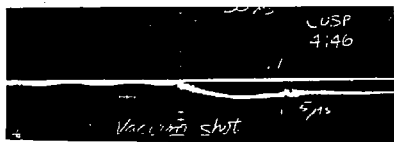
FIGURE 2.23 CURRENT WAVEFORMS.



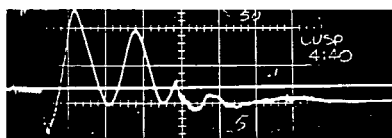
VACUUM SHOT
NO CUSP CURRENT



PLASMA SHOT
36 mTORR GAS FILL
NO CUSP CURRENT



VACUUM SHOT
WITH CUSP CURRENT



PLASMA SHOT
36 mTORR GAS FILL
WITH CUSP CURRENT

FIGURE 2.24

PLASMA CURRENT WAVEFORMS, 23 kAMPS/DIV

CUSP BANK = 15 kV PREIONIZE BANK = 30 kV

cross-section (flux loop), and a Rogowski coil to monitor the total current I_z giving rise to the field. I_z would also change as the plasma would modify the inductance of the total system.

For a total current I_z , the vacuum total of flux is

$$\psi_v = \int_{\text{vessel}} \vec{B} \cdot d\vec{A} =$$

$$\text{Defining a toroidal, } \beta_T, \beta_T = 1 - \frac{B_T(\text{inside})}{B_T(\text{outside})}$$

and a plasma cross section, gives the excluded flux.

Ampere's law shows that the toroidal field anywhere outside the plasma must be simple $B_T = \frac{I_z}{5R}$

(B in gauss; I_z in amps; R in cm)

Figure 2.25 is an example of the flux loop and Rogowski coil waveforms with and without the plasma. The fraction of excluded flux is

$$A = 1 - \frac{\psi_{\text{plasma}}/I_{z,\text{plasma}}}{\psi_{\text{vac}}/I_{z,\text{vac}}}$$

This fraction is small and, when measured, yields about 3% at all times except during the first onset of compression.

In order to improve this measurement, a subtraction circuit was used so that the fraction is approximated by

$$A = \frac{\psi_{\text{plasma}} - I_{z,\text{plasma}} \left(\frac{\psi_{\text{vacuum}}}{I_{z,\text{vacuum}}} \right)}{\psi_{\text{plasma}}}$$

The vacuum fraction is simply a gain adjustment on the

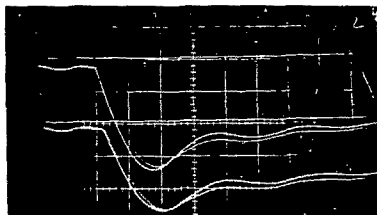
subtraction circuit so the signal nulls out on a vacuum shot, and A is read directly on the trace (Figure 2.26).

If one assumes simple flux exclusion, these numbers are consistent with our temperature and density if the plasma radius is 3.3 cm. However, this measurement can be foiled by force free currents in the plasma, in that the fraction of toroidal and poloidal fields in the vessel is not constant between vacuum and plasma shots. Thus a calculation based on these two measurements does not properly account effects of the cold background plasma.

2.5.2 Small probes: description

Two probes, each containing two coils, were wound on Q-tip sticks and sheathed by a 4 mm diameter quartz tube (Figure 2.27). These could slide into the vessel through compression fittings to make local measurements of the toroidal and poloidal magnetic fields: B_t and B_z . The compression fittings were used on two of the Thomson scattering ports. The R probe moved radially through the viewing port, down the center line of the plasma. The Z probe moved through the innermost laser port.

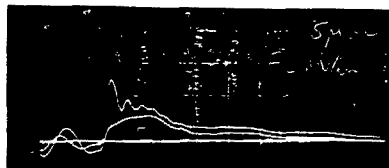
The Z probe moves parallel to one field component. Hence one coil is a solenoid of 45 turns of #37 wire, 2.5 mm diameter, 7 mm long. The B_t coil and both coils on the R probe are wound of 15 turns of #37 wire, threaded through tiny holes drilled into the wooden support, 7 mm apart. On



FL FLUX LOOP SIGNAL
VERTICAL .5V/DIV

RC ROGOWSKI COIL
VERTICAL 1V/DIV
HORIZONTAL 5 USEC/DIV

FIGURE 2.25



SUBTRACTION CIRCUIT

$$Y = FL - \frac{FL_0}{RC_0} RC$$

VERTICAL .1V/DIV
HORIZONTAL 5 USEC/DIV

FIGURE 2.26

FLUX EXCLUSION MEASUREMENTS.

BRIGHT TRACE -- VACUUM SHOT

WEAK TRACE -- PLASMA SHOT, 45 MICRON FILL

15 kV CUSP BANK

1 MSEC INTEGRATOR ON EACH SIGNAL

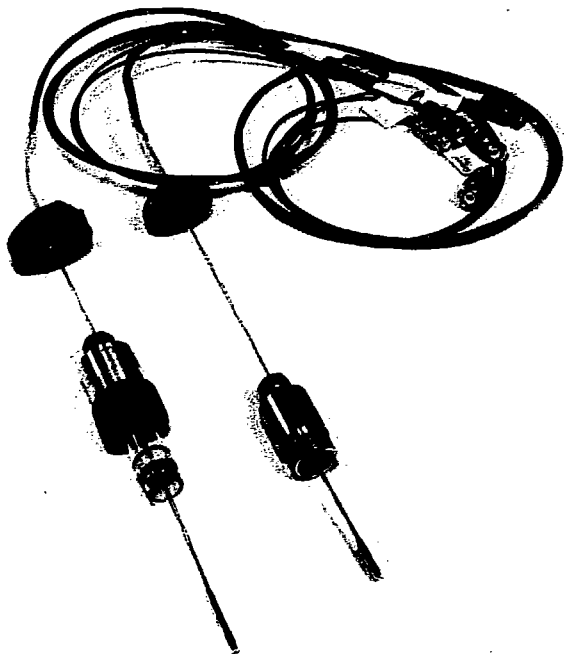


FIGURE 2.27 SMALL PROBES.

XBB 789-12492

Small magnetic probes are wound on 2.5 mm forms and held inside 4 mm quartz tubes. The probes are pushed through compression fittings on the Thomson scattering ports.

the R probe the coil centers are 1 cm apart.

The leads of each coil form a twisted pair, which carries the signal through the 12 inch long quartz tube to the miniature 50 Ω RS196 cables. A third dummy twisted pair is included in the probe and is just shorted at the end. This measures any electrostatic pickup or magnetic signal in the leads.

The probes were absolutely calibrated against a large probe of well-known dimensions. The calibrator consists of a 6 inch wide shorted stripline which rings down a capacitor when a mechanical switch is dropped. The probe is inserted between the stripline plates where the field is very uniform.

The signal induced in the probe measures dB/dt, which is converted to a signal proportional to B by a passive RC integration circuit. The resulting signal is too small to be recorded by the computer data acquisition system, so Poloroid photographs of scope traces are used. Each integrator and scope channel are calibrated using a standard square pulse.

The stripline calibrator is designed to have a risetime close to that of the device to avoid problems of frequency response. Its field is much lower than the device. Hence the calibration signals were not integrated. Since the waveforms are identical for the signals from the probes and the standard, the amplitudes of any given peak can be compared. The response is given as the area NA in cm².

Standard probe	14.2
R probe, B_T	2.54
B_z	2.20
Z probe, B_T	2.28
B_z	2.25

2.5.3 Small probe data

Magnetic probes are often inappropriate for high density plasmas¹³ due to boil-off from the probe surface and perturbations to the local current distribution. Lovberg has tabulated this information, and for our plasma a quartz probe should be good for 100 μ sec.

Probe measurements were made at 1 cm intervals with and without plasma, and with and without the extra conducting rings. Data has been measured from the photographs with a ruler and magnifying graticule and reduced by hand.

Figure 2.28 shows typical probe waveforms taken without plasma. They were taken at a position where the poloidal field is less than half its maximum to point out the effect of the pre-ionize field on the total poloidal field. Figure 2.29 shows the measured vacuum field radial and lateral profiles and compares them with the theoretical fields from computer calculations.

With the plasma there are three distinct regions: inside, outside, and in the boundary of the compressed plasma. Typical waveforms, superimposed with the vacuum waveforms, are shown in Figure 2.30 a, b, and c. These were taken at a fast time

scale as the interesting behavior (fluctuations, exclusion from the plasma) occurs only for the few microseconds during and immediately after the cusp rise.

Figure 2.30 a, deepest into the plasma, shows the toroidal field delayed for 2 μ sec, a time consistent with Alfvén propagation, followed by low amplitude oscillations. The poloidal field also shows some oscillations but is excluded for 7 μ sec.

Figure 2.30 b in the boundary shows violent oscillations in both toroidal and poloidal fields. An important aspect of these oscillations is that they are repeatable from shot-to-shot, and they appear in phase throughout the plasma. They do vary with fill pressure (Figure 2.31), and slow down as the cusp current rises.

Figure 2.30 c, outside the plasma, shows poloidal field enhancement outside the plasma in r, while no such enhancement in z. The toroidal field shows a brief delay in r and then rapid convergence to the vacuum value.

This enhanced poloidal field is not due to a high- β effect, i.e. exclusion and compression of field lines. The presence of the plasma modifies the timing and coupling between the cusp current and the crowbarred pre-ionize current. The result is a larger current in the pre-ionize coils and a larger poloidal field.

Figure 2.32 shows radial and lateral profiles of the vacuum and plasma fields at a) 1 μ sec into compression

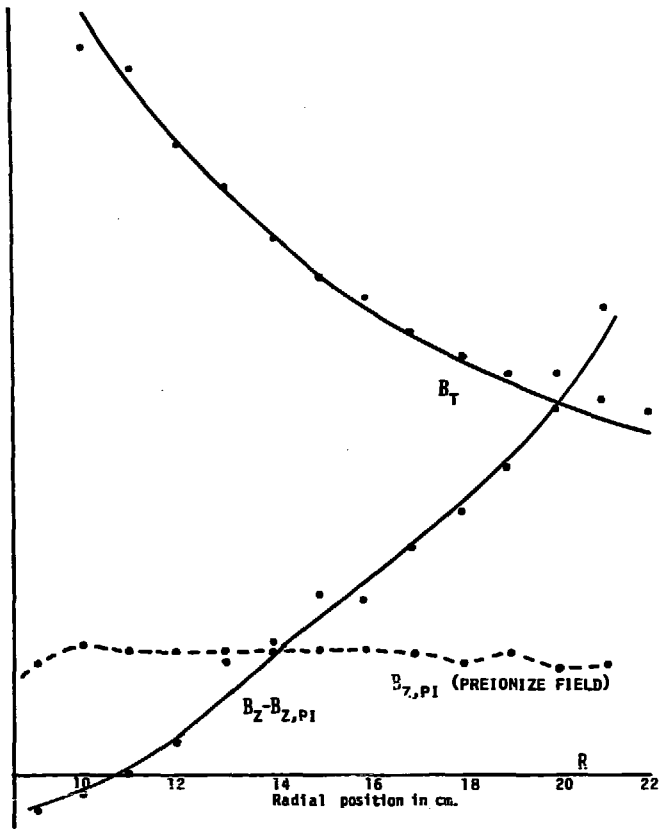
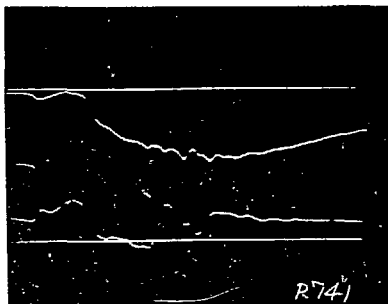


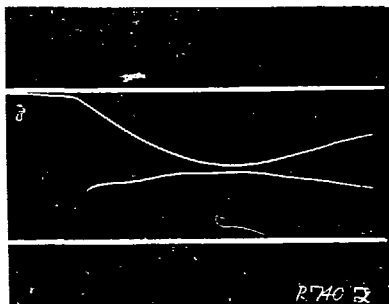
FIGURE 2.29 VACUUM MAGNETIC FIELD RADIAL PROFILE.



PLASMA SHOT
36 MICRON GAS FILL

B_T 1935 GAUSS/DIV

B_Z 433 GAUSS/DIV

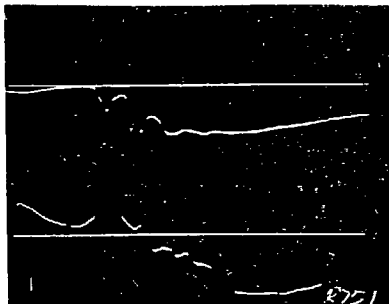


VACUUM SHOT

B_T 1935 GAUSS/DIV

B_Z 433 GAUSS/DIV

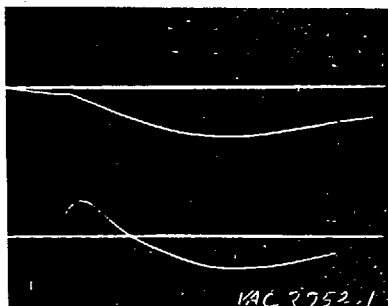
FIGURE 2.30A
SMALL PROBE WAVEFORMS, NEAR INNER WALL
 $R = 10$ CM. $Z = 0$ CM.
CUSP BANK = 15 KV
HORIZONTAL 2 USEC/DIV



PLASMA SHOT
36 MICRON GAS FILL

B_T 1935 GAUSS/DIV

B_Z 433 GAUSS/DIV



VACUUM SHOT

B_T 1935 GAUSS/DIV

B_Z 433 GAUSS/DIV

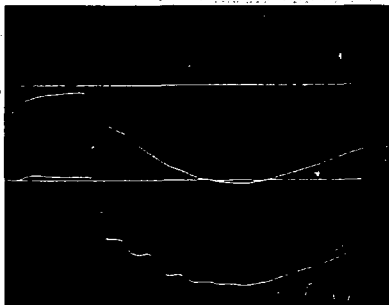
FIGURE 2.30B

SMALL PROBE WAVEFORMS, NEAR CENTER

$R = 15$ CM. $Z = 0$ CM.

CUSP BANK = 15 kV

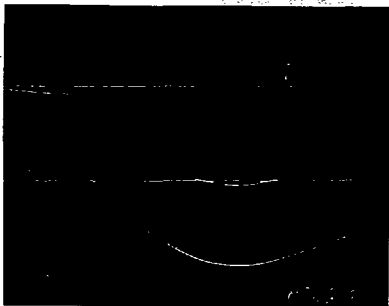
HORIZONTAL 2 USEC/DIV



PLASMA SHOT
36 MICRON GAS FILL

B_T 774 GAUSS/DIV

B_Z 866 GAUSS/DIV



VACUUM SHOT

B_T 774 GAUSS/DIV

B_Z 866 GAUSS/DIV

FIGURE 2.30c

SMALL PROBE WAVEFORMS, NEAR OUTER WALL

$R = 20$ CM. $Z = 0$ CM.

CUSP BANK = 15 kV

HORIZONTAL 2 USEC/DIV

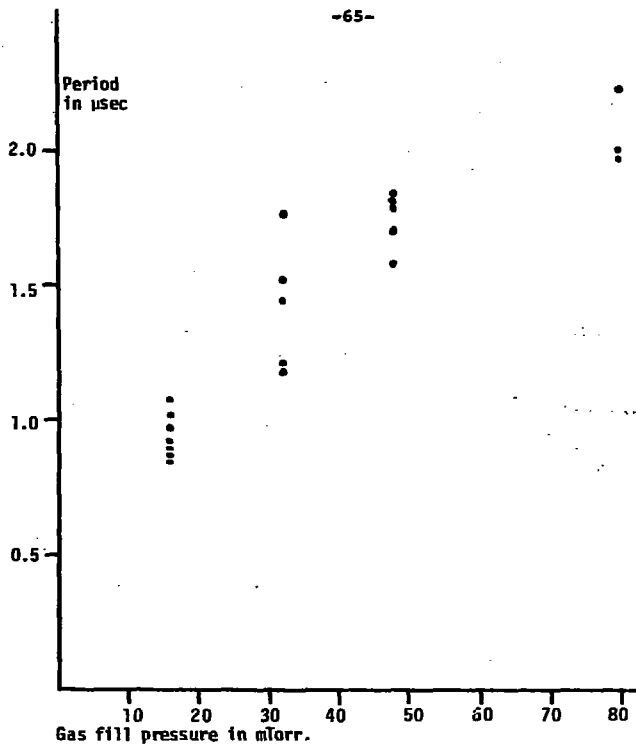


FIGURE 2.31 FIELD OSCILLATION PERIOD VS.
GAS FILL PRESSURE.

The separation between the different peaks in the toroidal field small probe waveform are measured as a function of the initial gas filling pressure.

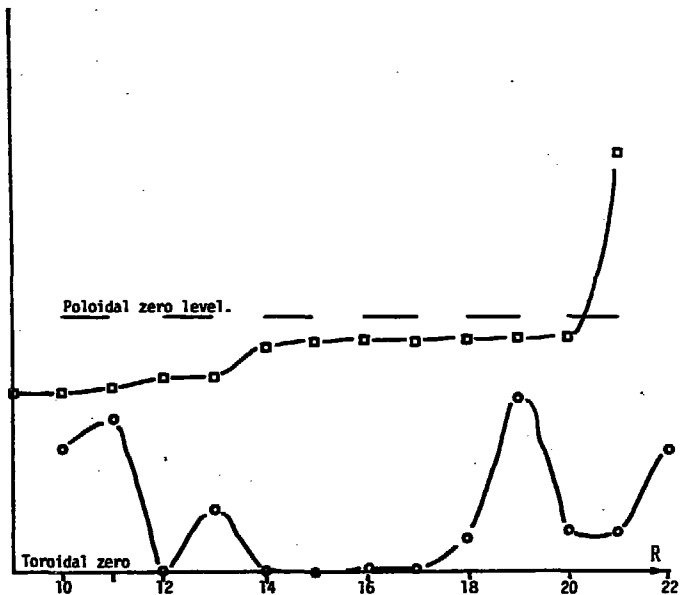


FIGURE 2.32A RADIAL FIELD PROFILES.

Small probe data of B_z (squares) and B_t (circles) measured 1 μ sec into the compression.

XBL 789-11340

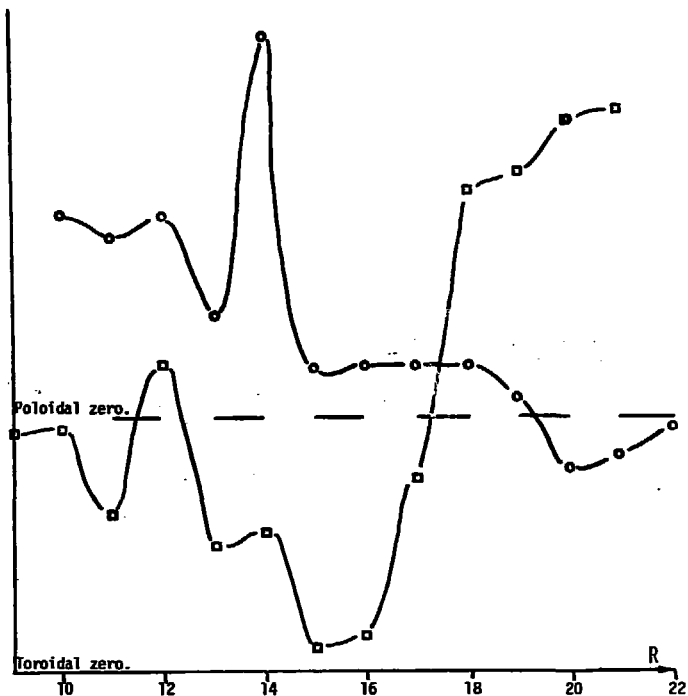


FIGURE 2.32B RADIAL FIELD PROFILES.

Small probe data of B_z (squares) and B_t (circles) measured at the peak of the first oscillation, about 5 μ sec into the compression.

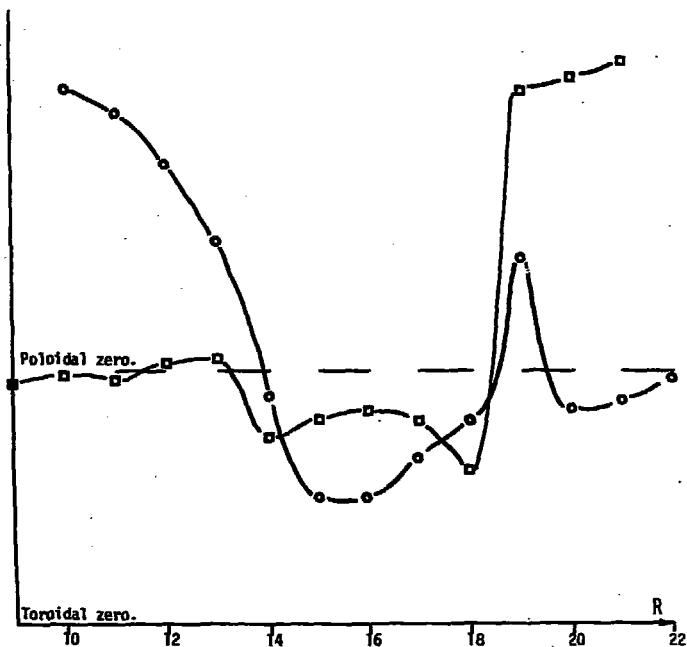


FIGURE 2.32c RADIAL FIELD PROFILES.

Small probe data of B_z (squares) and B_t (circles) measured at the valley after the first oscillation, about 6 μsec into the compression.

XBL 789-11338

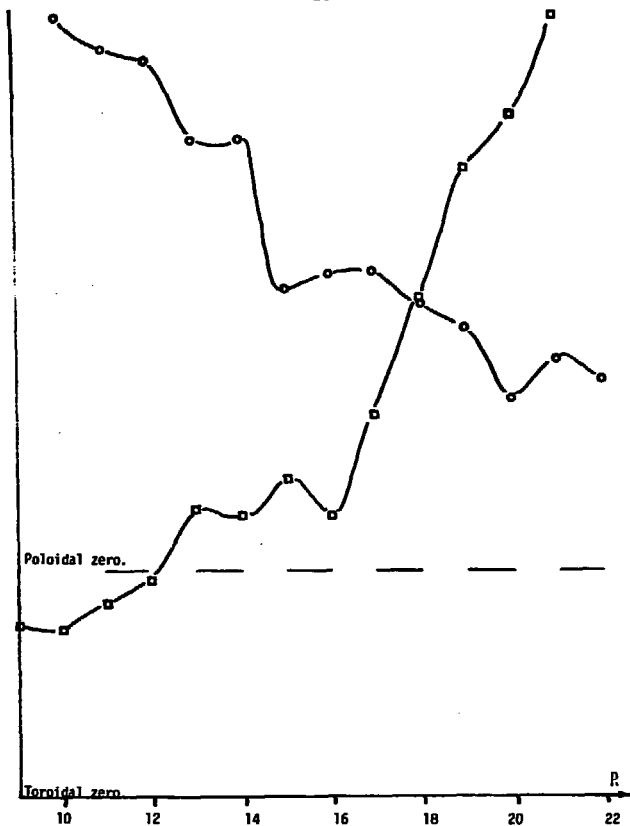


FIGURE 2.32d RADIAL FIELD PROFILES.

Small probe data of B_z (squares) and B_t (circles) measured at the peak of the cusp current.

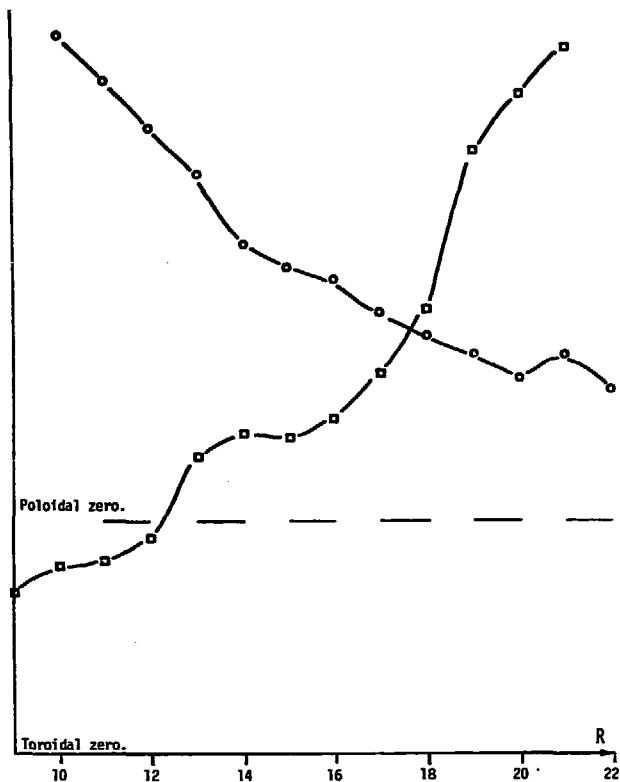


FIGURE 2.32E RADIAL FIELD PROFILES.

Small probe data of B_z (squares) and B_t (circles measured at 4 μ sec after the peak of compression.

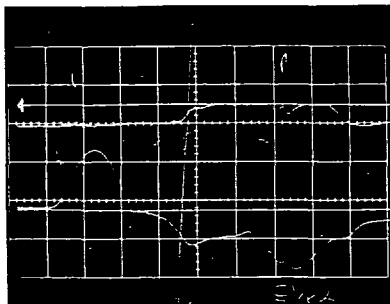
(during exclusion of toroidal field) b) peak of the first oscillation c) valley of first oscillation, d) peak of cusp current, and e) 4 μ sec later.

All of these data support the picture observed in the spectral and interferometer data: that the plasma is compressed into the inner wall (small values of R) by the poloidal field. The toroidal field does not push the plasma or penetrate diffusively, but penetrates abruptly, accompanied by large fluctuations.

Probe data were also taken during pre-ionization. Figure 2.33 shows some waveforms. There is strong exclusion after the first half cycle, and some fluctuations. The appearance of a burst of toroidal field correlated with the one big fluctuation indicating an Alfvén sort of field line oscillation.

I suspected the disturbance might be an Alfvén instability driven by pressure anisotropy, as the equilibration time is not much shorter than the observed period. The ion collision time, however, is shorter than the gyro period, implying that the ions are not strongly coupled to the field.

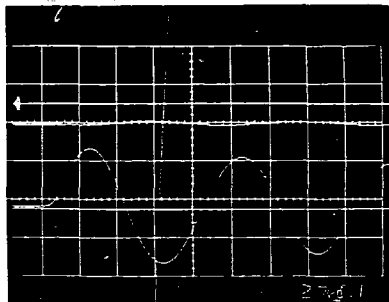
This regime is well-suited to the simulation mentioned in Section 1.6. The Hamasaki code considers fluid electrons and particle ions, and can consider different angles between the bias and compression field. Large amplitude magneto-sonic waves appeared in these simulations, even though the backwards differencing scheme used is expected to err in the direction of over-damping such disturbances.



PLASMA SHOT
36 MICRON GAS FILL

B_T 506 GAUSS/DIV

B_Z 554 GAUSS/DIV



VACUUM SHOT

B_T 506 GAUSS/DIV

B_Z 554 GAUSS/DIV

FIGURE 2.33

SMALL PROBE WAVEFORMS, DURING PREIONIZATION

$R = 11.4$ CM. $Z = 2.2$ CM.

CUSP BANK = 15 KV

HORIZONTAL 2 USEC/DIV

2.6 Interferometer Measurements

We used a Michaelson interferometer to measure the line integral of electron density at different radii. An interferometer measures the phase shift in electromagnetic radiation (microwave or laser) caused by the index of refraction of the plasma.

For a laser in which $\omega > \omega_p, \omega_c$, the index of refraction of a magnetized plasma is essentially that of an unmagnetized one:

$$[2.7] \quad N^2 - 1 - \frac{\omega_p^2}{\omega^2} = 1 - \frac{4\pi e^2 n_e}{\omega^2 m_e}$$

The phase shift along the beam path is

$$[2.8] \quad \Delta\phi = \int_{\text{vac}} k dx - \int_{\text{plasma}} k dx = \int k(1-N) dx \\ = \int k \frac{(1-N^2)}{2} dx = k_{\text{vac}} \frac{4\pi e^2}{m_e 2\omega^2} \int n_e dl$$

Our interferometer uses a 4 mw He-Ne laser with a 6328 angstrom line giving $\omega = 3 \times 10^{15}$. This gives

$$[2.9] \quad \int n_e dl = 6 \times 10^{16} \Delta\phi_{\text{radians}} = 10^{15} \Delta\phi_{\text{degrees}}$$

In practice the beam passes through the plasma twice. Hence this must be divided by two.

2.6.1 Description and access

Our interferometer was designed and built for Tormac IV-a by Booth Myers and rebuilt by Ben Feinberg.¹⁴ It is constructed on a single, rigid C-shaped frame made of G-10

4-11-58

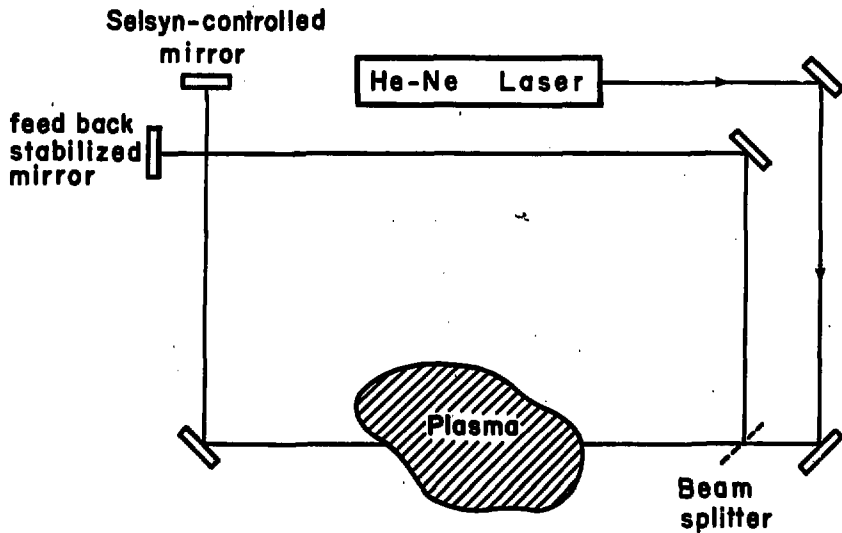
fiberglass channel which hangs over the vessel suspended by two springs. The entire system can be raised and lowered by two vertical, adjustable shop supports. Figure 2.34 diagrams the apparatus and Figure 2.35 shows it in place.

The internal optics are set up to have the plasma and reference lengths equal. The beams are split and rejoin at a prism beamsplitter. The interfering spot passes through a filter to reject plasma light, then is focused by a lens onto a light fiber bundle. The light fibers carry the signal outside the cage to a photodiode mounted in the electronics package.

A key feature of this interferometer is that it is stabilized against mechanical vibrations by a closed servo loop. The photodiode output is amplified and sent to a transducer which adjusts the mirror on the reference beam. When the loop is closed the interferometer is locked to an intermediate phase. (Fringes vary the output from +1.5 to -1.5 volts. The feedback loops stops it at 0 volts.) The servo response time is the order of 1 msec, so it does not cancel any shift occurring at the plasma time scale.

The beam shines through the vessel, along z, through holes in the winding support, and through the glass end plates to the vessel.

The reinforcing winding end plates have 12, 1/4 inch access holes, equally spaced at different radii spaced 1 cm. apart. A set of interferometer data means moving the

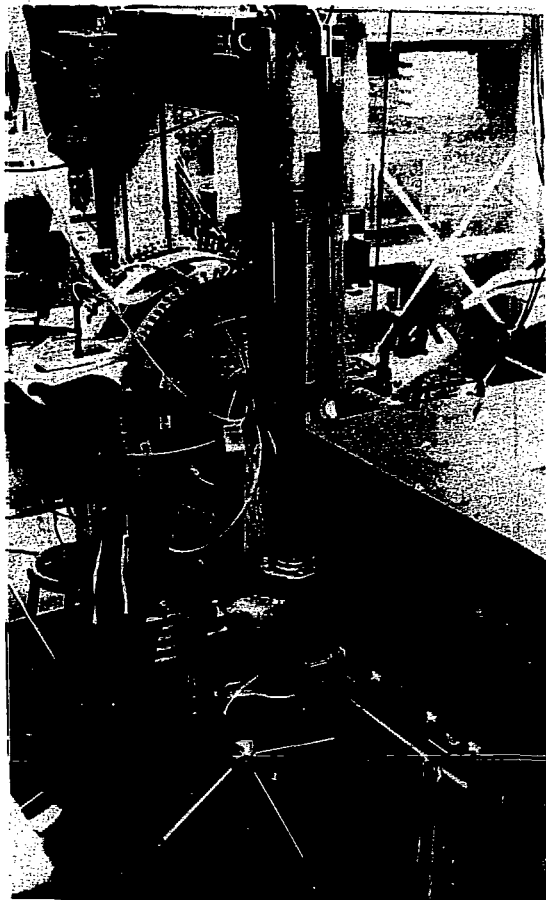


-75-

He-Ne Interferometer

FIGURE 2.34

XBL 789-2207



XBB 789-12552

FIGURE 2.35 INTERFEROMETER IN POSITION.

The He-Ne laser interferometer is suspended between two floor stands. The 12 holes for the laser beam are visible on the winding endplate. The large box, center right, is the Thomson scattering input optics. The selsyns are visible, upper left.

interferometer from hole to hole; the 12 holes are in 2 straight vertical lines (Figure 2.35) so that most of the motion is done by lowering the supports.

At each hole shots are taken at three different fill pressures with and without the cusp so that the pre-ionized plasma can be studied.

2.6.2 Alignment and calibration procedure

The laser and beamsplitter are fastened firmly to the fiberglass frame while all the mirrors are adjustable. Alignment is not only critical where the beams interfere. There are a number of other constraints. I found that adjusting it in the following order worked.

1) Adjust the first two mirrors so that the beam hits the splitter square in the center.

2) Adjust the selsyn-controlled mirror on the "plasma" path beam so that it returns exactly on itself, by letting it pass through a hole in a white card. This is necessary to have the beam pass through the 1/4" access holes in the winding.

3) Adjust the reference beam mirror so the beam hits the small feedback mirror in the center.

4) Adjust the micrometer screws on the feedback mirror so that the beams interfere. This can be viewed by removing the light pipe assembly or by setting a slip of paper between it and the exit hole. Continue adjusting the reference beam

until a single, centered fringe is found. Do not do this by adjusting the selsyns.

The electronics are adjusted by allowing the interferometer to vibrate; this is done by activating the selsyn motors. The output amplifier is adjusted to provide 3 V peak to peak, centered about 0 V. The selsyns are then released. The feedback stabilization is engaged and adjusted to flatten the output.

Frequency response is checked by removing the interferometer light pipe, and pulsing the photodiode with square wave signals from an LED.

2.6.3 Analysis technique

At the Tormac IV densities many of the recorded phase shifts exceed 90° , which means the analysis of the data must determine whether and where the signal is going above and falling below 90° . This was done in a semiautomated way by a series of programs:

GIDNEY removes the interferometer data from a sequence of data shots, storing them in an intermediate file.

UNCLOYD unfolds all the data assuming shifts are always $< 90^\circ$.

CLOYD is interactive for shifts $> 90^\circ$. It makes a guess as to where to locate the left and right limits for the waveform representing $\Delta\phi > 90^\circ$, then asks the user whether it should keep guessing.

BORIS plots all the raw or unfolded shots corresponding to one profile.

ROCKY displays radial profiles at given times, and integrates the profile to give total ionization vs time.

2.6.4 Radial density profiles

Several hundred traces were analyzed. Data for the radial profiles was taken for:

2	configurations (with and without conducting hoops)
x 12	access hole locations
x 3	gas fill levels
x 3	shots, 2 with the cusp, 1 with only the preionizer
<u>216</u>	total shots and extras

Figures 2.36 a, b show the 12 raw and unfolded shots for one radial profile. Figures 2.37 a-f, 2.38 a-o show the final output for the configuration without hoops. The data with the hoops to more closely emulate Tormac IV-a) was nearly identical.

The final radial profiles allow the calculation of diffusion rates and recombination rates. These are plotted in Figure 2.39 and compared with the theoretical classical values.

2.7 Overall Particle Accounting

The inside dimensions of the glass vessel are

$R_1 = 8.3$ cm, $R_2 = 22.2$ cm, $L = 24.3$ giving a total volume

$$[2.10] \quad V = \pi(R_2^2 - R_1^2)L = 3.2 \times 10^4 \text{ cm}^3$$

FILE=INTF 0GAS & CASE?3.2

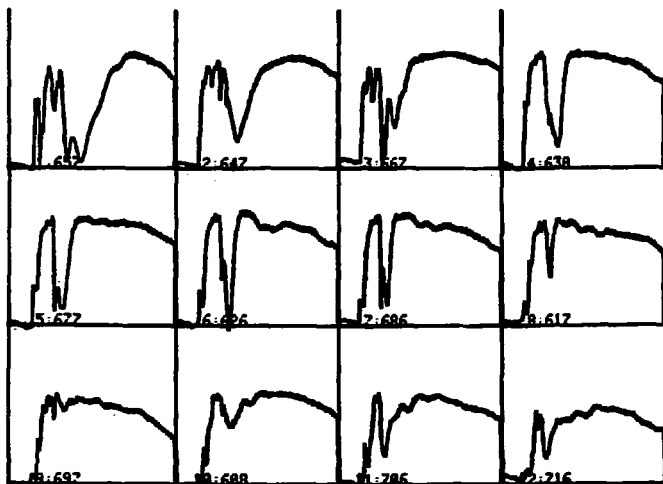


FIGURE 2.36A RAW INTERFEROMETER DATA FOR ONE CASE.

Interferometer waveforms at 12 positions. Radius increases from left to right, then top to bottom. Data was taken with cusp=15kV and gas fill=36 mTorr.

XBL 789-11335

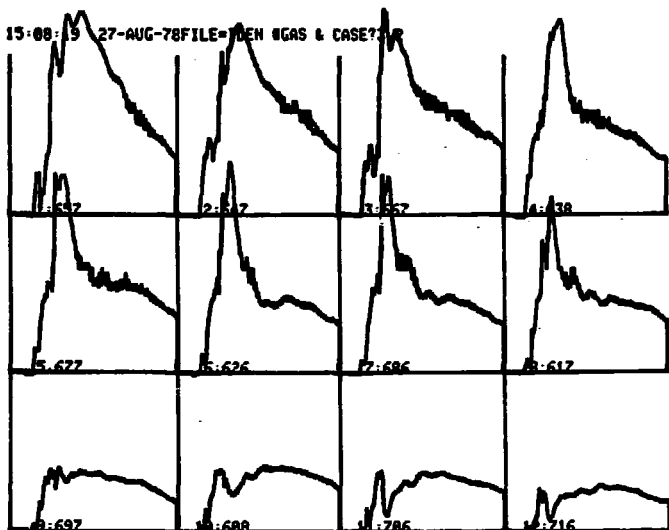
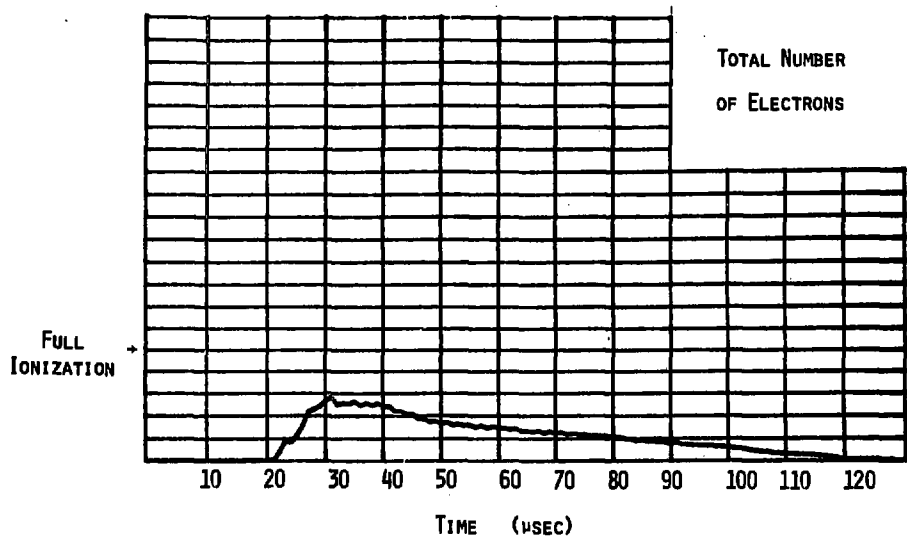


FIGURE 2.36B UNFOLDED INTERFEROMETER DATA FOR ONE CASE.

The raw waveforms from 2.36a have been unfolded by the computer to show electron line density. Interactive programs are used to determine where in the waveform the phase shift exceeds 90 degrees.

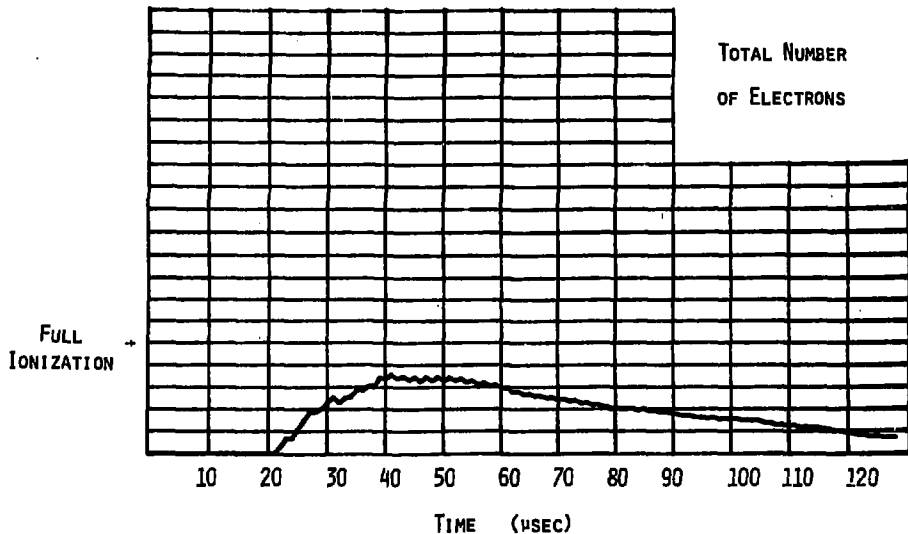
XB1 789-11334



TOTAL IONIZATION VS TIME. LEVEL OF FULL IONIZATION IS INDICATED. FILL PRESSURE WAS 12 MTORR. NO CUSP FIELDS WERE APPLIED.

FIGURE 2.37A

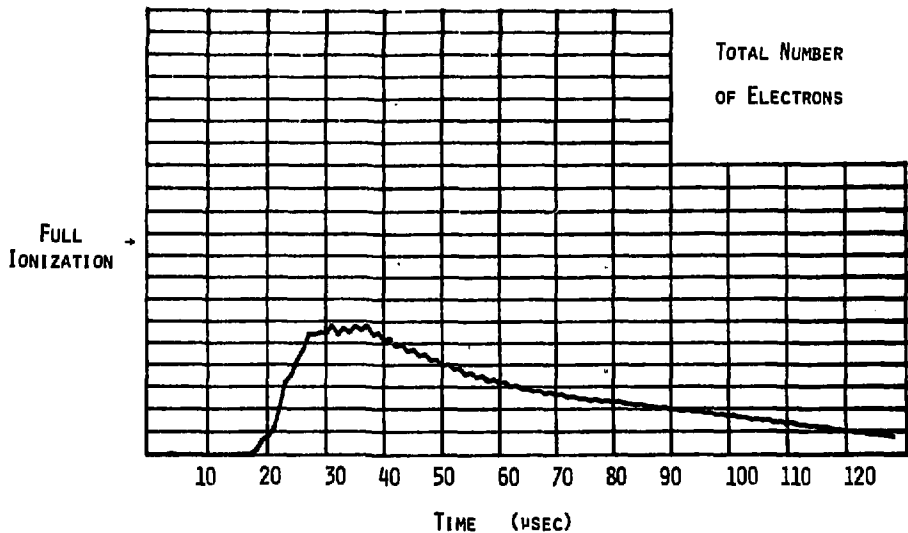
XBL 789-10877



TOTAL IONIZATION VS TIME. LEVEL OF FULL IONIZATION IS INDICATED.
 FILL PRESSURE WAS 12 MTORR.

FIGURE 2.37B

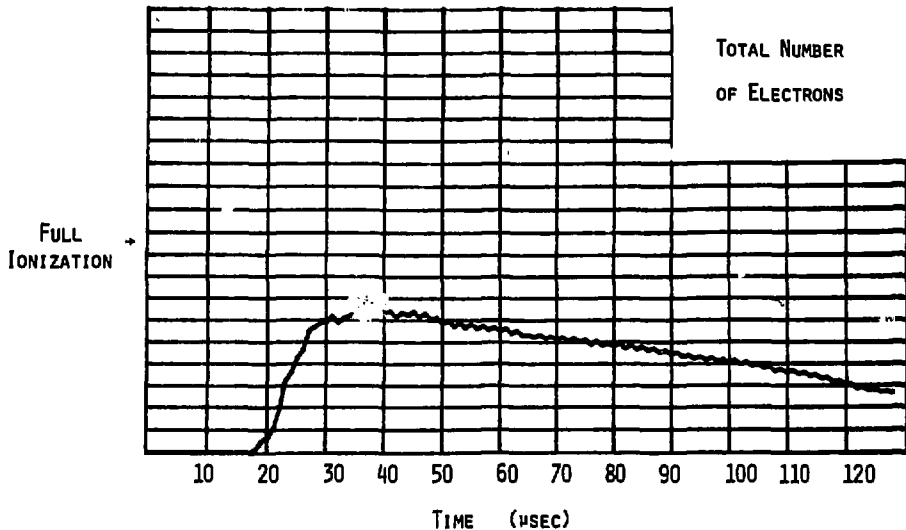
XBL 789-10878



TOTAL IONIZATION VS TIME. LEVEL OF FULL IONIZATION IS INDICATED. FILL PRESSURE WAS 24 MTORR. NO CUSP FIELDS WERE APPLIED.

FIGURE 2.37c

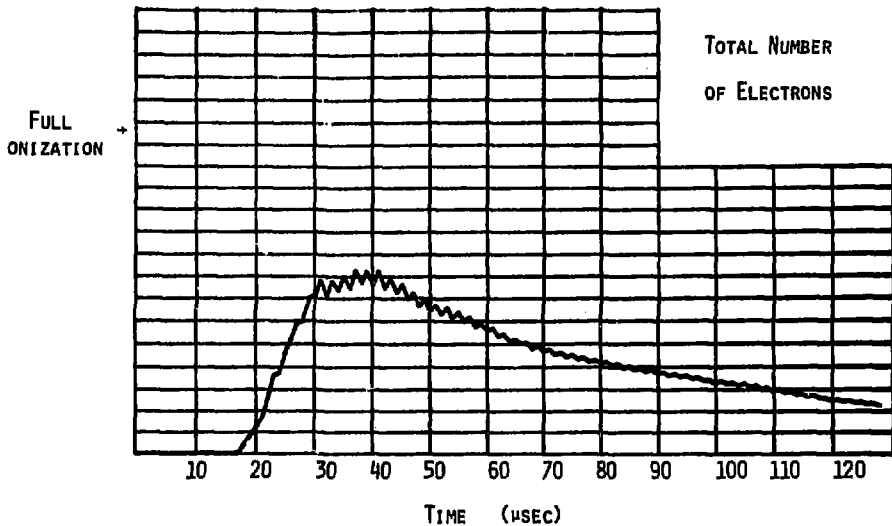
XBL 789-10879



TOTAL IONIZATION VS TIME. LEVEL OF FULL IONIZATION IS INDICATED.
 FILL PRESSURE WAS 24 mTORR.

FIGURE 2,37D

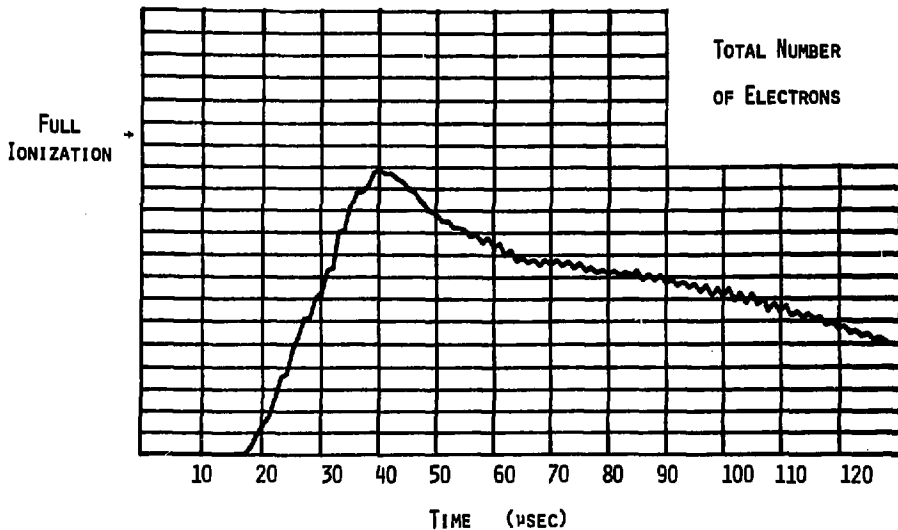
.XBL 789-10875



TOTAL IONIZATION VS TIME. LEVEL OF FULL IONIZATION IS INDICATED.
 FILL PRESSURE WAS 36 MTORR. NO CUSP FIELDS WERE APPLIED.

FIGURE 2.37E

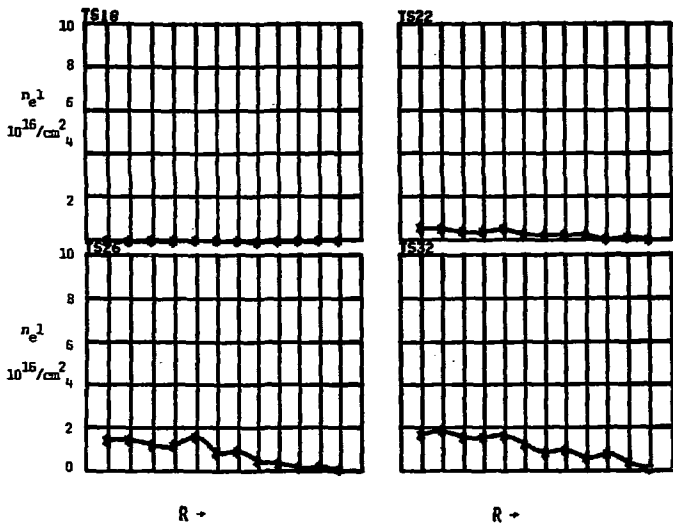
XBL 789-10880



TOTAL IONIZATION VS TIME. LEVEL OF FULL IONIZATION IS INDICATED.
 FILL PRESSURE WAS 36 MTORR.

FIGURE 2.37F

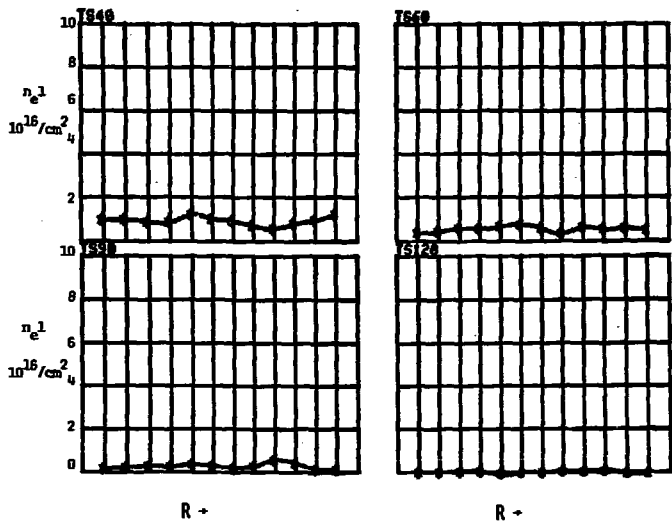
XBL 789-10874



Profiles of $\int n_e dl$ vs R at four times. Times are given above each graph. Each horizontal division represents 1 cm. Fill pressure was 12mTorr. No cusp fields were applied.

FIGURE 2.38A

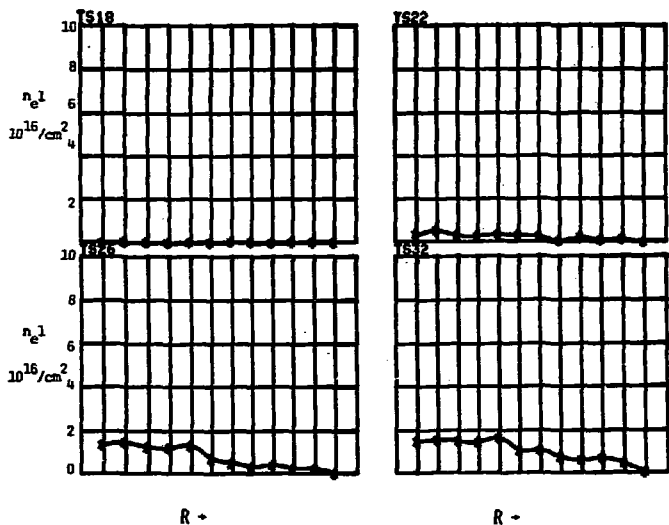
XBL 789-10872



Profiles of $\int n_e dl$ vs R at four times. Times are given above each graph. Each horizontal division represents 1 cm. Fill pressure was 12 mTorr. No cusp fields were applied.

FIGURE 2.38B

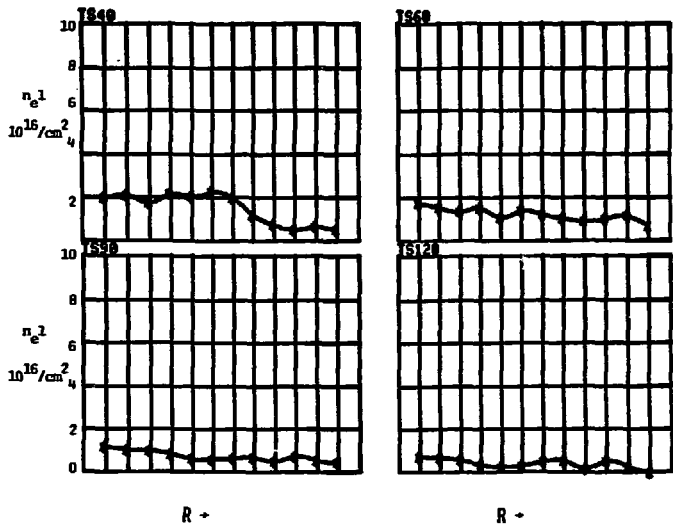
XBL 789-10871



Profiles of $\int n_e dl$ vs R at four times. Times are given above each graph. Each horizontal division represents 1 cm. Fill pressure was 12 mTorr.

FIGURE 2.38c

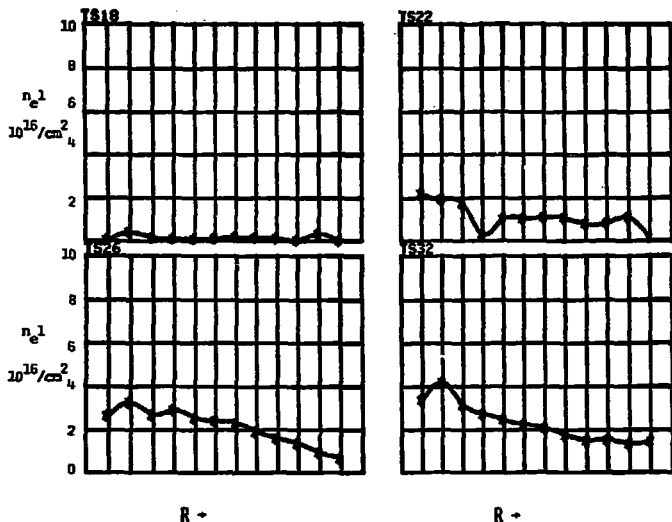
XBL 789-10858



Profiles of $\int n_e dl$ vs R at four times. Times are given above each graph. Each horizontal division represents 1 cm. Fill pressure was 12 mTorr.

FIGURE 2.38D

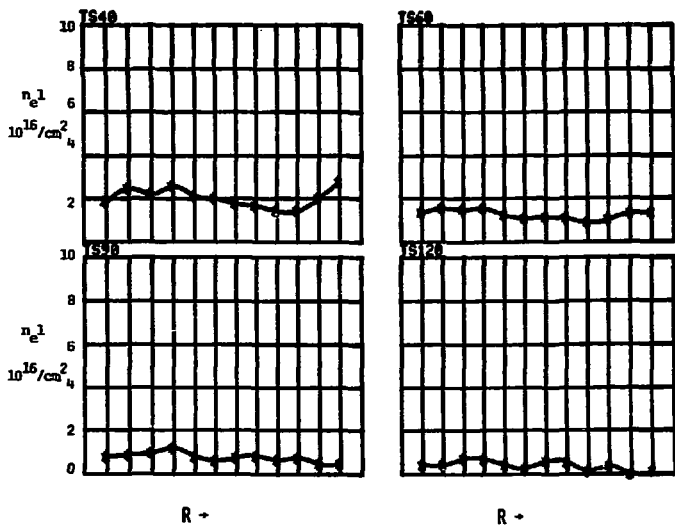
XBL 789-10859



Profiles of $\int n_e dl$ vs R at four times. Times are given above each graph. Each horizontal division represents 1 cm. Fill pressure was 24 mTorr. No cusp fields were applied.

FIGURE 2.38E

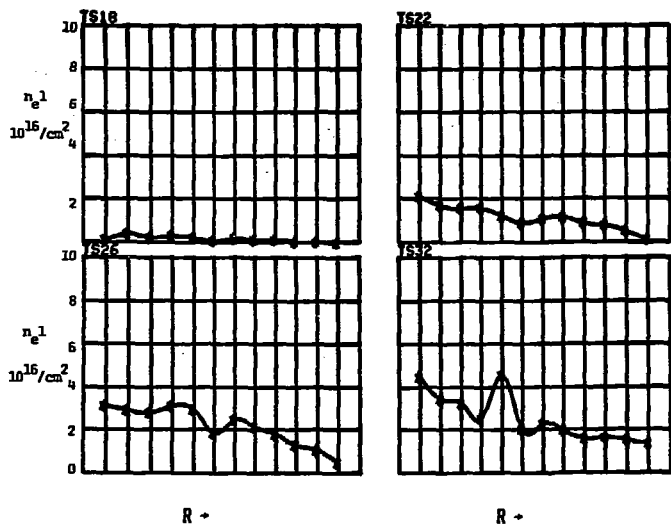
XBL 789-10860



Profiles of $\int n_e dl$ vs R at four times. Times are given above each graph. Each horizontal division represents 1 cm. Fill pressure was 24 mTorr. No cusp fields were applied.

FIGURE 2.38F

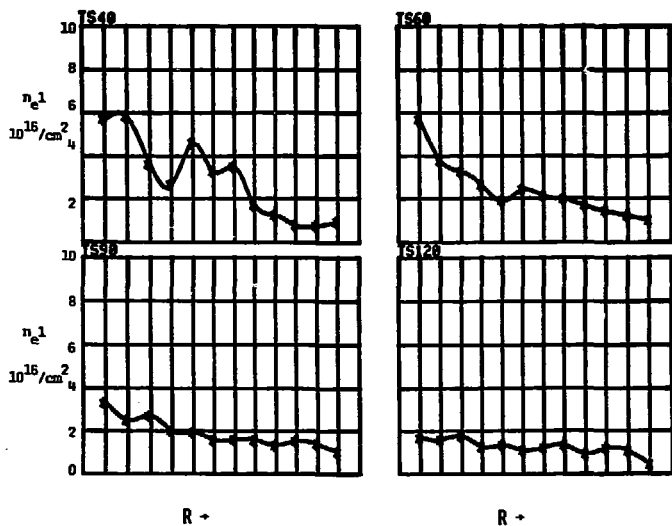
XBL 789-10861



Profiles of $\int n_e dl$ vs R at four times. Times are given above each graph. Each horizontal division represents 1 cm. Fill pressure was 24 mTorr.

FIGURE 2.38G

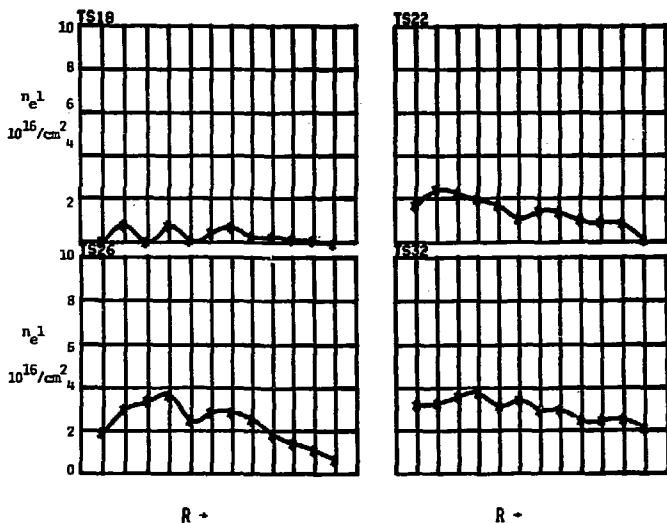
XBL 789-10862



Profiles of $\int n_e dl$ vs R at four times. Times are given above each graph. Each horizontal division represents 1 cm. Fill pressure was 2^4 mTorr.

FIGURE 2.38H

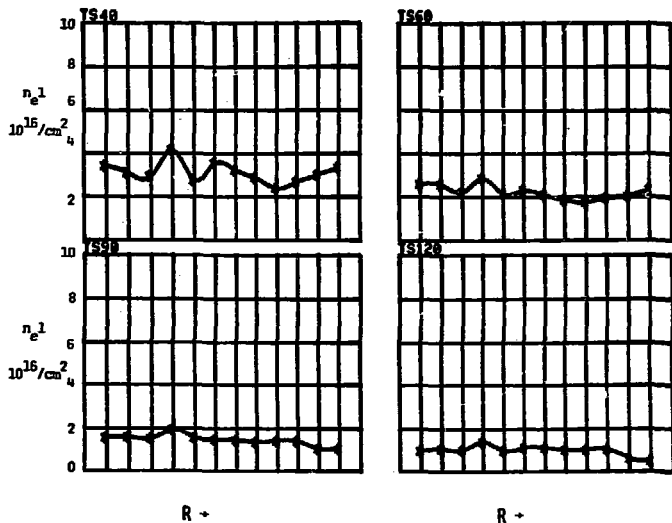
XBL 789-10863



Profiles of $\int n_e dl$ vs R at four times. Times are given above each graph. Each horizontal division represents 1 cm. Fill pressure was 36 mTorr. No cusp fields were applied.

FIGURE 2.38i

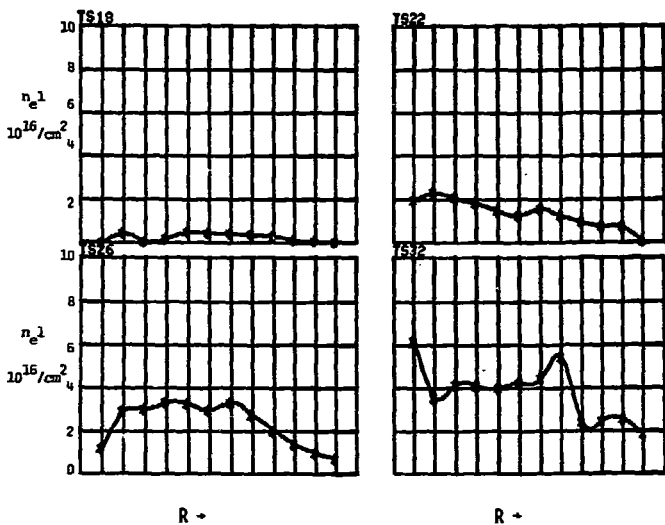
XBL 789-10864



Profiles of $\int n_e dl$ vs R at four times. Times are given above each graph. Each horizontal division represents 1 cm. Fill pressure was 36 mTorr. No cusp fields were applied.

FIGURE 2.38J

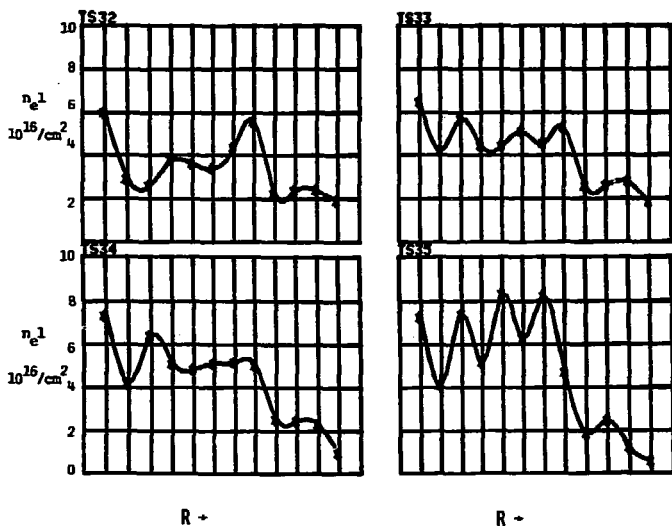
XBL 789-10866



Profiles of $\int n_e dl$ vs R at four times. Times are given above each graph. Each horizontal division represents 1 cm. Fill pressure was 36 mTorr.

FIGURE 2.38k

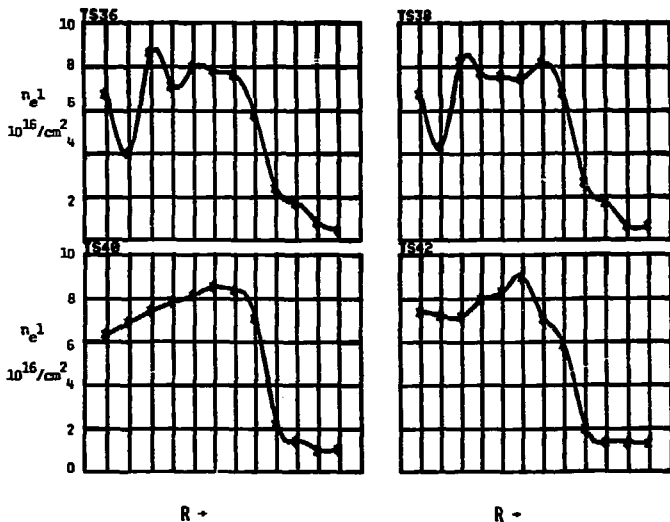
XBL 789-10865



Profiles of $\int n_e dl$ vs R at four times. Times are given above each graph. Each horizontal division represents 1 cm. Fill pressure was 36 mTorr.

FIGURE 2.38L

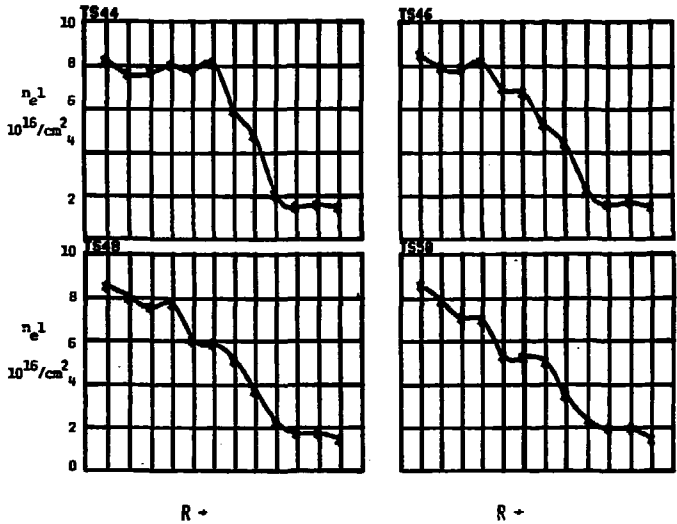
XBL 789-10867



Profiles of $\int n_e dl$ vs R at four times. Times are given above each graph. Each horizontal division represents 1 cm. Fill pressure was 35 mTorr.

FIGURE 2.38M

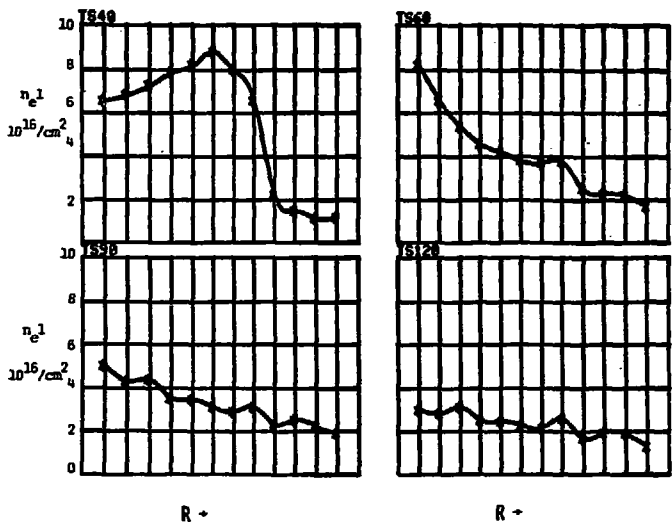
XBL 789-10868



Profiles of $\int n_e dl$ vs R at four times. Times are given above each graph. Each horizontal division represents 1 cm. Fill pressure was 36 mTorr.

FIGURE 2.38N

XBL 789-10869



Profiles of $\int n_e dl$ vs R at four times. Times are given above each graph. Each horizontal division represents 1 cm. Fill pressure was 36 mTorr.

FIGURE 2.380

XBL 789-10870

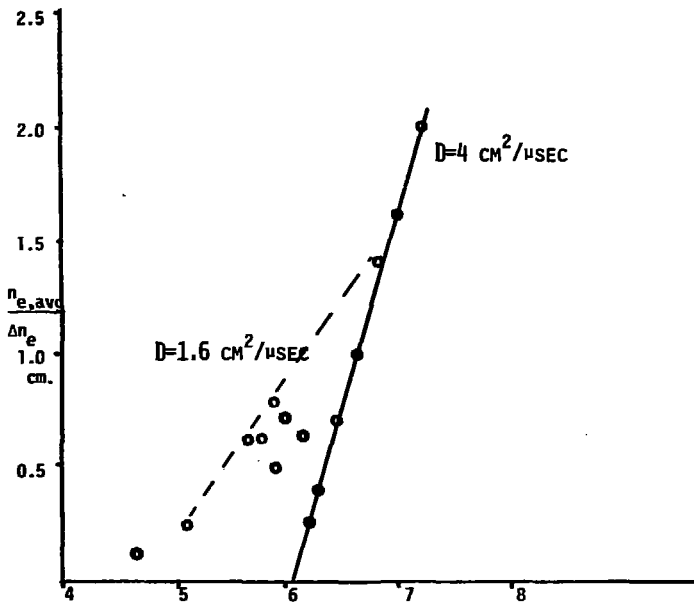


FIGURE 2.39 EVOLUTION OF DENSITY GRADIENT.

An estimate of diffusion, taken from the interferometer data gives results consistent with the classical value of $1.8 \text{ cm}^2/\mu\text{sec}$.

XBL 789-11351

At 20°C, 1 mTorr of gas contains 3.3×10^{13} particles/cm³ which, for our mixture (85% D₂, 15% He), when ionized yields 6.6×10^{13} electrons, 5.6×10^{13} deuterons, and 5.0×10^{12} helium nuclei. Both Tormac IV-a and c were operated frequently at 50 mTorr, for an initial fill of 5.3×10^{19} molecules, and the possibility of 2.1×10^{20} total charged particles.

From this inventory, we can calculate the effectiveness of the sweep-up and pre-ionization, and calculate the necessary energy to heat the plasma. If we estimate 20 eV/atom necessary to ionize the deuterium, then full preionization of the hydrogen would require 290 J. By comparing the damping of the pre-ionizer with and without plasma, one can see that 1/2 of the circuit energy is being absorbed by the plasma. The peak energy in the pre-ionize bank is 900 J, so considering that energy will be lost from the plasma during this time, it is not surprising that the pre-ionizer does not ionize the gas further than 35%.

To test Tormac confinement, the plasma needs to be collisionless, and this occurs at some $T > 300$ eV. To heat all the particles to that temperature would require over 10 kJ, which is most of the energy of the cusp bank, or many times the size of the heater. For such an experiment much larger banks would be required or a way of operating at much lower densities.

The effectiveness of the sweep-up could be measured

as the ratio of the observed density compression to volume compression. From the interferometer profiles and D_B derived densities we can model the compressed plasma as a rectangular torus $R_1 = 8.3$, $R_2 = 15.3$, $L = 13$. $V = 6750 \text{ cm}^3$, for a compression of 4.8. For a 36 mTorr fill, the peak electron density is 6×10^{15} , or three times the uncompressed, 100% ionized density. The result is 63% effective sweep-up.

2.8 References

1. R.N. Bracewell and A.C. Riddle, *Astrophys. J.* 50 427 (1967).
2. G.T. Herman and S.W. Rowland, *Comp. Graphics and Image Proc.*, v. 2, 151 (1973).
3. B.R. Myers and M.A. Levine, *Rev. Sci. Instr.*
4. Rory Niland, LBL, Private memo.
5. G.T. Herman, A. Lent, and P.H. Lutz. Tech. Rpt. 93 SUNY, Buffalo N.Y. (1975).
6. H.R. Griem, Plasma Spectroscopy, p. 305, McGraw-Hill, N.Y. (1964).
7. Ibid., p. 293
8. R. Shaw, M.C. Vella, to be published.
9. H.J. Kunze, Plasma Diagnostics, W. Lochte-Holtgrave, ed. Chap. 9, North-Holland, Amsterdam (1968).
10. Ibid.
11. M. Greenwald and W.I.B. Smith. *Applied Optics* 16, 587 (1977).

12. Gallagher and Levine, *op. cit.* (1974).
13. R.H. Lovberg, in Plasma Diagnostic Techniques, R.H. Huddlestone and S.L. Leonard, ed. ch. 3 Academic Press, N.Y. (1965).
14. B.R. Myers, *Bul. Am. Phys. Soc.* 21, 844 (1976).

3. EXPERIMENT LAYOUT AND CONSTRUCTION

3.1 Glass Vessel

The vessel is made of pyrex (Figure 3.1 a,b). It is the same dimensions as Tormac IV-a and is modified for diagnostic ports and a larger vacuum port. The pieces are ground to fit and assembled using a strong, high vacuum epoxy, Stycast 1266.

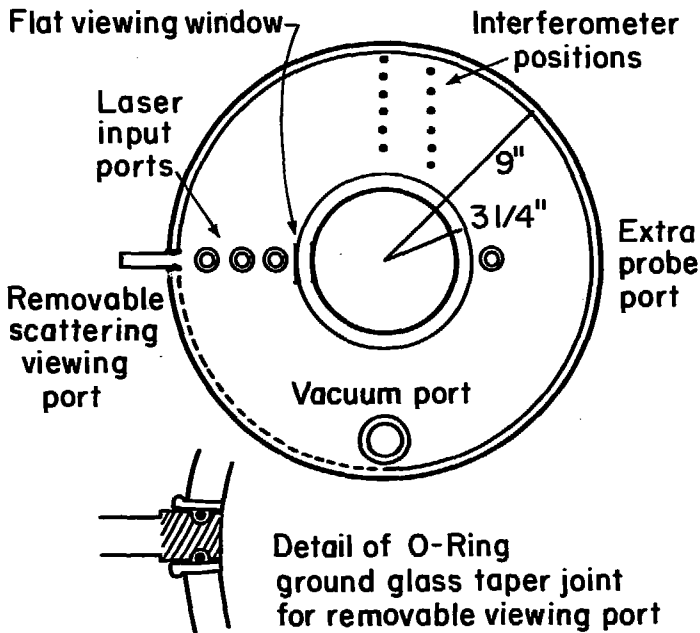
The flat sides are 1/2" thick pyrex plates drilled for the ports and the center post. The inner wall is cut from a glass pipe, the outer is a segment of an 18" OD bell jar. The ports mounted on the sides are simple tubes. When the vessel is centered in the windings, the winding end plates can slip right over them.

The laser viewing ports are special and are mounted on the outer cylinder. A tube would not fit under the windings, so O-ring ground glass 19/38 taper joints are used. The female joint is made nearly flush with the inner glass surface, which entails cutting the joints to half their normal length. This is still adequate for a good seal.

The vacuum port is made strong, as this is the only solid connection from the vessel to the mechanical world. It has a 1 1/2" ID, which allows about 10 times the pumping rate of Tormac IV-a.¹

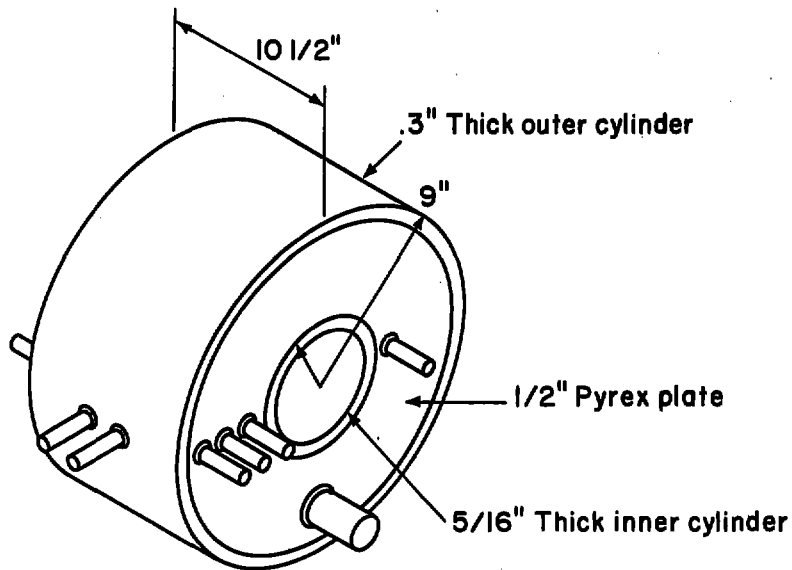
The assembled vessel sits on a heavy rubber pad inside the windings. Other pieces of rubber insulate it from mechanical shock from the outer sides and center conductor.

Glass vessel / access



XBL 789-2220

FIGURE 3.1A PYREX VESSEL FOR TORMAC IV-C



-109-

Glass vessel and access

FIGURE 3.1B PYREX VESSEL FOR TORMAC IV-C XBL 789-2219

3.2 Cusp Winding

The main cusp winding is assembled around the vessel in four pieces which can be taken apart again by simply removing bolts (Figure 3.2). There is a solid copper center conductor, two end plates, and an outer cylinder. Current is fed from a 6" wide strip line into a flange on the center conductor. The winding is built to operate at up to 40 kilovolts and mechanically sustain 50 kilogauss at the cusp lines.

The plates and cylinder are made with 100 parallel #14 wires, imbedded in epoxy and fiberglass cloth tape. The plates are reinforced by 1/4" thick G-10 fiberglass disks 21" in diameter. These are drilled for ports, interferometer access, and supporting rods. Eight 1/4" fiberglass supporting rods are threaded at each end and tie the plates together like drumheads. They run outside both the outer cylinder and the pre-ionize and heater windings.

The wires on the plates are soldered and strapped to the center cylinder flanges, and spiral 28% of a circumference as they radiate out (Figure 3.3).

The cylinder was built on a laminated plywood form. Four lines of 100 teflon pegs circled the form to bend and hold the wires. Layers of fiberglass tape were laid down, both along z and θ , then every other pair of wires, then more tape, then the other 50 wires, and final layers of tape. This created a basket weave effect of wires and

Coil assembly

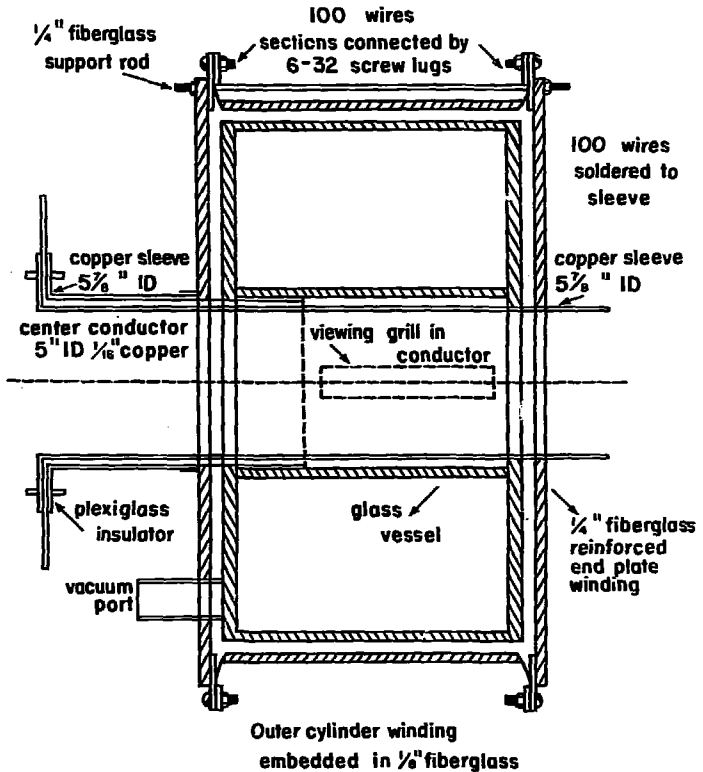
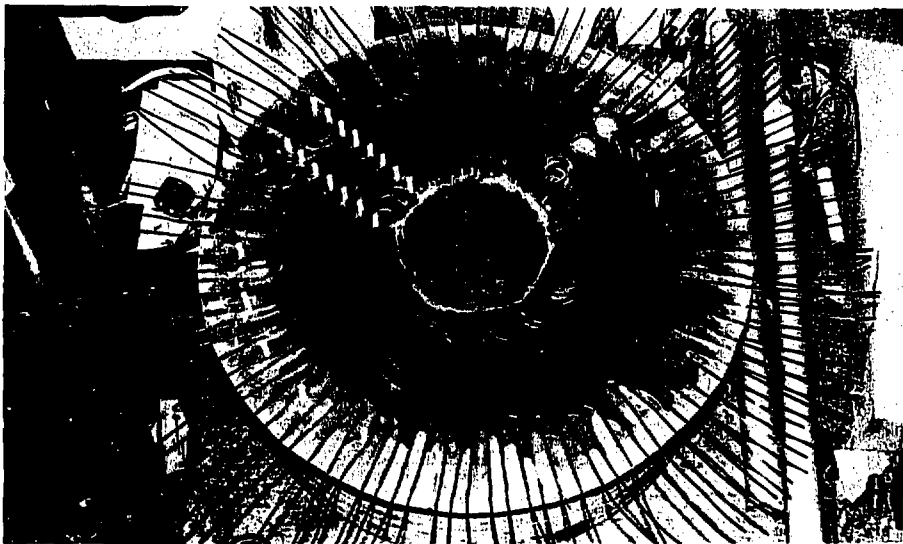


FIGURE 3.2

XBL 789-2213



XBB 789-12554

FIGURE 3.3 WINDING END PLATE.

100 wires spiral radially on the inside of a 1/4 inch thick fiberglass disk. The wires are held by epoxy and glass cloth. Teflon pegs are stuck in the port and viewing holes.

fiberglass computed to be strong enough for all the static forces and prevent adjacent wires from spreading or crossing one another.

This entire assembly was soaked in epoxy (Epon 815, Versamid 140 catalyst, Figure 3.4) and pulled tight by nylon straps. A motor rotated the form under heat lamps to set the epoxy, and the result was a very thin, strong, single-layer coil.

Each end plate is connected to the cylinder by 100 #6 screws through lugs soldered to each wire.

The wires in the outer cylinder reverse their spiral twice to form the cusps $3 \frac{1}{4}$ " apart. The turns are +21%, -35%, and +21% of a circumference, respectively.

A solid $\frac{1}{4}$ " thick plexiglass insulator separates the two flanges and extends along the center cylinder to avoid a path in the air from the endplate. The flanges have bolts hard soldered to them to connect the strip line.

The vessel is supported by a heavy plywood stand, with the axis at 53" high. Nylon straps hold the winding in place on a heavy rubber pad.

3.3 Cusp Bank and Switches

The capacitor banks on Tormac IV-c are electrically unchanged from IV-a, although some connections were rebuilt to the new vessel.² A full schematic of the high voltage system is Figure 3.5. Note all the banks are located in a



XBB 789-12555

FIGURE 3.4 APPLYING EPOXY TO WINDING OUTER CYLINDER.

Gary Tabler (right) squeezes the epoxy into the layers of glass cloth as Martin Greenwald (left) brushes more on.

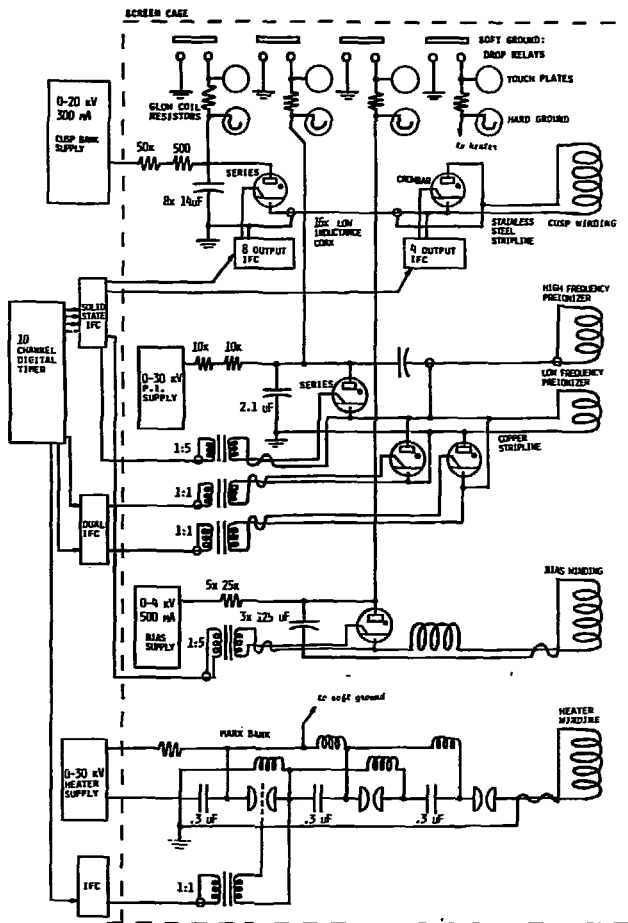


FIGURE 3.5 HIGH VOLTAGE SYSTEM SCHEMATIC

screen cage with the vessel.

The cusp bank consists of 8 14 μ f 20 kV capacitors, each with its own 7703 ignitron switch mounted right on the capacitor lead. The eight fire in parallel. Current is carried over 16 low inductance cables to the crowbar circuit and then by stripline to the vessel.

The eight series ignitrons are triggered by an ignotron firing chassis (IPC) mounted on the bank. It consists of a 3 kV supply, an ignitron and 8 trigger capacitors. It, in turn, is triggered by a solid state firing chassis outside the cage. The 600 volt pulses from the solid state chassis are upped by a 5:1 transformer.

The cusp crowbar consists of 4 large 555 ignitrons mounted in parallel on a stripline table of heavy copper plates. These are triggered by a similar chassis to the series ignitrons.

3.4 Bias Circuit

The purely toroidal bias field is produced by a loose 8 turn torus strung about the vessel. The center conductor of a RG213 cable is used and is brought to the bank as a twisted pair. The bank consists of three capacitors in parallel, a single 7703 series ignitron and a dummy series inductance to slow the rise time.

3.5 Preionizer Circuit

The preionizer circuit is more complicated than the

others. The main circuit rings at 200 khz for four cycles prior to the cusp and is then crowbarred. A high frequency circuit rings at 2 mhz and is driven by the onset of the main circuit.

The low frequency windings are two single turn hoops, 2" wide, circling the outer cylinder near the edges. They are insulated in alternating layers of polyethylene and mylar tape to hold a voltage of 60 kV. They are connected in parallel to the 2 μ f capacitor through a single series ignitron. Two 7703 ignitrons crowbar the circuit in opposite directions for either current polarity. The series ignitron is driven by the solid state IFC through a 5:1 transformer, and the crowbar ignitrons are driven by a thyrotron tube IFC through 1:1 transformers.

The high frequency circuit consists of two capacitors in parallel and two parallel loops mounted on the endplates. Current is carried through RG8 coax and the loops are made from the coax center conductor.

3.6 Heater Circuit

Several "shaker" heating experiments have been performed on Tormac IV with various circuits. However, these were not used for Martin Greenwald's and my experiments. The basic circuit is a high voltage bank which rings down through a single turn hoop around the outer cylinder at the midplane. The capacitor banks have included simple capacitors, Marx

banks, and ³Lausanne lumped constant lines. We designed the IV-c experiment to include the Lausanne line connection through a 10 foot long, 8" wide strip line.

3.7 Floor Plan

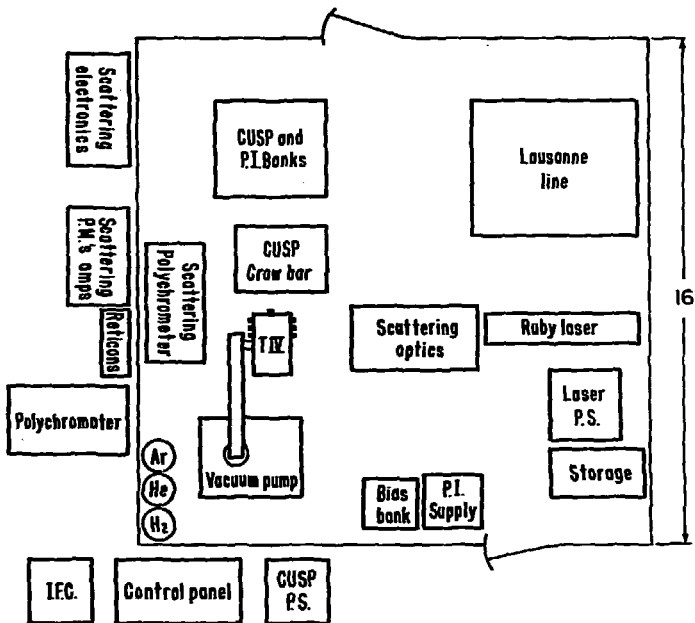
The Tormac IV-c experiment is located in the same 16 foot square screen cage used for Tormac IV-a. The addition of the Thomson scattering equipment was the major limitation in re-arranging the experiment (Figure 3.6). The arrangement is crowded but it works.

All the scattering optics are located at the 53" height of the vessel axis. The three vessel ports for the laser are at the same height so that the scattering position can be changed by moving the input optics around on the optics table. This table is a 1" aluminum slab mounted on stacks of cement blocks and covered with an interlocked PVC plastic box.

3.8 Vacuum System

The vacuum system is designed to create a vacuum better than 10^{-6} torr inside the vessel at the time gas is injected. This assures that impurities in the gas are less than .01%.

The limit in the vessel pump access is the 1 1/2" vacuum port, limited by the allowable perturbation in the magnet winding. The pump is a Welch 3102 turbo molecular pump with a mechanical force pump. When blanked off it can create a vacuum in the range 10^{-9} torr, and it pumps at



Tormac IV-c screen cage

XBL 789-2226

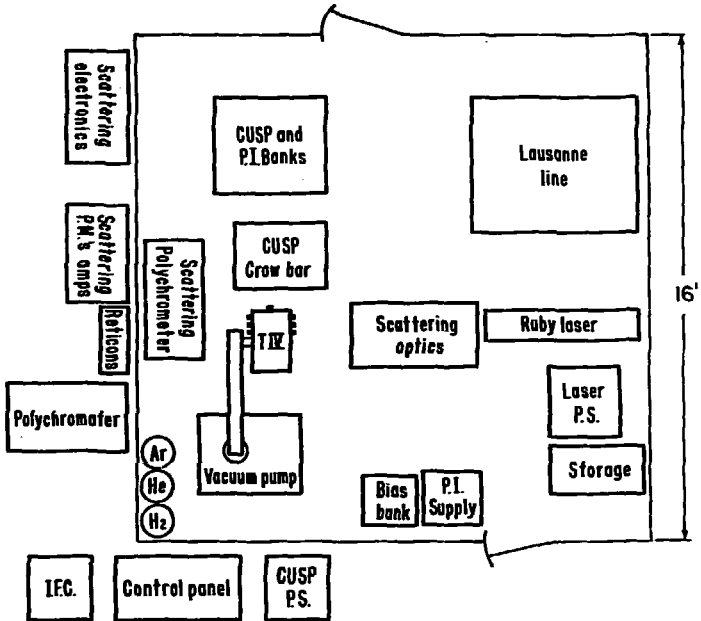
FIGURE 3.6 EXPERIMENT FLOOR PLAN.

the rate of 260 liters/sec.

The connection from the pump is a 4" pneumatic bellow-sealed stainless steel gate valve and a 4" stainless vacuum line four feet long (Figure 3.7). The combined impedance of this is less than the vessel port. This is an improvement from Tormac IV-a, which had a 1/2" port and a 1 1/2" line.

A bellows is in the line at the gate valve to adjust the position. The connection at the vessel is a segment with a Varian flange to the line and a compression fitting to the vessel. Fittings are welded to the line for connecting gauges, probes, roughing pumps and gas fill lines. These are either 3/4" Rad-lab style fittings or compression fittings. Viton O-rings are used throughout, so the valve and line can be heated to 200°C using heater tape and surrounding it in fiberglass insulation. O-rings and taper joints are lightly greased with Apiezon L.

The system is measured by 6 gauges. A Barocel differential manometer is connected on the two sides of the gate valve and is used primarily to measure gas filling pressures. There are thermocouple gauges at the forepump, the vessel and the gas fill mixing plenum (see below). There are two ion gauges, one as close as possible to the vessel; the other at the pump throat. These can measure the range 10^{-9} to 10^{-3} torr. With the valve open they give the vacuum and the pressure drop across the 4" line; thus the actual vacuum inside the vessel can be extrapolated. It



Tormac IV - c screen cage

XBL 789-2226

FIGURE 3.6 EXPERIMENT FLOOR PLAN.

usually falls to between 6×10^{-8} and 2×10^{-7} . When the valve closes, the absolute base pump pressure can be measured, usually between 5×10^{-9} to 5×10^{-8} . The second gauge gives the vessel "leak up" rate which allows the vessel pressure to rise to near 10^{-6} during the 5 seconds between closing the gate valve and firing the shot.

The gas mixing and fill assembly is mounted on the pump frame. Gas is fed from deuterium and helium bottles to a 1/2 liter mixing plenum, which can be evacuated by a separate roughing pump. A regulator after the plenum sets a fixed pressure for gas going to the fill line. In the fill line are two solenoid valves 2" apart. Gas goes to the vessel in increments: the first solenoid fills the 2" of line to the regulated pressure and the second allows it into the vessel. A set of timing relays outside the screen cage automatically cycle this for certain number of puffs of gas.

3.9 Safety Interlocks

The doors to the screen cage and all the power supplies are linked to an interlock system.⁴ Whenever the chain is broken, relays automatically soft ground all the capacitors through resistors, and all the supplies are turned off. The drop relays are mounted together by the cage entrance. The same mounting board contains the grounding hooks which are first touched to the soft ground and then hung on a hard

ground connection before anyone is permitted to enter the cage.

When the interlock is closed at the control panel, a 5 second bell rings to insure everyone has left the cage before the drop relays are lifted and the charging supplies are enabled.

A second interlock system exists on the Thomson scattering system to prevent the lasser from being fired if the optics are not covered or if there is insufficient cooling water.

3.10 References

1. Op. cit., Gallagher and Levine (1974).
2. B.R. Myers, private memo on Tormac IV-a results (1977).
3. A. Lietti, Rev. Sci. Instr. 40, 473 (1969).
4. E. Hartwig, ed. LBL Electrical Safety Standrds, UCID 3927.

4. NUMERICAL CALCULATIONS

4.1 Vacuum Code PSIVAC

The desired Tormac confinement field requires complicated current windings as it produces both poloidal and toroidal fields. Early Tormacs were designed using an electrolytic tank analog;¹ however, I found this to be incorrect for our problem and difficult to relate to real winding patterns.

The field resulting from a set of windings can be numerically calculated in a straightforward way. The complete winding is considered to be a pure torus (actually a single axial current) plus a set of toroidal current loops. The contribution to the vector potential A_0 is found for each loop using elliptic integrals and these are simply summed into a scalar flux function ψ . Then $\vec{B}_p = (B_r, B_z)$ can be found by differentiating ψ on a grid of points (r, z) .

That is, consider a set of $L - 1$ to N coaxial coils, each carrying current I_L and having a location r_L, z_L . To find ψ at a point (r, z) ²

$$[4.1] \quad \psi(r, z) = \sum_L I_L \psi_L(r, z)$$

$$[4.2] \quad \psi_L(r, z) = 4I_L \sqrt{\frac{r_L}{r}} \frac{r}{k} \left(\frac{2-k^2}{2} K(k) - E(k) \right)$$

$$[4.3] \quad \text{where } k^2 = \frac{4r_L r}{((r+r_L)^2 + (z-z_L)^2)}$$

and K and E are the complete elliptic integrals of the first and second kind.

$$\{4.4\} B_r = \frac{\psi(x-\delta, z) - \psi(x+\delta, z)}{2r\delta}$$

$$\{4.5\} B_z = \frac{\psi(x, z+\delta)}{r+\delta} - \frac{\psi(x, z-\delta)}{r-\delta} \frac{1}{2\delta}$$

The toroidal field, $B_T =$

For all these formulas, r and δ are in cm

I is in abamps

B is in gauss

I have written programs to simulate the vacuum fields which plot contours of $|B|$, B_p and ψ . Contours of ψ are the poloidal projections of the field lines themselves. A polynomial expansion for the elliptic integrals was copied from the MAPCO program used at Lawrence Livermore Laboratory.³ My vacuum program, PSIVAC, was originally run on the MFE computer center CDC 7600, using the polynomial expansions. The speed was greatly increased by using a table of 2000 values for the function

$$\frac{4}{k} \left(\frac{2-k^2}{2} K(k) - E(k) \right)$$

and this permitted to program to run on a small PDP-11/45 at LBL, and on our PDP-1134.

This simple program does not solve the design problem, however. Large currents are induced in other conductors such as the pre-ionizer coils and the copper center conductor which modify the field. The plasma is another conductor which must be included.

The first problem may be solved by fixing a set of current loops at the conductors and iterating the program to exclude flux from inside the loops. Each iteration, the currents are adjusted proportional to the bounding flux value.

Ben Feinberg⁴ has adapted this scheme further to model a perfectly conducting $\beta = 1$ plasma. Current loops are placed at the plasma boundary. The currents are adjusted to exclude flux. Then the boundary can be moved in steps proportional to the magnetic field pressure. This cycle continues until a constant pressure boundary is found.

4.2 CGL Plasma Equilibrium Code

I have simulated a diffuse plasma by developing a program similar to one written by Killeen and Whiteman⁵ to examine stuffed cusp equilibrium. The program solves the CGL equilibrium equations for a given class of solutions developed by J.B. Taylor.⁶ These find solutions for P_{\perp} and P_{\parallel} as a function of $|B|$; that is, for a plasma with equal magnetic pressure around the boundary. These solutions must obey the stability criteria for the

$$\text{firehose instability} \quad B - \frac{dP_{\parallel}}{dB} > 0 \quad [4.6]$$

$$\text{and mirror instability} \quad B + \frac{dP_{\perp}}{dB} > 0 \quad [4.7]$$

The CGL force balance equation can be put in the form

$$\begin{aligned}
 & B \left[\left(\frac{P_{\parallel} - P_{\perp}}{B^2} - 1 \right) \vec{j} + v \left(-\frac{P_{\parallel} - P_{\perp}}{B^2} \right) \times \vec{B} \right] \\
 & = \nabla (P_{\perp} + \frac{1}{2} \left(-\frac{P_{\parallel} - P_{\perp}}{B^2} \right) B^2) + \frac{1}{2} B^2 \nabla \left(-\frac{P_{\parallel} - P_{\perp}}{B^2} \right) \quad [4.8]
 \end{aligned}$$

This simplified by defining $\mu = \left(-\frac{P_{\parallel} - P_{\perp}}{B^2} \right)$ [4.9]

$$v = \mu - 1 \quad [4.10]$$

giving $\vec{B} \times \nabla \times v \vec{B} = \nabla P_{\parallel} - 1/2 \mu v B^2$ [4.11]

For our class of solutions where $P = P(B)$ this becomes

$$\nabla \times v \vec{B} = 0 \quad [4.12]$$

and the current density is given by $\vec{j} = \frac{\nabla v \times \vec{B}}{-v}$ [4.13]

The simulation program solves the differential equation gotten by expressing the force balance equation in terms of ψ , the flux function in cylindrical coordinates; v , and the vacuum field B_0

$$\begin{aligned}
 & \frac{\partial^2 \psi}{\partial r^2} + \left(\frac{1}{v} \frac{\partial v}{\partial r} - \frac{1}{r} \right) \frac{\partial \psi}{\partial r} + \left(\frac{1}{v} \frac{\partial v}{\partial z} \right) \frac{\partial \psi}{\partial z} + \frac{\partial^2 \psi}{\partial z^2} \\
 & = - \frac{1}{v} [B_{z0} \frac{\partial v}{\partial r} - B_{r0} \frac{\partial v}{\partial z}] \quad [4.14]
 \end{aligned}$$

The functions for $P(B)$ used to get v are

$$P_{\parallel} = CB(B_0 - B)^m \quad [4.15]$$

$$P_{\perp} = CmB^2(B_0 - B)^{m-1} \quad [4.16]$$

The program starts with the vacuum fields found by the

PSIVAC program and iteratively solves the above differential equation by the Alternating Direction-Implicit method.⁷ The iteration cycle is $\psi \rightarrow B \rightarrow P \rightarrow \psi$.

I discovered that such a code is inappropriate for studying the actual Tormac equilibrium. The solutions are only guaranteed stable for values of $\beta < \sim .3$, and the use of a fixed geometrical grid causes problems at sharp boundaries. The parameter C in [4.15, 4.16] is adjusted to raise β , and as this approached the critical values found by Killeen, the numerical solution did not converge. A convergent solution locates a plasma in a minimum-B region, digging the magnetic well deeper. A non-convergent solution keeps digging the well deeper and deeper and spreading out. I stopped this behavior by adding an artificial limit to the iteration loop: a limit on plasma energy. Whenever the volume integral of plasma pressure exceeded a certain value, the parameter C was decremented. This led to convergent solutions of uncertain physics. The purpose of the exercise, though, was not to study the plasma physics but to obtain a reasonable magnet design.

Figure 4.1 shows a vacuum and plasma run for a Tormac V design. The principle conclusion I reached was that for this design purpose the plasma simulation was unnecessary. For all the convergent solutions, the plasma location did not move from the location of the vacuum magnetic well. Thus the vacuum program alone is adequate for design work

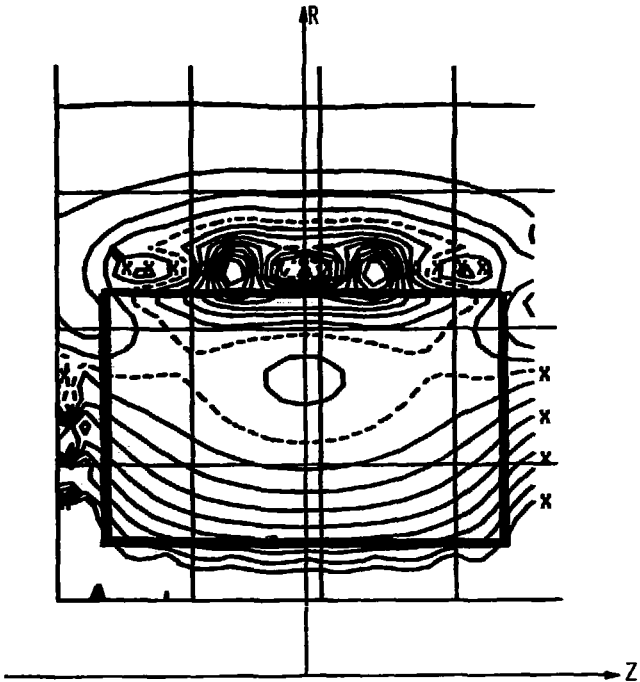
and the plasma codes can be used to confirm this.

4.3 Tormac IV-c Results

Figures 4.2 and 4.3 show the vacuum field $|B|$ contours and field lines (flux contours) for the windings actually built. A profile of these results is shown with the actual probe measurements in Figure 2.29.

4.4 References

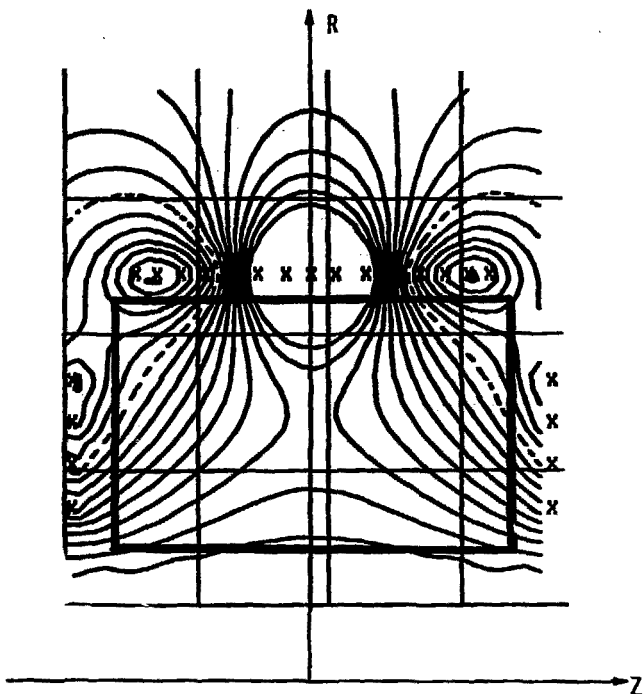
1. L.S. Combes, C.C. Gallagher and M.A. Levine. Rev. Sci. Inst. 37, 1567 (1966).
2. W.R. Smythe, Static and Dynamic Electricity, p. 271 McGraw-Hill, N.Y. (1950).
3. W.A. Perkins and U.C. Brown, LLL report UCRL-7744 Rev. II (1966).
4. B. Feinberg, J. Coonrod, to be published.
5. J. Killeen and K.J. Whiteman, Phys. Fluids 9, 1846 (1966).
6. J.B. Taylor and R.J. Hastie, Phys. Fluids 8, 323 (1965).
7. R.D. Richtmeyer and K.W. Morton, Difference Methods for Initial Value Problems. Interscience, John Wiley, N.Y. (1967).



|B| CONTOURS, OUTPUT FROM VACUUM FIELD PROGRAM. THE POSITION OF THE GLASS VESSEL IS SHOWN BY HEAVY LINES.

FIGURE 4.2

XBL 789-11084



POLOIDAL FIELD LINES (Psi CONTOURS)
OUTPUT FROM VACUUM FIELD PROGRAM. THE
POSITION OF THE GLASS VESSEL IS SHOWN BY
HEAVY LINES.

FIGURE 4.3

XBL 789-11085

5. DATA ACQUISITION

5.1 Reticon System¹

Tormac diagnostics require an acquisition system which can digitize and record many transient waveforms. The polychromator, for example, requires 16 channels to determine the line shape, and we would like that recorded at many time steps per shot.

It is impractical to use poloroid pictures of oscilloscope traces for so many channels. The standard solution is to use fast digitizing circuits which directly convert the waveform to digital measurements

Data Acquisition Requirements

3 experiments

- x 24-32 analog waveforms, < 1 mhz, 4 volt peak to peak, < 1% noise
 - x - 100 time steps per shot
 - x - 100 shots per day
-

and store them in a buffer memory.² One such system would be required for each waveform, and the assembled group could be read out individually by the computer during the delay time between shots.

Directly digitizing transient waveforms is very expensive, > \$2000 per channel using commercially available systems made by Biomation³ or circuits available in CAMAC⁴ modules.

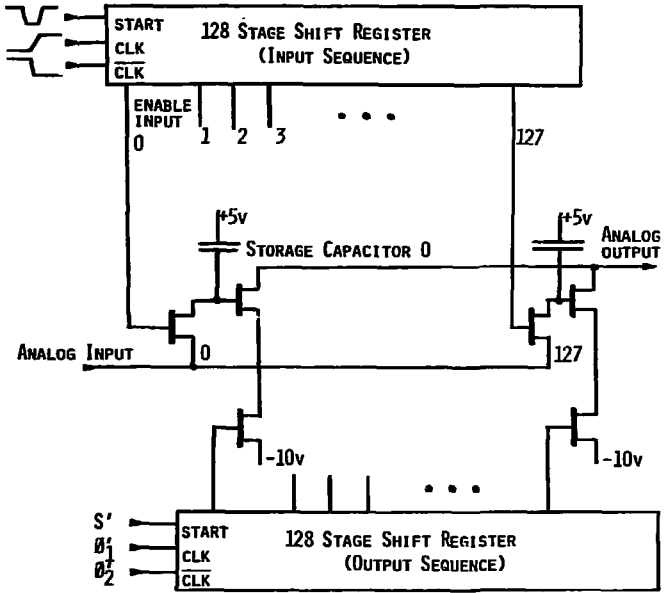
For our requirements and budget this was prohibitive. Fortunately, the development of new integrated circuits, serial analog memories (SAM), permitted a new approach.

A serial analog memory is a linear array of sample and hold circuits, and the logic necessary to sequence them. It can store a waveform as a series of discrete time samples, and then read it out at a different frequency after a brief delay. Within the limits of its retention time the single integrated circuit replaces one buffered digitizer or scope channel. Presently these circuits are made by Reticon Corporation and Fairchild Semiconductor.⁵

5.1.1 Organization

The system for Tormac uses the Reticon SAM128V⁶ (Figure 5.1). Each SAM contains 128 sample and hold circuits and gating circuitry from common analog input and output lines. Two independent 128 stage shift registers control the sequencing of the input gates and output buffers. The sequence is shifted at each edge of a complementary clock signal running at half the sample rate.

A complete system is assembled from 32 SAMs, a control circuit, and a single, medium speed ADC (Figure 5.2). When an event occurs, all 32 inputs are clocked in parallel to record the signals, after which the computer is notified. The computer then commands the control board to read and digitize the signals from each SAM in series until 128



INTERNAL ORGANIZATION OF SAM128V

FIGURE 5.1

XBL 789-11082

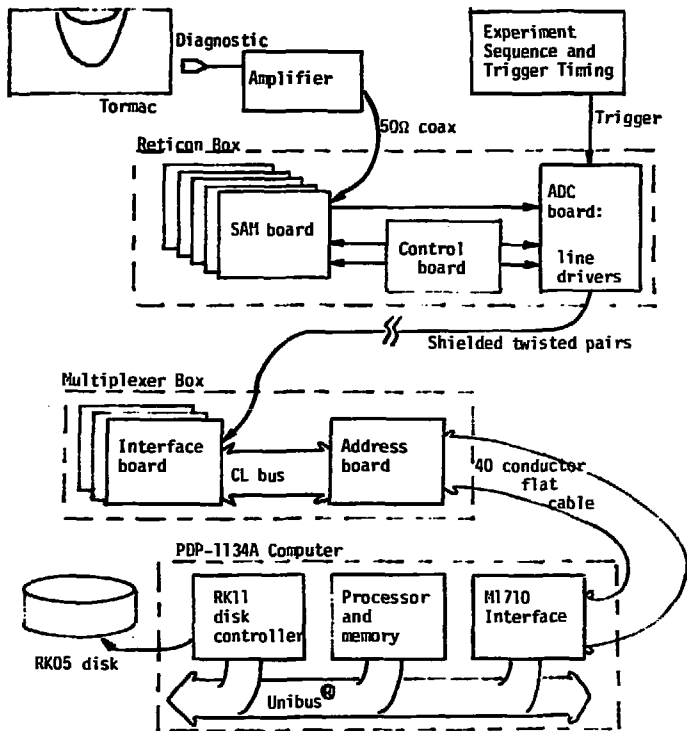


FIGURE 5.2 DATA PATH FROM DIAGNOSTIC TO DISK STORAGE.

XB1 789-11359

time samples times 32 SAMs equals 4096 signals are recorded. The inputs can sample at up to 5MHz, for a total bandwidth of 160 MHz. The readout is performed at 7 μ sec per sample. Hence this method has expanded the bandwidth by over 1000.

Three such systems have been built and installed on Tormac IV, V and Pl. Each unit is contained in a heavily shielded box adjacent to the experiment. It communicates over optically-isolated high speed serial lines to a multiplexer at the computer across the room. The multiplexer interfaces each system separately and could, in principle, read out all three systems simultaneously.

5.1.2 Data Transmission Scheme

The computer and Reticon system must exchange commands and data words each 7 μ sec, over 50 feet of electrically hostile territory. This is done serially over 5 optically-isolated twisted pairs:

- 1) READ pulse: the computer tells Reticons it has read a word into memory and has readied a command.
- 2) CLOCK: a train of ten 2.5 mhz pulses which synchronize the serial exchange
- 3) COMMAND: an 8 bit serial word from the computer
- 4) DATA: a 10 bit serial word from the ADC in the Reticon box
- 5) DONE: a flag from the Reticon box telling the computer it has read in a shot and is ready to be read out

The pairs are driven by type 8830 differential line drivers, and are isolated at the computer-end by HP4360 opto-isolaters.⁷

Figure 5.2 is a schematic of the data path from instrument to computer. It includes each of the circuit boards which are described in detail below.

5.1.3 Channel control and selection

The 8 bit command word contains a 5 bit channel address and clear, trigger and reset bits. The channel address is decoded to select 1 of 4 chips on 1 of 8 SAM boards (Figure 5.4).

The clear bit resets the timing circuitry for a read-in cycle. The trigger acts like an external trigger to initiate a read-in cycle. The start bit indicates the first cycle of a channel read-out: this gates the card select.

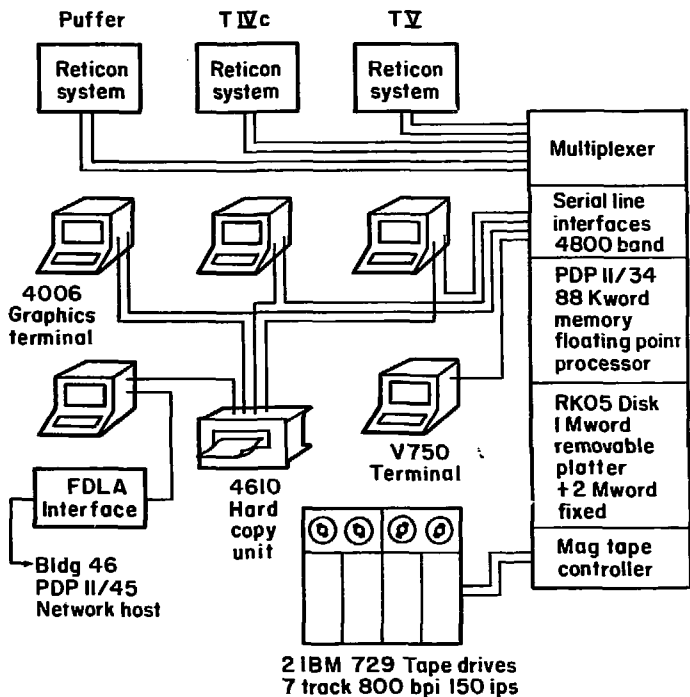
Each SAM board has gating circuits to combine the card and chip select lines into chip read-out start pulses.

5.1.4 Operation cycles

To prepare to take a shot, the computer toggles the reset bit in the Reticon box and then waits to see the done flag.

When an event is triggered, the control board sends a read-in start signal to all SAM cards and starts the read-in clock. The start signal drops after the first clock transition, and the next 128 transitions load all the SAMs.

Tormac data acquisition computer system



XBL 789-2225

FIGURE 5.3

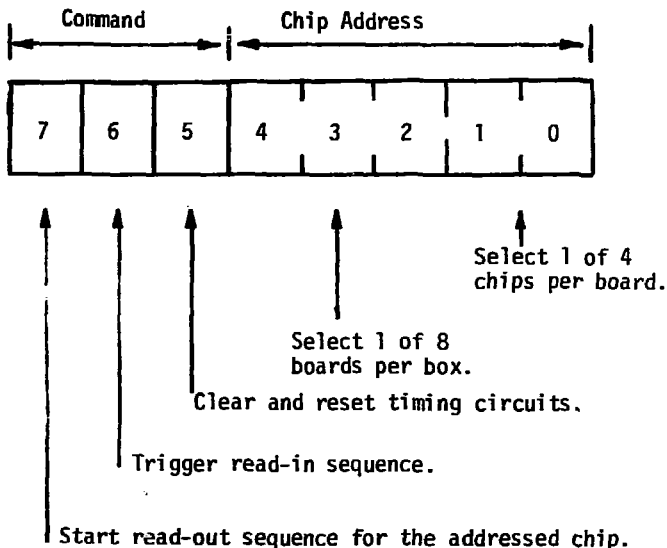


FIGURE 5.4 COMMAND WORD FORMAT.

An 8 bit command word is transmitted from the computer to the Reticon box, synchronized with the serial transmission of the data word back to the computer.

The clock continues for 128 more transitions (64 pulses) to create a slight delay: this period becomes the DONE flag.

After DONE falls the computer sets the chip address and start bit for the first channel and reads it. The start bit is dropped and 128 more read cycles completely read out that channel. This continues until all channels are read out.

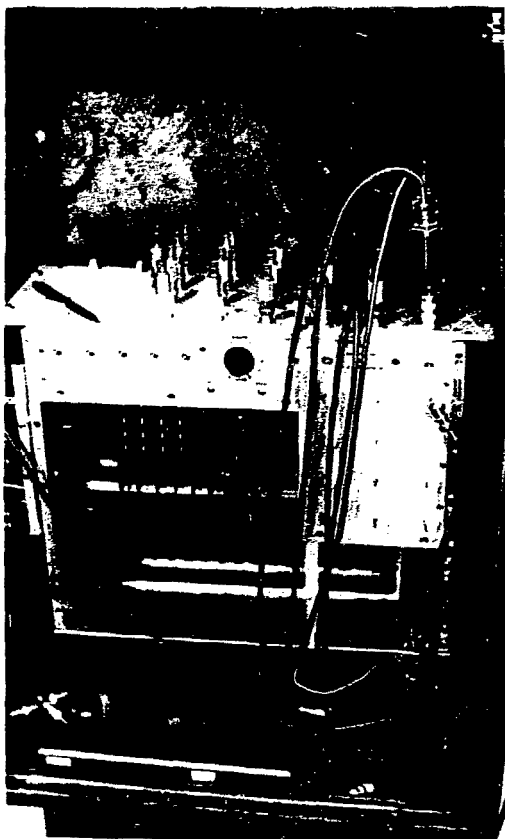
5.1.5 Circuit description

The Reticon system and multiplexer are constructed with standard Control Logic boards, racks and power supplies. Each of the three Reticon systems is electrically identical, and the boards are interchangeable.

5.1.5.1 Reticon system circuitry

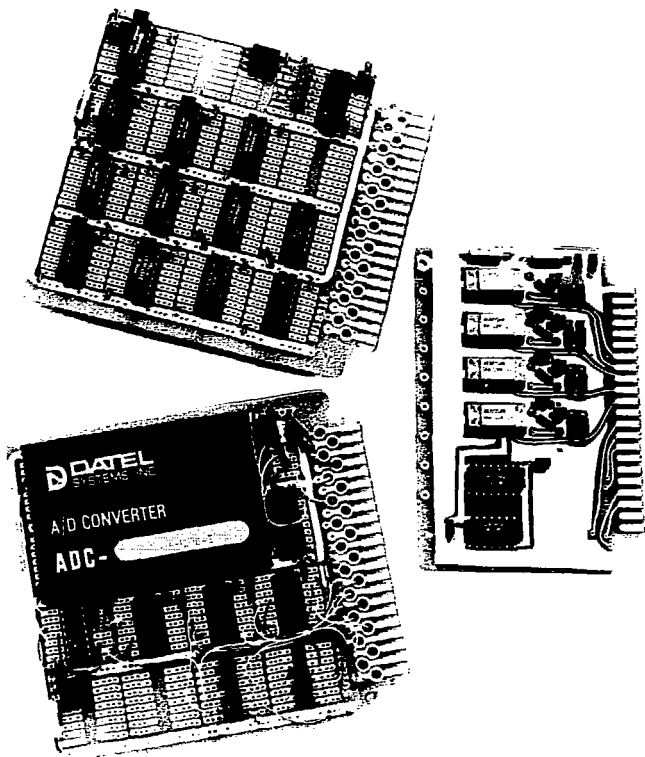
The Reticon box holds the circuit cords and power supplies and connects them to external BNC (analog) and Bendix (digital) signal connectors (Figure 5.5). The analog signals run through small co-ax lines, and through a simple switch. The switch allows the SAM cards to sense either a front panel BNC or an internal calibration signal, adjustable from -3 to +3 v.

SAM boards contain 4 SAM chips, gates and buffers for the clock and start signals, and Darlington emitter followers to drive the SAM outputs onto the analog bus. The SAM chips operate from +5 v and -10 v signal and power lines. Hence CMOS circuits are used for the gates. The boards are two-sided printed circuits with careful ground planes



XBB 789-12553

FIGURE 5.5 RETICON BOX IN SHIELDED CABINET.



XBB 761-628

FIGURE 5.6 PHOTO OF BOARDS.



XBB 789-12551

FIGURE 5.7 MULTIPLEXER BOX, SHOWN WITH PDP-1134.

Wirewrapped interface cards and flat cable connector are shown behind hinged front panel. Twisted pair cables from Reticon boxes connect through Bendix connectors on the rear.

(Figure 5.6, 5.7).

The control board is also CMOS and is wirewrapped (Fig. 5.8). It has two sections. The command section converts the serial COMMAND signal to a parallel word and buffers it in latches. The output of these latches goes to the select decoders, which drive the SAM boards. The loading of the command buffer is synchronized with the READ pulse from the computer. This pulse toggles the clock flip flop for the read out clock ϕ_1^i , ϕ_2^i .

The second section controls the read-in timing. The trigger and trigger command pulse are gated into a one-shot D4, which prevents retriggering for 30 msec. From there it sets a clock enable and a start flip flop. The oscillator runs, generating ϕ_1 , ϕ_2 clock signals for 128 pulses counted by A4, which then clears the enable line.

The TTL level signals from the computer and ADC board are converted to CMOS levels in two stages on the control board. First the pulses are offset from ground to -10v by optoisolators. Then they are amplified to the full 15 volt swing by open collector buffers at D1.

The ADC board contains the line drivers and receivers, and the Datel Analog to Digital converter (Figure 5.9). When the analog bus enters the board, it is terminated to +6v through 330 Ω . This was chosen as a compromise to minimize both noise susceptibility and bus driver current.

The Datel ADC converts the bus voltage to a 10 bit

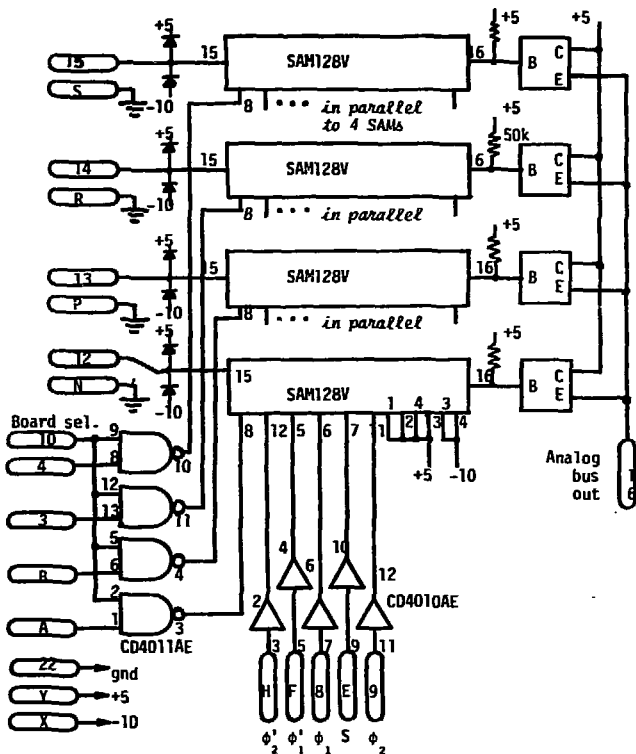
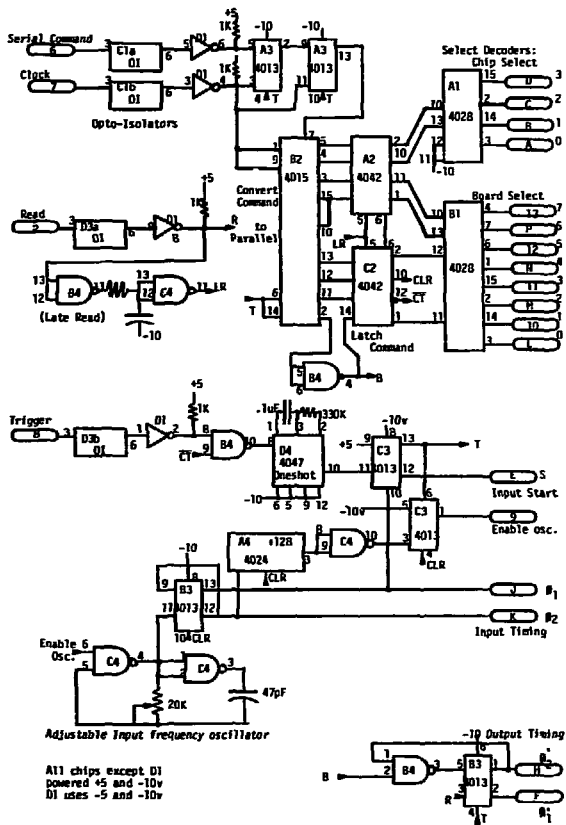


FIGURE 5.8 RETICON SYSTEM SAM BOARD

Each Reticon system holds 6-8 boards, each containing 4 Serial Analog Memory (SAM) integrated circuits. Each SAM stores one signal waveform.

RETICON SYSTEM DIGITAL CONTROL BOARD



XBL 789-11083

FIGURE 5.9

digital word by successive approximation in 4 μ sec. The internal 10 pulse clock becomes the CLOCK line for the system serial transmission scheme.

5.1.5.2 Multiplexer circuitry

The purpose of this interface is to permit the computer to operate up to 4 Reticon systems simultaneously. In addition it provides a simple means of interfacing other devices to the PDP-11 Unibus.⁸

The strategy used is to create a Control Logic⁹ (CL) style board box with its own data bus (Figure 5.10). This data bus is simpler than the full Unibus and is buffered into it through an interface board within the computer.

Interfaces to individual devices are constructed on Control Logic boards. Any cables leaving the computer screen cage are optically isolated and carried on twisted pair cables. The cables are connected to the box by round Bendix connectors.

The CL bus carries 4 address, 12 data, read, and write lines over flat cable from the computer (Figure 5.11). In the multiplexer box the data lines run to all cards while the address, read and write lines are decoded by the Address board.

The Address board contains a decoder and buffers the READ and $\overline{\text{WRITE}}$ lines to each interface. Both polarities, READ and $\overline{\text{READ}}$, are buffered when the address lines read 0 to

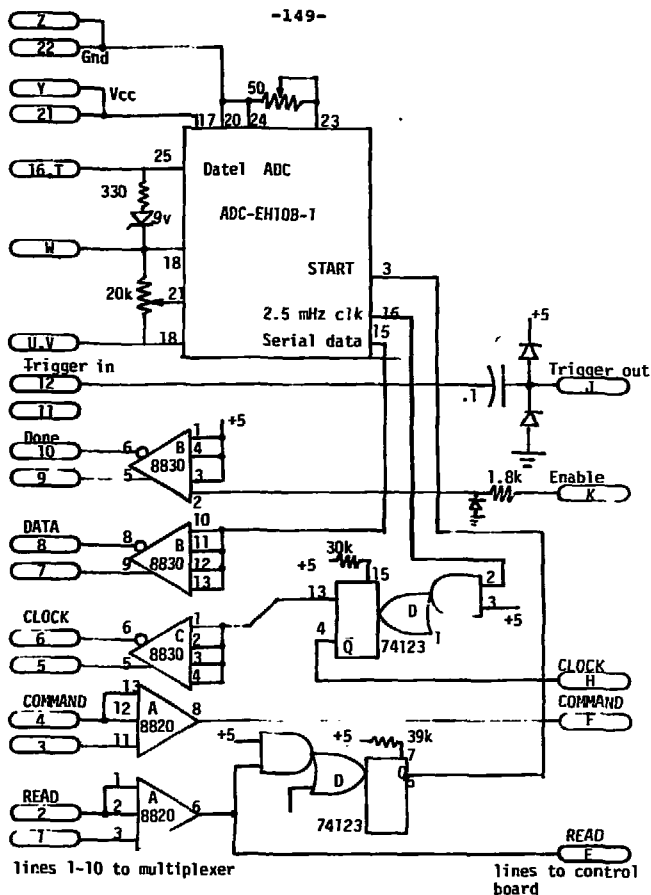


FIGURE 5.10 RETICON SYSTEM ADC BOARD

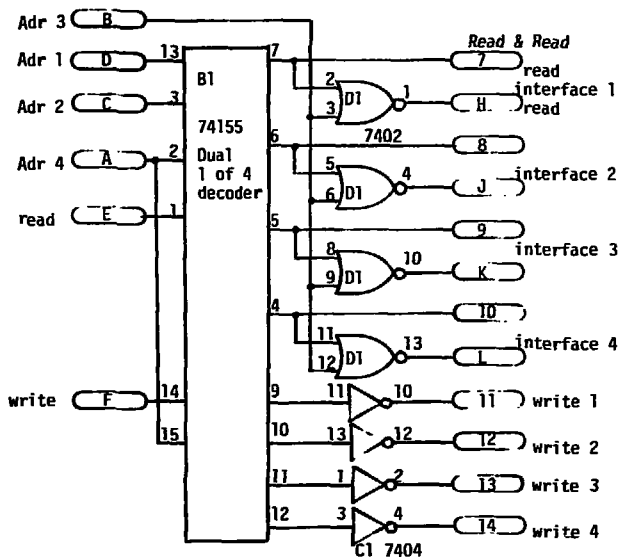


FIGURE 5.11 MULTIPLEXER ADDRESS BOARD.

Each Reticon interface has a pair of addresses on the computer Unibus. The M1710 interface partially decodes the address, and this board in the multiplexer completes it.

XBL 789-11357

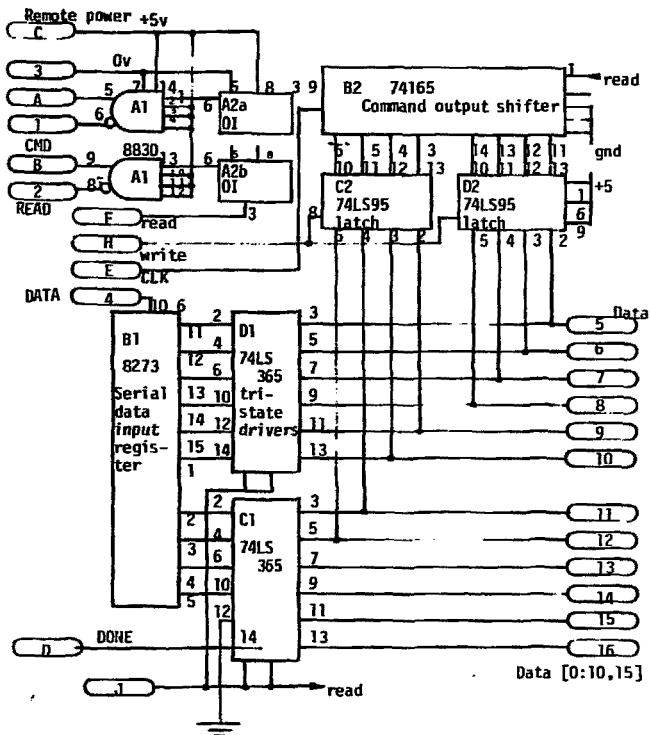


FIGURE 5.12 MULTIPLEXER INTERFACE BOARD.

Each Reticon system is interfaced to the computer through a separate interface board in the multiplexer. The twisted pair lines are optically isolated, and powered from the Reticon box end.

3. Addresses 4 to 7 are the same as 0 to 3 except READ is inhibited. Addresses 8 to 15 are not currently used and are available for expansion.

Each interface board works in conjunction with half a hex isolator board. The line drivers from the interface are powered by +5v brought over the twisted pair cable from the Reticon box power supply and are particular to each interface. Hence their associated optoisolators are located on the interface board. The line receivers for the 3 pairs from the Reticon box are optoisolators powered by the signal. As they require no remote power, they can be grouped into lab stock hex isolator boards.

The interface card contains shift registers to receive the Reticon data word (B1) and transmit the command (B2). The command word is loaded from the data bus when a $\overline{\text{WRITE}}$ pulse clocks latches C2 and D2. The data register is read onto the bus when gated through C1 and D1 by the $\overline{\text{READ}}$ pulse. The READ pulse is sent to the Reticons through the driver A1. READ and $\overline{\text{READ}}$ can be addressed separately so the data line can be read without cycling the computer. This is done to read bit 11, the DONE flag, while waiting for a shot.

5.2 Computer System

The first law of computer systems is that they grow. The second, and naturally more frustrating, is that the

better they work, the faster your demand outgrows them. The third is that computer problems are like heroin: they are so intriguing you had best stay ignorant of them.

Our computer system has been very successful and has evolved through three generally interesting stages. This development has been aligned with the laboratory's Real Time System Group. There are about a dozen similar, but not identical, systems at LBL used for data acquisition.

The purpose of the computer is to allow the experimenter to collect data and learn its significance quickly, flexibly, and with no attention to idiosyncracies of a computer. The intended results are:

- 1) Raw data can be quickly stored, displayed and permanently recorded.
- 2) Data can be analyzed by interactive programs (that is, programs which can be changed quickly while they are in use).
- 3) A fast, powerful general computation facility.
- 4) A simple-to-use general graphics plotting facility.
- 5) No failures or lost data.

5.2.1 Present configuration

The present system allows three experiments and a fourth programmer to operate concurrently from one computer while a fifth terminal runs programs on ours, or switch onto a larger, remote system. Both our PDP-1134A and the remote network host PDP-11/45 run compatible RSX-11M¹⁰ operating system software. The FORTRAN, BASIC and graphics library

are the same. All three experiments may use identical data acquisition programs, and they don't have to.

5.2.1.1 Hardware

The Digital Equipment Corp. PDP-1134A computer¹¹ is a quick, powerful and brilliantly sophisticated minicomputer, and the most widely used in physics. The wealth of experience people have on PDP-11's have perpetuated the machine's near-monopoly in the field, and in this case the monopoly is well-deserved.

The key feature useful to us is the computer's memory management system, which allows it to divide up large amounts of memory between different users and protect them from each other.

Our processor is equipped with a floating point processor, 24 k words of DEC core memory and 64 k of additional Standard core memory (Figure 5.12).

Programs and short term data storage goes on 3 M words of RK05 disk. Long term storage is provided by two IBM 729 7 track magnetic tape units. The tapes are compatible with the LBL computer center and other PDP-11's equipped with 7 track tapes.

The system console terminal is a simple refresh CRT, the DEC VT50. There are four identical user graphics storage display terminals, Tektronix 4006-1's. These display 35 lines of text and/or vector plots with 1024 line resolution.

Each 4006 is connected to the Tektronix 4610 hand copy printer/plotter.

5.2.1.2 Software

We need to run several large programs at once, yet be able to freeze everything during a data acquisition cycle. DEC's RSX11-M real time operating system allows this. Each program becomes a "task", and the system automatically juggles tasks on and off disk, and into different segments of core.

Each user's files are catalogued separately and protected. Most programs are written in FORTRAN IV-plus, and make use of libraries of subroutines used by the whole group. These include routines for

MAGNETIC TAPE: subroutines for reading and writing data in several different formats: DEC DOS standard, straight binary, CDC display format, ASCII standard.

DATA TAKING: subroutines to operate the Reticon system multiplexer, standard data taking programs, polychrometer automatic calibration routines

GRAPHICS: subroutines to plot on the Tektronix terminals: points, lines, grids, contour diagrams, spline fit curves.

ANALYSIS: best fit solvers to various functions, Runge Kutta integrators, elliptic integral routines for magnetic field codes.

5.2.2 System evolution

The initial data acquisition system was quite small. It provided the same services, although with less convenience and smaller scale. A PDP-11/10 computer allowed a single user to take data and perform simple manipulations using interactive BASIC. Data could be plotted on an XY scope or an XY plotter.

The system had no local program on data storage. Instead, the computer was linked to a remote PDP 11/45 running RSX-11M. All programs and data were transferred over this 9600 band phone line link and stored on the disks of the 11/45.

There was a second mode available in which the user terminal was "directly" connected to the network host via local software. This allowed the user to program and run data analysis programs directly on the 11/45 in Fortran.

This network mode of operation became popular at LBL and is still in use by other groups. Its primary limitations were:

- 1) limited access to the heavily loaded 11/45,
- 2) slow data transfer time.

The Tormac group was the network "charter member". I wrote the original software and coordinated the protocols with Jeff Gallup of the Real Time Systems group. He, the RTSG and particularly Sytko Andrae then took responsibility for rewriting it in a more professional way and maintaining

it for the community. In addition, most of the research groups use CAMAC data acquisition hardware, and the RTSG Network Basic supports that too.¹²

Network BASIC is an expansion of DEC stand-alone BASIC and thus has no operating system per se. Adding adjuncts to this BASIC is very simple and allowed me to quickly add service routines for various other devices such as the 4006 graphics terminal, xy plotters, mag tape and disk. Whenever the RTSG intended to also support these things later, formats were chosen to be compatible.

The first expansion of the system was to add local magnetic tape drives. I resisted this as long as possible: an enormous advantage to our small network link was that it had no moving parts like disks, tapes, or printers. These are usually the most prone to failure, and our lab environment is electrically and thermally rough. The central LBL computer center, though, had dozens of IBM 729 tape drives available. Our demand for storage had grown to where we had to have something, and a decision was made by the PDP-11 network community to use the 729's interfaced through a Kinetic Systems controller.

Two sets of Magtape formats were used. Binary format routines allowed BASIC programs and data to be stored in 16 bit words. CDC decimal format was used to store standard data shots in a way easily accessible at the LBL computer center.

5.2.3 Descriptions of special programs

The following pages are detailed notes on operating and maintaining the programs written for the system which are common to all users.

Software Description: PDP-1134 RSX-11M

TAKE.FTN: Standard Data Taking Program

Purpose: Allow all the Tormac experiments to take data in a standard way.

Intended Results: -24 Reticon channels may be read each shot. (ch. 1 to 24)

- Shots may be stored and recalled from disk and are named by a prefix (P1, T4, T5, TC) and a sequence number.
- A descriptive header is stored with each shot, containing date, time, voltage and timing settings, and a comment.
- A separate file (e.g. T4 HEAD.HDR) stores the header each time the program exits so that it starts where it previously left off.
- Raw data is displayed and labeled for each shot.
- Data analysis routines, such as line fitting, are included.
- Channels 9-24 are assumed to be a 16 channel polychromator.

Setup Instructions: Take must be linked to the ADC, graphics and fit routines.

```
TKB commands    TAKE/FP/CP=TAKE,ADC,FIT,KLEE,GRAF
                 /
                 COMMON=10PAGE:RW:7
                 //
```

Each day the program is used it must be installed at high priority so that data taking can't be interrupted.

```
>INS TAKE/PRI=100./CKP=YES
```

It can then be run or aborted using the task name TAKE

```
>RUN TAKE
>ABO TAKE
```

Use Instructions: The program responds to 2 letter commands, to the prompt CMND>

```
NE  Take NEXT data shot, and display it
ST  STORE the present shot on disk
RC  RECALL a shot from disk (it prompts for the shot
    number)
EX  EXIT from TAKE, storing the header
AB  ABORT TAKE (exit without storing header)
PKnn find the PEAK of channel nn, integer nn
TE  TEST the Reticon unit
```

- TSnnn** print the data values for 4 time steps starting at nnn, for all 24 channels. Calibrate and print the polychromator levels on the last 16 channels ($=Data \times PC(i) \times 10^{**}(GS(i)/20)$) These 4 can be averaged in response to a prompt, and sent to FIT
- FINnn** FIT the polychromator channels to a Gaussian, display it and find an equivalent ion temperature for a Doppler broadened HeII 4686 line.
- PA** display all the PARAMETERS in the heater and change them in response to the prompt CHANGE>. Parameters are changed by type, number and value. Values must be followed by a decimal point.

Types and examples

- GSnn** polychromator gain setting, in dB, for polychromator channel nn (data channel nn + 8)
GS07=30.
- PC** polychromator calibration PCI3=1.097
- RE** Reticon read out order mapping RE23=22.
- BIAS** bias bank
- CUSP** cusp bank Timing and voltage settings
- PREI** pre-ionizer e.g. CUSP/V=15000
- RUBY** Apollo laser BIAS/T=230
- LAUS** heater bank
- COMP** computer
- INTF** interferometer
- FILE** file name in header FILE=TC0123.BIN
- NO** stop taking changes, go back to commands.

Program Structure and Modifying Instructions

- The main loop goes from table 10 to 30. The command is accepted, located in a table ICMD, and a computed GOTO jumps to the relevant program section
- To add commands, put the letters into the DATA statement for ICMD, enlarge the table lookup loop at 11, and add the service routine table to the GOTO list at 30.

Arrays

- ID(128,24)** main data array, 128 time steps x 24 channels equivalenced with D(512,6) so the display routine can easily display 4 channels per line.
- HEAD(256)** header array. It contains
AF shot name in ascii
ITIME,IDATE shot date and time in ascii
- S(25)** Reticon channel select array, integers

PC(16) Real polychromator calibration coefficients
GS(16) Integer polychromator gain settings
CMNT(64) Ascii comment
VOLT(8),TIMING(8) integer bank parameters
ANAME(8) 4 letter ascii bank names
ICMND(24) 2 letter commands
IB,IIN,IPNAM 2 letter pieces of the file name.

Software Description: PDP-1134 RSX-11M

ADC.MAC: Reticon system interface package

Purpose: Simply interface the data taking hardware to FORTRAN and BASIC programs

Intended Results:

- Select a Reticon unit through the multiplexer.
- Take baseline and data shots.

Setup Instructions: ADC must be assembled using MAC. Any program it is linked to must also have access to the IO portion of the Unibus, using the
COMMON=IOPAGE:RW:7
option in TKB.

Use Instructions:

MUX(IMUX) tells all following routines which multiplexer channel is to be used. IMUX is a two integer array. Before calling, IMUX(1) is the channel number; after calling it contains the two device addresses. BASE(D,S) takes a baseline shot. S is an integer array of pointers of which Reticon channels to read. It stops when it comes to a -1. D is an integer data array, 128 time steps x of channels. BASE triggers the Reticon unit itself. AADC(D,S) takes a shot, as above, but an external trigger must be used for the Reticons. SADC(D,S) like AADS, but the data is subtracted from D rather than stored there. MOVO (ISOURCE,IDESTINATION), MOVI (IS,ID) move out, from an integer variable to a Unibus location move in, from a UNIBUS location to an integer variable e.g. CALL MOVI (-136,I) reads the switch register, as octal 177570=decimal -136.

Program Structure:

- When FORTRAN or BASIC calls a routine, it points to the argument list from register 5. The argument list contains the number of arguments, followed by a list of argument addresses. Hence:
MOV 2(5),R0; fetches first argument address
MOV #4(5),R0; fetches second argument value.
- BASE, AADC, SADC are entry points to the same general routine. They set up the pointer for storing or subtracting data (MVLOOP,SBLOOP) on the stack, and a word = 100 if the Reticon unit is to be automatically triggered.
- ADCENT is then the common entry point. The Reticon is cleared, triggered if necessary, and then waitloops

are performed to watch the Reticon DONE signal go up and down.

- At STLOOP, the programs selects one Reticon channel after another, asserting their start bit, then reading them out.
- Commands are sent to the Reticon unit by loading them into the command register, then reading the data register. When the read pulse falls, the command is serially transmitted in sync with the data being read.

Suggested Change:

It would be convenient to have the Reticons operate by interrupt rather than waitloops at high priority. Right now the entire computer waits each time the ADC routines are entered.

A system resident driver would need to be written and loaded into the RSX-11M executive.

The multiplexer hardware would need to be modified, so that the DONE bits are constantly transmitted to the computer.

The Unibus interface card would have to be jumpered to allow interrupts.

Software Description: PDP-1134 RSX-11M

TV.FTN Integer Tektronix Graphics package.

Purpose: Give Fortran and Basic programs full access to the graphic capabilities of the Tektronix 4006-1 terminal.

Intended Results: - Pictures may be plotted and tabled with very few small subroutines.
- Plotting will occur as fast as the terminal will allow.

Setup Instructions: the routines are compiled with F4P and linked by TKB or FTB. e.g. >FTB X=X,TV

Use Instructions:

TVCL clear the screen, pause for .75 sec, home cursor
TVPU(IX,IY) set the terminal to graphics mode, move the cursor to IX,IY on the terminals 1023 x 780 grid.

TV Pen Up.

TVPD(IX,IY) draw a line to position IX,IY.

TV Pen Down

TVST(IX,IY,A,N) print an N character string A at position IX,IY

DOQIO(A,N) output N character string A without going through the normal terminal routines (i.e., skip all carriage control conventions)

Program Structure:

Most of the work happens in a subroutine TVQQ, where IX and IY are broken into 5 bit pieces, turned into characters, and sent out via DOQIO.

Software Description PDP-1134 RSX-11M

GRAF.FTN Real Number Plotting Package

Purpose: Provide standard routines for common mapped plotting tasks on Tektronix terminals.

Intended Results:

- Plot real numbers, lines, curves and symbols linear or logarithmic mappings.
- Plot grids on sectors of the terminal screen which reflect that mapping.

Setup Instructions:

This package contains TV.FTN, so that needn't be linked separately. GRAF is compiled by F4P and linked by TKB or FTB, e.g. >FTB X=X,GRAF

Use Instructions:

GRID (XL,XH,IXL,IXH,NX,YL,YH,IYL,IYH,NY)

Set up a mapping to the physical integer screen space (IXL→IXH,IYL→IYH) from a real numerical space (XL→XH,YL→YH). The mapping is either linear or log for each coordinate

if NX or NY > 0 then linear, N divisions
< 0 then log, -N divisions per decade
= 0 then linear, no grid.

The grid is drawn. For log mappings, the data range (e.g. XL,XH) gives the number of decades.

PLOT(X,Y,N,M)

X and Y are either points or arrays of points X(N),Y(N)

There are several modes

- N>1 M<2 connect N points by line segments
 - N>0 M>1 plot N points using ascii symbol M
 - N=1 M=0 move "PEN", like TVPU
 - N=1 M=1 move "PEN", like TVPD
- The position X,Y is determined by the GRID mapping

Program Structure:

GRID and PLOT communicate via some common variables and logical flags.

XLOG,YLOG flags for linear or log plots
XLO,YLO,DX,DY real intercept, slope for mapping
IXL,IYL,SX,SY integer intercept, slope for mapping.

For linear plots

$IX=IXL+(X-XLO)*SX$ $SX=(IXH-IXL)/(XH-XL)$

For log plots

$IX=IXL+DX*LOG_{10}(X/XLO)$
 $DX=(IXH-IXL)/(# of decades)$

Software Description: PDP-1134 RSX-11M

CONTUR.FTN Plot contour maps on the Tektronix

Purpose: provide a simple way of interpreting 2D arrays.

Intended Results:

- Develop and use a simple algorithm for plotting contours.
- Plot fairly smooth contours using line segments which are linearly spaced over a given range.

Setup Instructions:

CONTUR is compiled with F4P and can be linked with FTB or TKB. It calls routines in the GRAF package.
e.g. >FTB X=X,CONTUR,GRAF

Use Instructions:

CONTUR (A,N,M,AL,AH,NC)
plot NC contours, linearly spaced over the range AL to AH, for the N by M array A. GRID must have been called, for the real range (1-N,1-M).

Program Structure, Description of Algorithm:

- The array A is treated as a 3D surface intersected by planes at the different contour heights. The planes have array values at the corners of grid squares (see Figure 5.13).
- The program marches through the grid, one square at a time, starting at A (2,2); i.e., squares are indexed by their upper right corner.
- The values are remapped, linearly, into the 5 element B array. $B = f(A)$
- $NC(A-AL)/(AH-AL)$

While A runs from AL to AH, B runs from β . to NC, where NC is the number of contours. Thus the contours fall on integers. This is found by $IB=B$.

- The program finds the range of contours crossing a square by finding MIN and MAX of IB (ik=1 to 4). The point where the contour crosses is linearly interpolated: For contour K,

$$Z = (K-B(ik))/B(ik+1)-B(ik)$$

Z is an offset from the corner, along one side.

A logical flag L is set if a contour crosses a boundary. There are six possible vectors to draw for the four boundaries.

- In summary
For I,J=2<NX,2<NY
Map A into B and IB

Find range of $IB = [IC3 - IC1]$
For each contour in range:
 find crossings,
 draw vectors.

- An additional feature is that the central contour of the range is dotted to provide a reference.

Software Description PDP-1134 RSX-11M

TAPE.MAC Magnetic Tape Service Routines

Purpose: Provide simple, long-term data storage.

Intended Results: - Tapes can be read and written from FORTRAN and BASIC programs.
- Tapes are compatible with the CDC 6600 system, and with the older Network BASIC formats.

Setup Instructions:

The magtape is assigned to logical unit 2, so this must not be used for disk files in the calling program. TAPE is assembled by MAC and can be linked with FTB or TKB.
e.g. >FTB X=X, TAPE

Use Instructions:

MTSL(I) select tape unit I. This routine must precede any other TAPE operation
MTRW rewind the tape
MTSB(N) if N>0, skip N blocks forward
if N<0, skip N blocks back
MTSF(N) skip N files, forward or back
MTRB(A,N) read an array A of N words in packed binary format
MTWB(A,N) write a packed binary array
MTEF write an end of file mark
MTRH(B) read a 128 byte header, in CDC display code
MTWH(B) write B as a CDC display code header
MTRD(N,M,D,B) read N blocks of M words each, into array D. Data is on tape in 4 digit CDC decimal notation, B is a conversion buffer array, at least 4 x M bytes long.
MTWD(N,M,D,B) write data, as above.
MTCL Clear the controller of any error conditions.

Program Structure:

The routines use QIO monitor calls; these are documented in the DEC RSX-11M executive manual.

Conversion from CDC format for the headers is done by tables for the special characters, and bit manipulation for the letters and numbers.

The data routines, MTRD, MTWD, can only work with numbers in the range 0 to 9999. Reticon unit data falls in a range -300 to 300, so a constant 1000 is added to the data when it is written, and subtracted when it is read.

Software Description PDP-11/34 Network Basic

DISK.MAC simple disk routines for
stand alone Network Basic

Purpose: - Provide disk storage software for the period
August to October 1977, after the disk arrived but
before the RSX-11M software was prepared
- Provide a disk operating system which can run with
only one disk and still collect data. RSX-11M
requires ~.7 disk for system overhead.

Indended Results:

- Callable from Basic
- Store and recall programs and data from numbered files
- Boot the system from disk.

Set Instructions:

DISK is assembled by MAC and linked to basic modules
via TKB on the Network

```
TKB>BASIC/-HD=BASICL,DISK,FPMP,BASICH
```

```
 /  
STACK=0
```

```
 //  
It is loaded over the LBL Network download program  
>LBL TI:=BASIC.TSK.  
and then copied onto disk.
```

Use Instructions:

DKRD(A,N,E) read a 3072 word array (24 Reticon channels)
into array A from file N, where N = 1 to 199. Any error
flags are returned in E.
DKWD(A,N,E) write a data array.
DKBO(N,E) store the current program into program file
N, N=0 to 19. Disk Boot Out
DKBI(N,E,) Boot in program file N

Program Structure and Disk Organization:

The DEC RK05 disk is structured as 1.2 million words:
2 surfaces x 200 tracks x 12 sectors x 256 words. For this
system, surface 0 is used to store data files, 1 per track.
Track 0 is reserved for a bootstrap routine.

Surface 1 is used for program files. Each file is
ten consecutive tracks, holding 1 30K word core image. Hence
not only the program, but the variables and Basic interpreter
are stored with each file.

This format is not compatible with any DEC operating
system. The DEC PRESRV utility routine can be used in image
mode to save the disk on magtape.

The routines do nothing more than pass arguments to the
RK11 controller. No error checking or recovery is included.

Software Description: PDP-1134 RSX-11M

BASIC.TSK DEC RSX-11M BASIC with TORMAC subroutines

Purpose: Allow simple interactive program support for experiments.

Intended Results:

- Basic programs can access the same support sub routines as can FORTRAN programs: the ADC,TAPE and TV packages.

Setup Instructions:

Linking BASIC is complex and is described in detail in the BASIC user's manual. The important consideration is that a symbol table entry must be supplied for each subroutine which contains the routine name and starting address.

Use Instructions:

- subroutine names must be enclosed in quotes, e.g. CALL "TVCL"
- Integer variables always have a percent sign suffix; e.g. X%, A%(23)
- Integer constants passed as arguments must also have a percent sign, or they will be passed in floating point format. e.g. CALL "TVPU" (100%, 100%)

Program Structure:

- The subroutines are identical to the Fortran versions, with the addition of the symbol table entry. They may not access any functions special to Fortran.
- In some cases it is useful to call subroutines internal to the BASIC interpreter. To do this, register R5 must be reloaded to the value it had prior to execution of the call, e.g.
MOV R5,-(SP); push present R5 on stack
MOV-4(5),R5; fetch old R5
JSR 1,MSG; call a subroutine
.ASCII"!";<0>
MOV(SP+,R5; restore present R5

5.3 References

1. J.W. Coonrod, *Bul. Am. Phys. Soc.* 21, 844 (1976).
2. J.G. Zornig and J.F. McDonald, *Rev. Sci. Instr.* 44, 1217 (1973).
3. Biomation Inc., 1070 E. Meadow Circle, Palo Alto, CA.
4. W. Hopmann, *Proc. 8th Symposium on Fusion Technology*, Noordwykerhout, EUR-5182e, p. 519 (1974).
5. CCD 311 Data Sheet. Fairchild Semiconductor, 464 Ellis St., Mountain View, CA 94042.
6. Reticon Corp. 910 Benicia Ave., Sunnyvale, CA 94086.
7. Hewlett Packard, Palo Alto, CA 94301.
8. Digital Equipment Corp., 146 Main St., Maynard, MA 01754.
9. Control Logic Corp.
10. RSX-11M documentation, Digital Equipment Corp.
11. Digital Equipment Corp.
12. PDP-11 BASIC manual, with additional chapters, Real Time Systems Group, LBL (1976).

ACKNOWLEDGMENTS

This project has been funded by EPRI and the U.S. Department of Energy. I want to thank:

- Wulf, Mort and the Tormac staff for their guidance and support, and for the opportunity to join them in an experiment worth doing. Of them I particularly want to acknowledge
- Gary Tabler, for his impeccable assistace in assembling IV-c
- Michael C. Vella, for sharing his insight and experience
- My partner, Martin Greenwald, for his ability and patience
- The staff of LBL, all the groups and shops which have contributed to Tormac
- Michele Marram, for typing this tome. Her diligence surpasses my unconsciousness.

This thesis is dedicated to my parents.